Elucidation of lipid metabolism pathways mediated by AMPK and nuclear receptors PPARδ and LXRα in human macrophages

Dissertation

for attaining the PhD degree of Natural Sciences

submitted to the Faculty of Biochemistry, Chemistry and Pharmacy

of the Goethe University

in Frankfurt am Main

by

Marina Kemmerer

from Sumy – Ukraine

Frankfurt am Main, 2015

(D30)

Accepted by the Faculty of Biochemistry, Chemistry and Pharmacy

Goethe University Frankfurt am Main

Dean: Prof. Dr. Michael Karas

Referees: Prof. Dr. Bernd Ludwig

Prof. Dr. Bernhard Brüne

Prof. Dr. Robert Fürst

Prof. Dr. Klaas Martinus Pos

Date of Disputation: 26. 11. 2015

We are here for experience,
and experience is a preparation
to know the truth when we meet it.

- Henry Ford -

Index

Index

List of figures

List of tables

Abbreviations

AA	amino acid(s)
Ab	antibody
ABC	ammonium bicarbonate
ABCA1	ATP-binding cassette transporter A1
ACAA	acetyl-CoA acyltransferase
ACADVL	acyl-CoA dehydrogenase, very long-chain
ACAT	acyl-CoA cholesterol ester transferase
ACC	acetyl-CoA carboxylase
acLDL	acetylated LDL
ACN	acetonitrile
ADRP	adipose differentiation-related protein/PLIN2
AICAR	5-aminoimidazole-4-carboxamide ribonucleotide
AMP	adenosine monophosphate
AMPK	AMP-activated protein kinase
AMPK OE	overexpression of truncated, constitutively active AMPK$\alpha 1^{1-334}$ subunit
Angptl4	angiopoietin-like 4
ANOVA	analysis of variance
Apo	apolipoprotein
APS	ammonium persulfate
ATF1	activating transcription factor 1
ATP	adenosine triphosphate
BCL6	protein B cell lymphoma 6
bp	base pairs
BSA	bovine serum albumin
C/EBP	CCAAT/enhancer binding protein
cAMP	cyclic AMP
CD	cluster of differentiation

Abbreviations

CE	cholesterol ester
ChIP	chromatin IP
CHOP	C/EBP-homologous protein
CPT1	carnitine palmitoyltransferase 1
CV	scrambled control shRNA/lentiviral particles
DC	dendritic cells
DEPC	diethyl pyrocarbonate
DMEM	Dulbecco's Modified Eagle's Medium
DMSO	dimethylsulfoxide
DNA	desoxyribonucleic acid
DTT	dithiothreitol
e.g.	*exempli gratia* [Lat.], for example
ECAR	extracellular acidification rate
EDTA	ethylene diamine tetraacetic acid
eIF2a	eukaryotic translation initiation factor 2a
ELOVL6	long-chain fatty acid elongase 6
ER	endoplasmic reticulum
ERK1/2	extracellular signal-regulated kinase 1/2
ETFDH	electron transfer flavoprotein-ubiquinone
FABP4	fatty acid-binding protein 4
FACS	fluorescence activated cell sorting
FAO	fatty acid β-oxidation
FC	free cholesterol
FCS	fetal calf serum
FFA	free fatty acid(s)
g	gramm
g	gravitational field
GAPDH	glyceraldehyde 3-phosphate dehydrogenase
GSEA	gene set enrichment analysis

Abbreviations

h	hour(s)
H_2O	water
HDAC	histone deacetylase(s)
HDL	high-density lipoprotein(s)
HMG-CoA	3-hydroxy-3-methylglutaryl-coenzyme A
i.e.	*id est* [Lat.], that is
IL	interleukin
IMPA2	inositol(myo)-1(or 4)-monophosphatase 2
IP	immunoprecipitation
kb	kilo basepares
KCl	potassium chloride
KD	knock-down
keV	kiloelectron Volt
KO	knockout
KOH	potassium hydroxide
LB	lysogeny broth
LBD	ligand binding domain
LCFA	long-chain fatty acid(s)
LDL	low-density lipoprotein(s)
LKB1	liver kinase B1
LPL	lipoprotein lipase
LPS	lipopolysaccharide
LXR	liver X receptor
LXRE	LXR element(s)
M	molar
m	metre
MCAD	medium-chain acyl-CoA dehydrogenase
MCP1	monocyte chemotactic protein 1
MCSF	macrophage colony-stimulating factor

MEF2	myocyte enhancer factor 2
MEM	Eagle's Minimum Essential Medium
min	minute(s)
mLDL	modified LDL
mRNA	messenger RNA
MS	mass spectrometry
MSFM	macrophage serum-free medium
mTOR	mammalian target of rapamycin
MΦ	macrophage(s)
Na_3VO_4	sodium vanadate
NaCl	sodium chloride
NAD^+	nicotinamide adenine dinucleotide
NaF	sodium fluoride
NEAA	non-essential amino acids
NFκB	nuclear factor-kappa of activated B cells
OCR	oxygen consumption rate
OE	overexpression
oxLDL	oxidized low-density lipoprotein
p	phospho-
PBS	phosphate buffered saline
PCR	polymerase chain reaction
PDC	pyruvate dehydrogenase complex
PDK4	pyruvate dehydrogenase kinase, isoenzyme 4
PGC1α	PPARγ co-activator 1α
PI	phosphatase inhibitor cocktail
PLIN2	perilipin 2 /ADRP
PMSF	phenylmethylsulphonylfluoride
PPAR	peroxisome proliferator-activated receptor
PPRE	PPAR response element

Abbreviations

qPCR	quantitative PCR
RCT	reverse cholesterol transport
RIN	RNA integrity number
RNA	ribonucleic acid
RPMI	Roswell Park Memorial Institute
RT	room temperature
RT-PCR	real-time PCR/quantitative PCR
RXR	9-*cis* retinoid X receptor
SDS	sodium dodecyl sulfate
sec	second(s)
SEM	standard error of the mean
shRNA	short hairpin RNA
SILAC	stable isotope labeling by amino acids in cell culture
siRNA	small interfering RNA
SIRT1	silent information regulator T1, sirtuin 1
SMC	smooth muscle cell
SMPDL3A	sphingomyelin phoshodiesterase acid-like 3A
SMRT	silencing mediator of retinoic acid and thyroid hormone receptor
STAT	signal transducers and activators of transcription
t	total
TBS	Tris-buffered saline
TBST	TBS with Tween 20
TEMED	tetramethylethylenediamine
TG	triglyceride(s)
TGF	transforming growth factor
TNF	tumor necrosis factor
TPA	12-O-tetradecanoylphorbol 13-acetate
U	unit(s)

UCHL1	ubiquitin carboxyl-terminal esterase L1
UCP2	uncoupled protein-2
V	Volt
VLDL	very low-density lipoprotein(s)
vs.	versus
VSN	variance stabilization and normalization
WB	Western blot analysis
WB	Wash buffer
WT	wild type

1. Summary

Disturbances in lipid metabolism are responsible for many chronic disorders, such as type 2 diabetes and atherosclerosis. Regulation of lipid metabolism occurs by activated transcription factors peroxisome proliferator-activated receptor δ (PPARδ) and liver X receptor α (LXRα) mediating transcription of different target genes involved in regulation of fatty acid uptake and oxidation or cellular cholesterol homeostasis. This is especially relevant for the macrophages, since pathways regulated by PPARδ and LXRα affect foam cell formation, a process driving the progression of atherosclerotic lesion. AMP-activated protein kinase (AMPK) plays a central role in energy homeostasis in every type of eukaryotic cell, but its role in human macrophages, particularly with regard to lipid metabolism, is not precisely defined yet. Thus, I investigated the impact of AMPK activity on PPARδ and LXRα and the expression of their target genes involved in fatty acid oxidation (FAO) and cholesterol metabolism.

As PPARδ has been described as a potential target for prevention and treatment of several disorders and AMPK as interesting drug target for diabetes and metabolic syndrome, the aim of the first part of my studies was to investigate their interaction in primary human macrophages. Completing the first challenge successfully, I was able to establish a lentiviral transduction system for constitutively active AMPK (consisting of a truncated catalytic AMPKα1 subunit bearing an activating T198D mutation) in primary human macrophages. Using genome-wide microarray analysis of gene expression, I demonstrate FAO as the strongest affected pathway during combined AMPKα1 overexpression and PPARδ activation. The most influenced genes were validated by quantitative PCR as well as by Western analysis. I found that AMPK increases the expression of FAO-associated genes targeted by PPARδ. Corroborating the results obtained using AMPKα1 overexpression, PPARδ target gene expression was increased not only by PPARδ agonist GW501516, but also by pharmacological allosteric AMPK activator A-769662. Additional enhancement of target gene mRNA expression was achieved upon co-activation of PPARδ and AMPK. Silencing PPARδ expression increased basal expression of target genes, confirming the repressive nature of ligand-free PPARδ, abolishing the increased target gene expression upon AMPK or PPARδ activation. Measurements of triglyceride contents of human macrophages incubated with VLDL following PPARδ activation demonstrated a reduction of intracellular triglyceride accumulation in cells, which may reflect the enhancement of fat catabolism.

Summary

In the second part of my studies, I concentrated on the regulation of cholesterol transporter ATP-binding cassette transporter A1 (ABCA1) expression by AMPK. ABCA1 facilitates cholesterol efflux from macrophages thus, preventing atherosclerosis progression. For the first time, AMPK implication in the regulation of the ABCA1 pathway could be presented. Both AMPK overexpression and activation lead to significantly increased ABCA1 expression, whereas AMPKα1 knock-down strongly reduced this effect. Besides, I was able to prove an enhanced activity of ABCA1 during AMPK activation in human THP-1 macrophages by measuring cholesterol efflux into apolipoprotein AI-containing medium.

Previous findings showed regulation of ABCA1 by LXRα. I confirmed these results by silencing experiments indicating an essential role of LXRα in ABCA1 regulation pathway. Here, ABCA1 mRNA as well as protein expression were positively mediated by LXRα. LXRα activation elevated ABCA1 levels, whereas its silencing down-regulated this effect. Interestingly, ABCA1 was found to be regulated only by LXRα and not through LXRβ. At the same time, knock-down of PPARα, -γ or -δ, which may be also involved in the regulation of LXR/ABCA1 axis, did not influence the activation of ABCA1 expression by an AMPK activator. To confirm that LXRE on *Abca1* promoter is essential for ABCA1 regulation, I performed luciferase reporter assay using constructs based on *Abca1* promoter with or without LXRE mutation. Mutation of LXRE abolished reporter activity, whereas AMPK activation increased luciferase activity of wild-type LXRE construct. Furthermore, I demonstrate AMPK-dependent LXRα binding to the LXRE site of *Abca1* promoter using the method of chromatin immunoprecipitation. AMPK activation significantly increased, whereas silencing of AMPK significantly attenuated LXRα binding, indicating AMPK as one of the most important regulators of ABCA1 expression.

In summary, I provided an evidence for AMPK involvement into lipid and cholesterol metabolism in human macrophages showing the regulation of PPARδ and LXRα target genes. The understanding of AMPK and PPARδ interaction allows the development of new approaches for treatment of metabolic syndrome and related diseases. Increased FAO during the activation of both proteins may exhibit better therapeutic benefit. On the other hand, I have shown the impact of AMPK activation on ABCA1 via LXRα up-regulation leading to increased cholesterol efflux in human macrophages for the first time. These findings thus may impact future improving of anti-atherosclerosis therapies.

2. Zusammenfassung

Akuter Herztod ist mit 4-5 Millionen Fällen pro Jahr weltweit eines der größten Todesrisiken, das durch eine bestimmte ventrikuläre Herzrhythmusstörung verursacht wird. 80% dieser Fälle sind mit koronaren Arterienerkrankungen assoziiert, u.a. durch das Metabolische Syndrom. Das Metabolische Syndrom kann mehrere Stoffwechsel-erkrankungen, inklusive Typ 2 Diabetes sowie Atherosklerose, einschließen. Beide Störungen werden durch einen Entzündungsprozess hervorgerufen. Durch die Ausschüttung pro-inflammatorischer Chemokine migrieren die Monozyten zu der Entzündungsstelle, wandern anschließend ins entzündliche Gewebe ein und differenzieren zu Makrophagen. Makrophagen gehören zu Immunzellen des angeborenen Immunsystems und entfernen während jedes entzündlichen Krankheitsverlaufs apoptotische und immunsystemfremde Körper aus dem Gewebe mittels Phagozytose und aktivieren das adaptive Immunsystem durch Zytokin-Ausschüttung. Der Lipidmetabolismus spielt bei diesen Prozessen eine große Rolle. Aus diesem Grund sind die Untersuchungen des Lipidstoffwechselwegs in Makrophagen notwendig, um neue Therapien entwickeln zu können.

Das Überangebot an Nahrung im Organismus führt zu einer Überproduktion von Triglycerid-reichen *very low-density lipoprotein* (VLDL) Partikeln im Blut, was schließlich zu einer Entwicklung der Insulinresistenz und dem Typ 2 Diabetes beitragen kann. Typ 2 Diabetes stellt gleichzeitig einen Risikofaktor für eine Atheroskleroseerkrankung dar und sollte deswegen möglichst früh erkannt und therapiert werden. Als ein vielversprechendes therapeutisches Zielmolekül bei der Behandlung des Typ 2 Diabetes, und des damit assoziierten Metabolischen Syndroms, ist die AMP-aktivierte Proteinkinase (AMPK) mehrfach beschrieben. Zudem ist bereits eine große Wirkung auf die Fettreduktion und Aktivierung der Fettsäure-Oxidation (FAO) durch einen ubiquitär-exprimierenden Transkriptionsfaktor Peroxisom-Proliferator-aktivierten Rezeptor δ (PPARδ) in vorklinischen Studien sowie in klinischen Studien der Phase II gezeigt. In Skelettmuskeln wurde die Zusammenwirkung von beiden Proteinen schon beobachtet. Aufgrund der großen Bedeutung von humanen Makrophagen, war es für mich von Interesse den Wirkungsmechanismus von AMPK und PPARδ auf zellulärer und molekularer Ebene in diesen Zellen zu untersuchen.

Um den Einfluss von AMPK auf die Stoffwechselwege festzustellen generierte ich eine monozytäre THP-1 Zelllinie, die den AMPKα1 *Knock-down* enthielt. Sowohl auf der mRNA, als auch auf Proteinebene konnte eine Reduktion der AMPKα1-Expression um 93% erreicht

werden. Außerdem gelang mir die Überexpression von AMPKα1 in primären humanen Makrophagen mittels einer lentiviralen Transduktion. In diesem Fall exprimierten die Makrophagen konstitutiv aktive AMPKα1-Untereinheit. Zusätzlich benutzte ich einen allosterischen AMPK-Aktivator A-769662, um die AMPK-Aktivität in Makrophagen pharmakologisch zu modulieren.

Zunächst verfolgte ich das Ziel neue Targets und Wechselwirkungen während gleichzeitiger AMPK- und PPARδ-Aktivierung in primären humanen Makrophagen zu finden. Wissend, dass die PPARδ-Aktivierung heilend in Menschen wirkt, war es spannend neue Einsichten über die Zielgene im Zusammenhang mit der gleichzeitigen AMPK-Aktivierung kennenzulernen. So wurde ein Mikroarray durchgeführt, bei dem die AMPKα1-exprimierenden primären Makrophagen mit dem PPARδ-Agonisten GW501516 stimuliert wurden. Bei der anschließenden Analyse konnten einige neue, aber auch bekannte Gene identifiziert werden, die durch beide Proteine reguliert sind. Die am stärksten hochregulierten Gene waren Pyruvatdehydrogenase 4 (PDK4), Carnitin-Palmitoyltransferase 1a (CPT1a), *fatty acid-binding protein* 4 (FABP4), Perilipin 2 (PLIN2) und Acetyl-CoA-Acyltransferase 2 (ACAA2). Sie alle sind am Lipidabbau oder -transport beteiligt. Die Regulation dieser Gene durch AMPK und PPARδ erfolgte additiv, aber nicht synergistisch. Die kombinierte Aktivierung führte zu einer signifikanten Erhöhung dieser Gene im Vergleich zu den Einzelbehandlungen. Auch die anschließenden Untersuchungen mit dem AMPK-Aktivator A-769662 zeigten die gleichen Ergebnisse wie das Mikroarray. Sie wurden durch quantitative PCR und Western Analyse bestätigt. Diese Tatsache weist darauf hin, dass AMPK die PPARδ Aktivität fördert und die Genexpression zusätzlich steuert. Der am stärksten beeinflusste Stoffwechselweg, der während der Mikroarray-Durchführung gefunden wurde, ist die Fettsäure-Oxidation und die damit verbundenen Wege. Allerdings konnte eine erhöhte Aktivität der Fettsäure-Oxidation nach der Kostimulation mit AMPK und PPARδ in humanen Makrophagen nicht nachgewiesen werden.

Die Lipoproteinlipase (LPL) wandelt die Triglyceride zu freien Fettsäuren im Blutplasma um. Ihre Aktivität wird durch das Protein *angiopoietin-like* 4 (Angptl4) inhibiert, das wiederum durch PPARδ reguliert wird. Im Gegensatz zu den primären Makrophagen kann die humane Leukämie-Zelllinie THP-1 verstärkt Angptl4 produzieren, was zu einer großen LPL-Inhibition führt. In den primären Zellen wird dagegen die Menge an durch LPL gebildeten und von Zellen aufgenommenen freien Fettsäuren kaum durch die PPARδ-Aktivität, sondern

durch die Nahrungsaufnahme und die Konzentration von VLDL Partikeln reguliert. Dabei wird der intrazelluläre Triglyceridspiegel nur durch die Fettsäure-Oxidation verändert. Die Behandlung von Makrophagen mit VLDL führt zu einer sogenannten Schaumzellbildung. Die Experimente an lipidbeladenen Schaumzellen zeigen, dass die PPARδ-Aktivierung signifikant zu einem Triglyceridabbau in primären Makrophagen führt. Dies geschieht vor allem mittels des erhöhten Fettsäureabbaus, um die Immunzellen vor der Lipidtoxizität zu schützen. Interessanterweise verminderte die zusätzlich induzierte AMPK nicht den Triglyceridstand der Schaumzellen.

Die Herunterregulation von PPARδ durch siRNA konnte die PPARδ-Abhängigkeit der Fettsäure-Oxidation-assoziierten Gene bestätigen. In den mit siRNA behandelten Zellen konnte keine PPARδ-Aktivierung durch GW501516 erfolgen. Gleichzeitig verlor A-769662 seine Wirkung während der PPARδ-Reduktion, so dass auf eine AMPK-Wirkung oberhalb des Transkriptionsfaktors PPARδ zu schließen ist.

Im zweiten Teil meiner Arbeit ging ich auf die Grundlagen einer anderen Krankheit ein, der Atheroskerose. Atherosklerose stellt eine Entzündungserkrankung dar, während deren arterielle Plaques durch die Ansammlung von Lipiden, Zelltod und Fibrose entstehen. Diese können schließlich zu einer Verstopfung von Arterien und zu einem Herzinfarkt führen. Bei der Entwicklung von Atherosklerose spielen verschiedene Risikofaktoren, wie zum Beispiel Fettleibigkeit, hoher Blutdruck, deregulierter Fettstoffwechsel im Blut, Diabetes, Insulinresistenz, Rauchen und physische Nichtaktivität, eine große Rolle. Auf zellulärer Ebene tragen Monozyten stark zur Entwicklung von Atherosklerose bei. Sie migrieren ins Gewebe, differenzieren dort zu den Makrophagen und werden zu den Schaumzellen, wenn sie viel Cholesterin und Lipide aufgenommen haben. Im Fall einer ständigen Nahrungsaufnahme lagert sich weiterhin Cholesterin durch den Chylomikron- und den VLDL-Kreislauf im Körper an und bildet zusammen mit den Zellresten wasserunlösliche Plaques. Diese atheroskerotischen Plaques stellen eine Bedrohung für die Gesundheit einerseits durch die Verengung der Blutgefäße, andererseits durch einen immer wieder wiederkehrenden Entzündungsprozess dar. Aus diesem Grund sollte bereits die Initiierung der Atherosklerose verhindert werden. Dies kann zum Beispiel durch einen therapeutischen Ansatz mittels Cholesterin-Export aus den Zellen geschehen. Der Cholesterin-Transporter *ATP-binding cassette transporter* 1 (ABCA1) ist ein wichtiges Zelloberflächenprotein, das einerseits freies Cholesterin aus den Zellen transportiert, andererseits sich positiv auf die anti-entzündliche

Vorgänge auswirkt. Die Untersuchungen des Mechanismus der ABCA1-Regulation in den Makrophagen sind deshalb entscheidend für die Erkennung neuer Therapiemöglichkeiten der Atherosklerose.

Am Anfang der Untersuchungen gab es Hinweise, dass AMPK die ABCA1-Expression in humanen Makrophagen regulieren könnte. Diese Tatsache konnte in meinen weiteren Experimenten nachgewiesen und bestätigt werden. Außerdem konnte ich den eindeutigen Mediator zwischen AMPK und ABCA1 identifizieren: *liver X receptor* α (LXRα). Dieser Transkriptionsfaktor ist für die Regulation der ABCA1-Transkription verantwortlich, wobei im humanen System, im Gegensatz zu Nagerzellen, eine Autoregulation von LXRα vorherrscht. LXRβ und *activating transcription factor* 1 (ATF1) konnten als Regulationsfaktoren von ABCA1 durch meine *Knock-down*-Versuche ausgeschlossen werden. Aber auch PPARs scheinen keinen Einfluss auf die ABCA1-Regulation zu haben. Interessanterweise ist jedoch die LXRα-Expression PPARγ-abhängig. PPARγ wirkt sich allerdings nicht auf die Aktivität von LXRα aus, so dass ABCA1-Expression PPARγ-unabhängig ist. Die erhöhte Aktivität von ABCA1 wies ich während der AMPK-Aktivierung in humanen Makrophage nach. So induziert die aktivierte AMPK die LXRα-Aktivität, die zu der Transkription von ABCA1 führt. Die Reduktion von LXRα-Expression hat damit eine negative Auswirkung, sowohl auf die LXRα-, als auch auf die ABCA1-Traskription und -Translation. Mittels der Luciferase-Experimente zeigte ich, dass LXRα die LXRE-Stelle im ABCA1-Gen für die Transkription benötigt und diese durch die A-769662-Stimulation signifikant verstärkt besetzt wird. Dabei konnte kein LXRα an eine mutierte LXRE-Stelle des ABCA1-Promotors binden. Im Gegensatz dazu führte die Überexpression von LXRα zu einer signifikanten Erhöhung der Luciferase-Aktivität im Vergleich zu nicht-überexprimierenden Zellen. Zusätzlich konnte die Aktivität mit der A-769662-Behandlung gesteigert werden. Im Rahmen des Chromatin-Immunopräzipitation (ChIP)-Experiments bestätigte ich meine vorigen Ergebnisse und zeigte die Bindung von LXRα an den ABCA1-Promotor. Diese Protein-DNA Bindung wurde durch einen AMPK *Knock-down* verhindert und konnte durch eine zusätzliche AMPK-Aktivierung nicht wiederhergestellt werden, was die AMPK-abhängige ABCA1-Regulation beweist.

Um den Mechanismus der Wirkung von AMPK-Aktivierung besser definieren zu können, wollte ich die post-translationale Modifikation von LXRα identifizieren, die für die LXRα-Aktivierung verantwortlich ist. Mit Hilfe von Massenspektrometrie und der spezifischen

Methode von *stable isotope labeling by amino acids in cell culture* (SILAC) ist es mir gelungen eine Modifikation von LXRα während einer 6-stündigen Stimulation mit A-769662 festzustellen. Dabei wurde LXRα überexprimiert, immunopräzipitiert, bei der Coomassie-Analyse durch einen zusätzlichen Western Blot identifiziert, aus dem Gel herausgeschnitten und trypsiniert. Die anschließende Massenspektrometrie-Analyse ergab eine Dephosphorylierung eines Serinrestes an der Stelle 197 oder 198 des LXRα-Proteins. Die Ergebnisse waren bezüglich des Serinrestes nicht eindeutig, wobei es eine starke Tendenz zu Serin 198 gibt. Der Befund einer Dephosphorylierung gibt den Hinweis, dass es sich zwischen AMPK und LXRα um eine Phosphatase oder eine Kinase als Mediator handeln muss. Um diesen Mediator zu identifizieren, müssen weitere Versuche in humanen Makrophagen folgen.

Zusammenfassend zeigt meine Arbeit das Zusammenspiel zwischen AMPK und PPARδ, das sich positiv auf den Fettsäureabbau in humanen Makrophagen auswirkt. Die Aktivierung von PPARδ vermindert in diesem Zusammenhang die Bildung von Schaumzellen, indem Triglyceride abgebaut werden. Diese Beobachtung ist ausschließlich auf die Aktivierung der Fettsäure-Oxidation zurück zu führen. Zudem zeigte ich zum ersten Mal die Regulation von einem wichtigen Cholesterin-Transporter ABCA1 durch AMPK. Als Mediator dient dabei der Transkriptionsfaktor LXRα, der sich auf die LXRE-Stelle des ABCA1-Promotors setzt und anschließend die Expression des Transporters ermöglicht. Wichtig ist auch die Tatsache, dass AMPK LXRα durch eine Dephosphorylierung steuert und es mindestens einen Faktor zwischen den beiden gibt. Dieser Faktor könnte zukünftig identifiziert werden und zum besseren Verständnis der ABCA1-Regulation beitragen. Die Ergebnisse meiner Arbeit könnten als Grundlage für zukünftige neue Therapiebehandlungen von Typ 2 Diabetes und Atherosklerose dienen.

3. Introduction

3.1. Inflammation and macrophages in metabolic diseases

Metabolic syndrome is defined as a cluster of multiple metabolic disorders including insulin resistance, glucose intolerance, dyslipidemia, abdominal obesity, and hypertension[1, 2]. It is associated with an elevated risk of type 2 diabetes mellitus and cardiovascular disease[3-5]. Type 2 diabetes is epidemic disease including features, such as hyperglycemia, hypertension, obesity, hypercoagulability, and insulin resistance[6]. According to National Diabetes Statistics, the number of people with diagnosed and undiagnosed diabetes reached 29.1 million in the United States in 2012[7]. Many factors causing the metabolic syndrome may be corrected by changing the own lifestyle. The major risk factors for cardiovascular disease are cigarette smoking, high blood pressure, and increased cholesterol levels, but also the age and sex play an important role in disease development[8]. However, for most of the affected persons, drug therapies are necessary. Thus, additional research about the most appropriate and individual therapy is needed[9]. In this section I will introduce macrophages and inflammation, as well as the importance of the transcription factors peroxisome proliferator-associated receptor δ (PPARδ) and liver X receptor α (LXRα) in progress of metabolic disease.

3.1.1. Inflammation

Immunity and metabolism are associated and coordinated by common regulatory pathways sometimes claiming the whole body[10]. Pro-inflammatory molecules, such as C-reactive protein (CRP), and pro-inflammatory cytokines are responsible for the development of peripheral vascular disease, myocardial infarction, stroke, and cardiovascular mortality[11-14]. Inflammation plays an important role in the pathogenesis of atherosclerosis and type 2 diabetes[15].

During atherosclerotic process, inflammatory signaling changes the behavior of blood cells at the artery wall and recruits further cells promoting lesion formation[16, 17]. Pro-inflammatory cytokines interleukin (IL)-6 and tumor necrosis factor (TNF) α induce leukocyte recruitment to the endothelium, promote adhesion molecule expression, and increase capillary permeability leading to atherosclerosis[16]. Accumulated cholesterol during atherosclerotic progress is able to induce inflammation through Toll-like receptor-dependent or -independent mechanisms[18, 19].

Inflammation plays also a key role in type 2 diabetes causing decreased insulin sensitivity by infiltration of macrophages which secrete pro-inflammatory cytokines, such as TNFα and IL-6[20, 21]. Thus, insulin resistance is closely associated with chronic inflammation[22]. The pro-inflammatory signaling cascades involve nuclear factor-kappa of activated B cells (NF-κB) and c-Jun N-terminal kinase pathways[21]. Additionally, saturated fatty acids act pro-inflammatory by induction of endoplasmic reticulum (ER) stress or activation of Toll-like receptors[23, 24].

3.1.2. Macrophages

Leukocytes, such as monocytes, are not only critical during processes of injury or infection, but also in the processes of chronic inflammation associated with metabolic overload, e.g. in adipose tissue during obesity[25]. They develop from hematopoietic stem cells in the bone marrow and get attracted to the sites of injury or infection by chemokines secreted by e.g. endothelial cells[26]. Chemokines interact with cognate chemokine receptors on monocytes and promote directional migration[23]. These monocytes differentiate into macrophages[27], which regulate inflammatory processes during initiation and resolution phase[28]. Macrophages are important effector cells of innate immunity[15]. They sense, integrate, and appropriately respond to foreign stimuli or their microenvironment transferring the information to adaptive immunity by different cytokines[1]. Besides, these immune cells perform several functions like host defense, clearance of cellular debris, remodeling of tissues, and regulation of inflammatory processes to restore tissue homeostasis[27] (Figure 1).

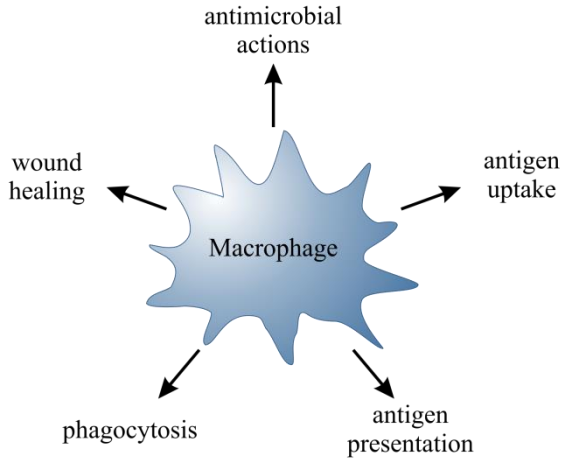

Figure 1: Functional heterogeneity in macrophages.

Macrophages regulate inflammatory processes providing defense against intracellular pathogens by antigen uptake, presentation, and initiating phagocytosis to activate adaptive immunity; by down-regulation of inflammatory responses; and by wound healing.

During the homeostatic adaptations, macrophages exhibit different phenotypes[26]. Bacterial infection results in macrophage activation and production of pro-inflammatory cytokines, such as IL-1β and TNFα, and reactive oxygen species, promoting peripheral insulin resistance to reduce nutrient storage[29]. Described pro-inflammatory or classically activated, M1 phenotype macrophages indeed facilitate the clearance of invading organisms, but they can also damage tissue by secretion of reactive oxygen and nitrogen species[30]. In case of ongoing inflammation, macrophages switch from a resting state to an active state producing host defense factors[10]. Enhanced antigen presentation or phagocytosis of apoptotic cells were shown to suppress an inflammatory response[31]. The alternative activated or, so called, M2 phenotype macrophages are induced by IL-4/IL-13 to achieve inflammatory resolution and tissue repair. They promote anti-inflammatory pathways and increase oxidative phosphorylation. Both phenotypes exhibit not only different functions, but also altered metabolism[32]. M1-like macrophages use glycolysis and oxidative phosphorylation of pyruvate, whereas M2 phenotype relies on high rates of FAO[33].

It is important to understand the phenotypic diversity of macrophages, because they are essential immune cells of many diseases[34] representing attractive therapeutic targets. Significantly, notable differences exist between human and murine macrophages. To bring forward different possibilities of therapy and understanding of dysregulated lipid metabolism pathways in humans, I decided to work with human but not mouse macrophages.

3.1.3. Type 2 diabetes mellitus

Type 2 diabetes mellitus has become a growing and global epidemic disease[6, 7]. Patients with diabetes exhibit elevated pro-inflammatory acting IL-6 and monocyte chemotactic protein 1 (MCP1) expression levels[35]. Not only adipose tissue is affected during diabetes. Liver, pancreatic islets, and muscles develop hyperglycemia, hepatic steatosis, and inflammation, whereupon macrophage population increases recruiting of further immune cells and secreting pro-inflammatory cytokines[36]. Nutrient excess and adiposity contribute to inflammatory signaling, lipotoxicity, ER stress, mitochondrial dysfunction, and finally to decreased insulin sensitivity[37-39]. Also TNFα promoting lipolysis and thus contributing to increased serum free fatty acid concentrations induce insulin resistance development[40].

Native triglyceride (TG)-rich very low-density lipoproteins (VLDL) represent the metabolic precursor of low-density lipoproteins (LDL). VLDL consist of free and esterified cholesterol, phospholipids, apolipoproteins, and TGs, which can be released by lipoprotein

lipase (LPL)[41-43]. The overproduction of VLDL commonly leads to insulin resistance and type 2 diabetes[44]. Thus, new therapeutic options are needed because the current therapies are not able to achieve significant increases of insulin sensitivity[35]. As type 2 diabetes is a common risk factor for the initiation and development of atherosclerosis[45, 46], targeting of an inflammation appears to be an attractive therapeutic approach.

3.1.4. Atherosclerosis

Cholesterol homeostasis is maintained by the movement between the liver and peripheral tissues. Besides, uptake, esterification, hydrolysis, and efflux of cholesterol determine its balance in different tissues[47, 48]. Free cholesterol serves as steroid hormone precursor and controls membrane fluidity, formation of caveolae, and developmental signaling[48]. It can derive from the diet or be endogenously synthesized by the body. Synthetized cholesterol secretes into the blood as VLDL[47]. Elevated cholesterol concentrations in cells and blood lead to a development of atherosclerosis[48], which is a chronic inflammatory disease developing at sites of disrupted laminar flow and arterial branch points by lipid deposition within the vessel wall[49-51].

The progression of atherosclerosis starts with accumulation of LDL or apolipoprotein (apo) B-containing lipoproteins in the subendothelial space, which is accompanied by recruitment of dendritic cells and monocytes[23]. Monocytes selectively attach to certain adhesion molecules on endothelial cells, transmigrate into the vessel wall[52] and its innermost layer, the tunica intima[53], and differentiate into macrophages facilitated by exposure to macrophage colony-stimulating factor (MCSF)[54]. Changes of endothelial permeability and the composition of extracellular matrix beneath the endothelium enhance the entry and retention of cholesterol-containing LDL[55]. Phagocytosis of matrix-retained and aggregated lipoproteins, but also fluid phase pinocytosis of non-retained native LDL by macrophages are involved in the atherosclerotic process[56, 57]. Macrophages ingesting modified and native lipoproteins form cytosolic lipid droplets, resulting in foam cell phenotype defining microscopic appearance of these lipid-laden macrophages. Inside of lipid droplets, free cholesterol gets re-esterified to cholesteryl fatty acid esters by the enzyme acyl-CoA:cholesterol ester transferase (ACAT)[58, 59]. Foam cells secrete pro-inflammatory mediators, such as cytokines IL-1β and TNFα, and matrix remodeling enzymes leading to chronic inflammation inducing the expression of adhesion molecules ICAM-1, -2, and VCAM-1, which in turn promote the migration of recruited leukocytes[60].

The intima of human arteries contains resident smooth muscle cells (SMCs). During the development of early and established atherosclerotic lesions, further SMCs and T cells infiltrate into intima[53]. Macrophages release nitric oxide[61] and matrix metalloproteinases, which degrade the extracellular matrix inducing apoptosis of SMCs[62] and contributing to an advanced state of atherosclerosis[23]. Prolonged ER stress induces unfolded protein response effector CCAAT/enhancer binding protein (C/EBP)-homologous protein (CHOP) causing macrophage apoptosis[63]. The progresses of inflammation, apoptosis as well as decreased efferocytosis of apoptotic cells, contribute to the formation of vulnerable plaques, characterized by lipid-filled necrotic core with thin fibrous cap[23, 53]. In case of plaque rupture a thrombus develops, underlying the pathology of myocardial infarction, sudden cardiac death, and stroke[23] (Figure 2).

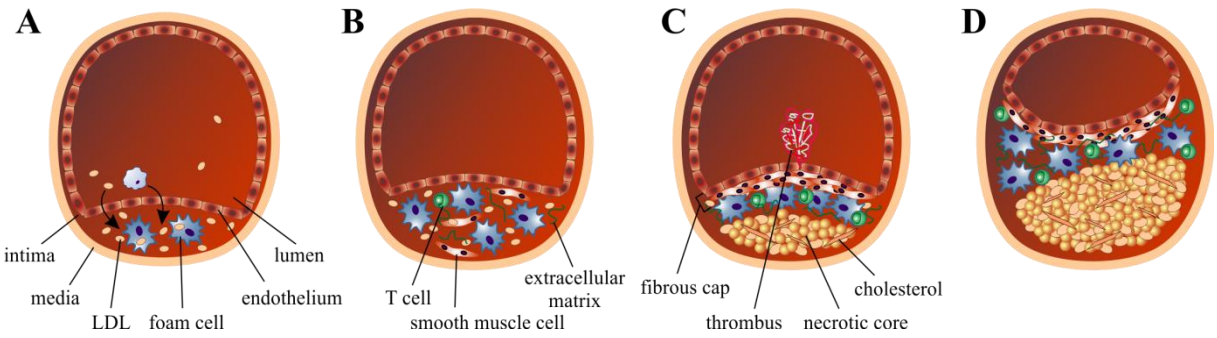

Figure 2: Initiation and progression of atherosclerosis.

Atherosclerosis occurs at sites of arterial walls. **A** Increased concentration of atherogenic lipoproteins, such as LDL or apoB, leads to migration into the intima. After the entry, lipoproteins get enzymatically modified (e.g. oxidized) and aggregate inside of the intimal space. Phagocytosis of these particles by recruited macrophages induces foam cell formation (fatty streak). **B** Recruited vascular smooth muscle cells (SMCs) secrete extracellular matrix components, such as collagen, contributing to retention and accumulation of atherogenic lipoproteins. T cells arrive and promote a state of chronic inflammation. Intermediate lesion grows, whereas the lumen size diminishes. **C** Foam cells die, releasing cellular debris and crystalline cholesterol and inducing plaque formation. SMCs form a fibrous cap beneath the endothelium. Formation of necrotic core leads to recruitment of further immune cells. The generated vulnerable plaque can rupture or the endothelium can erode, resulting in the exposure of thrombogenic material. This process can lead to a blockade of the artery, promoting an acute coronary syndrome or myocardial infarction. **D** The advanced obstructive lesion can encroach on the lumen and cause clinically obstructive disease. Adopted from [44].

The approaches for atherosclerosis therapy are modification of plasma lipoprotein metabolism, and cellular cholesterol metabolism on one side and inhibition of pro-inflammatory pathways, such as blockade of key adhesion molecules, on the other[44, 64]. The most abundant lipoproteins are LDL and high-density lipoprotein (HDL) in plasma. The main

lipid component of both is cholesterol[44]. LDL levels correlate with heightened cardiovascular risk in humans[53], whereas HDL can be anti-inflammatory and promote reverse cholesterol transport (RCT) *in vitro* and *in vivo*[65]. Increased levels of VLDL under conditions of overnutrition might increase the TG content of atherosclerotic plaques[42].

The question arises about a therapy of this epidemic cardiovascular disease. How immune cells interact with each other in the atherosclerotic lesion is poorly understood yet[66]. In my studies I concentrated on the cholesterol signaling in human macrophages to elucidate its role in atherosclerosis and to find a new possibility for treatment.

3.2. Transcription factors in lipid metabolism

Several nuclear factors lie at the nexus between inflammation and lipid metabolism[67]. Nuclear receptors are transcription factors activated by hydrophobic ligands, such as fatty acids, hormones, bile acids or oxysterols[60]. Conformational change of the receptor molecule upon ligand binding leads to the release of co-repressors, such as histone deacetylase (HDAC), and recruitment of co-activators, such as histone acetyl transferase, to regulatory elements of nuclear receptor target genes[68, 69]. The structure of nuclear receptors contains different domains with specific functions. The N-terminal activation function (AF)-1 region is variable and responsible for ligand-independent activation. The highly conserved DNA-binding domain (DBD) contains 2 zinc-finger motifs binding to specific DNA sequences, such as peroxisome proliferator-response element (PPRE) for PPARs or liver X receptor response element (LXRE) for LXRs (Figure 3). PPRE consists of a direct repeat of the consensus binding site 5´-AGGTCA-3´ separated by one nucleotide (DR-1). The DNA binding site of LXRs is LXRE containing 5´-AGGTCA-3´ sequence separated by four nucleotides, called DR4 motif. Response elements appear not only in proximal promoter regions, but also in introns of target genes[47]. The variable hinge domain of nuclear receptors connects DBD and the ligand-binding domain (LBD), which recognizes ligands and leads to dimerization of transcription factor with retinoid X receptor (RXR), and finally to its activation. The C-terminal AF-2 sequence is responsible for ligand-independent transactivation[32,33]. Post-translational modifications of PPAR poorly structured domains affect the transcriptional activity of both AF-1 and AF-2 regions.

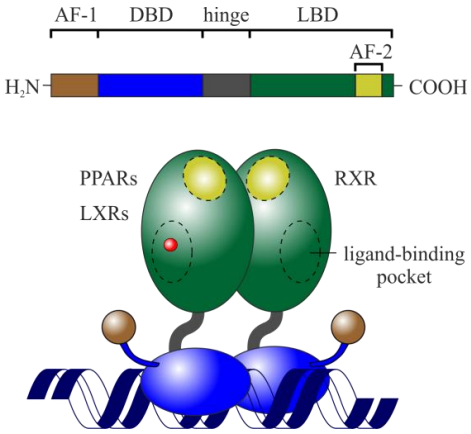

Figure 3: Structure of nuclear receptors dimerizing with RXR.
The colors of two-dimensional structure reflect the same colored domains of three-dimensional, in the bottom shown nuclear receptor structure. Each domain possesses its own function: AF-1 – transcription activation, DBD – DNA-binding domain, hinge – dimerization, LBD – dimerization and ligand-dependent transcription activation. AF, activation function; LBD, ligand-binding domain; PPARs, peroxisome proliferator-associated receptors; LXRs, liver X receptors; RXR, retinoid X receptor. Adopted from [67].

The superfamily of nuclear receptors contains a large number of adopted orphan receptors, e.g. PPARs or LXRs functioning as heterodimers with RXR and regulating metabolism, storage, transport, and degradation of lipids. PPARs and LXRs activate their target genes not only by endogenous or synthetic ligands, but also induce trans-repression of other transcription factors in ligand-dependent manner leading to inhibition of pro-inflammatory pathways[1, 70].

3.2.1. PPARδ - the regulator of lipid metabolism

There are three different PPAR isotypes: PPARα, PPARδ (/PPARβ), and PPARγ, which regulate lipid synthesis, transport, storage, and oxidation[71], sharing ~60% to 80% homology[72]. In addition, they regulate macrophage activation during inflammatory processes or metabolic diseases[27]. The expression and functions of particular PPAR subtype is highly cell type-dependent[73]. PPARα is abundantly expressed in liver and regulates not only fatty acid β-oxidation (FAO) during fasting[74], but also cell proliferation and inflammation[75]. Adipocytes, macrophages, and dendritic cells express PPARγ[76]. This nuclear receptor increases phagocytosis, and supports higher LDL uptake and cholesterol efflux in macrophages. Besides, this PPAR isotype is responsible for the lipid storage, adipocyte functions, and insulin sensitivity in the adipose tissue, and is a major regulator of adipogenesis[77-79]. Transcription factor PPARδ is ubiquitously expressed and influences different fatty acid

metabolism-associated pathways[71, 80]. Its role in carbohydrate metabolism is also investigated, and pathways associated with glycolysis, pentose-phosphate pathway and glycogen metabolism are found down-regulated in PPARδ$^{-/-}$ livers[81]. Mouse models with a myeloid-specific deletion of PPARδ show reduced numbers of alternatively activated macrophages and increased tolerance towards adipose tissue inflammation and insulin resistance[82, 83]. The β-oxidation in white adipose tissue, but also in skeletal muscle and heart is regulated by PPARδ[1, 84]. This transcription factor also controls cell proliferation, differentiation, as well as inflammation. PPARδ is described to prevent obesity by reduction of fat mass and lipid accumulation, energy uncoupling, and activation of FAO *in vivo*[85]. In summary, activated PPARδ possesses inflammation-suppressive, insulin-sensitizing, anti-obesity, and anti-diabetic properties[80, 83, 86–88].

3.2.1.1. Transcriptional regulation by PPARδ

Three different types of transcriptional regulation by PPARs are characterized: type I – ligand-independent repression, type II – ligand-induced activation and/or de-repression, and type III – ligand-independent activation. Types I and II are PPRE-mediated responses[89]. During the ligand-independent repression (type I), a high-affinity complex between PPAR-RXR and nuclear co-repressors forms, which blocks transcriptional activation of PPAR target genes[90]. The binding of the ligand (type II) induces a conformational change leading to a dissociation of co-repressors, binding to PPREs, and recruitment of co-activator proteins for transcriptional initiation[69]. In case of the anti-inflammatory response, the receptor-dependent trans-repression (type III) occurs through interaction with other transcription factors and suppression of their activities[91]. PPARs, but also LXRs, suppress transcription factors including NF-κB, activator protein 1, signal transducers and activators of transcription (STAT), and nuclear factor of activated T cells[70, 91, 92]. This process may be mediated via a direct interaction with other transcription factors, post-translational modification of the mitogen-activated protein kinase cascades, or competition for common co-activators[90].

There are three different anti-inflammatory mechanisms of PPARδ known: interaction with or dissociation of the BCL6 protein, inhibition of NFκB by extracellular signal-regulated kinases (ERK) 1/2 kinase phosphorylation, and induction of anti-inflammatory mediators such as transforming growth factor (TGF) β[86, 93, 94]. Unligated PPARδ interacts with the transcriptional repressor BCL6 preventing NFκB-dependent up-regulation of pro-

inflammatory gene expression, such as of *IL1B, MCP1,* and *matrix metallopeptidase 9*[86, 94-96]. In the absence of ligands PPARδ can also actively suppress its own target genes.

3.2.1.2. Activation of PPARδ

PPARδ can be activated by endogenous fatty acids, TGs, or pharmacological compounds, such as GW501516 possessing EC_{50} of 1.1 nM[97]. Free fatty acids are the primary fuel in mitochondrial oxidation[98]. Attenuation of FAO genes leads to reduced fatty acid utilization[79]. Unsaturated fatty acids can synergize with IL-4 to activate PPARδ target genes, whereas rising saturated fatty acid concentration inhibits PPARδ activity[83]. The treatment of PPARδ with agonist GW501516 has been shown to stimulate FAO in murine skeletal muscle cells *in vitro* and *in vivo*[80]. In adipocytes and hearts from high-fat diet-exposed mice, anti-inflammatory action of GW501516 is found activating PPARδ, preventing lipopolysaccharide (LPS)-induced cytokine expression and activation of NFκB pathway via extracellular signal-regulated kinase 1/2 (ERK1/2) [99, 100].

Several clinical studies were performed using GW501516. PPARδ agonist is described to decrease serum insulin and TGs in primates and partially to correct the hyperinsulinemia[101]. Treatment with GW501516 reduces plasma TG and increased HDL-cholesterol in healthy volunteers[102]. Another study also observes reduction of plasma TG in dyslipidemic men with central obesity during GW501516 application[103]. Clinical phase II trials for dyslipidemia are just running with compound GW501516[104]. In moderately obese men, GW501516 causes weight loss, decrease of plasma TG, total cholesterol, LDL-cholesterol, and hepatic fat content[105].

In macrophages PPARδ serves as a sensor for VLDL. Treatment with VLDL leads to the accumulation of triglycerides, activation of PPARδ, and induction of adipose differentiation-related protein/perilipin 2 (ADRP/PLIN2) associated with lipid droplets as a direct PPARδ target[42, 106, 107] (Figure 4). Another PPARδ target is angiopoietin-like 4 (Angptl4) functioning as an inhibitor of lipoprotein lipase (LPL), which hydrolyzes TG to free fatty acids[108-111]. The inhibition occurs by converting active LPL dimer into inactive monomers[112]. The fatty acid transporter CD36 is another PPARδ target, which itself facilitates an entry of PPARδ ligands inside the cells[113] producing a positive feedback to amplify PPARδ function. Pyruvate dehydrogenase kinase isoenzyme 4 (PDK4) is a prominent PPARδ target which facilitates a stimulation of FAO in mitochondria inhibiting pyruvate dehydrogenase complex and thereby

glucose oxidation[113, 114]. The inhibition of pyruvate conversion into acetyl-CoA by PDK4 causes attenuated synthesis of malonyl-CoA, an inhibitor of FAO[115]. PDK4 can be induced not only by PPARδ agonist[80], but also by fasting[113]. Further PPARδ target genes are identified by using skeletal muscle-specific PPARδ KO mice revealing down-regulation of medium-chain acyl-CoA dehydrogenase (MCAD), carnitine palmitoyltransferase 1a (CPT1a)[116], PPARγ co-activator 1α (PGC1α), and reduced LPL mRNA level to about 56%[117]. PGC1α is a transcriptional co-activator binding to transcription factors, including PPARδ, which increases their activity[85].

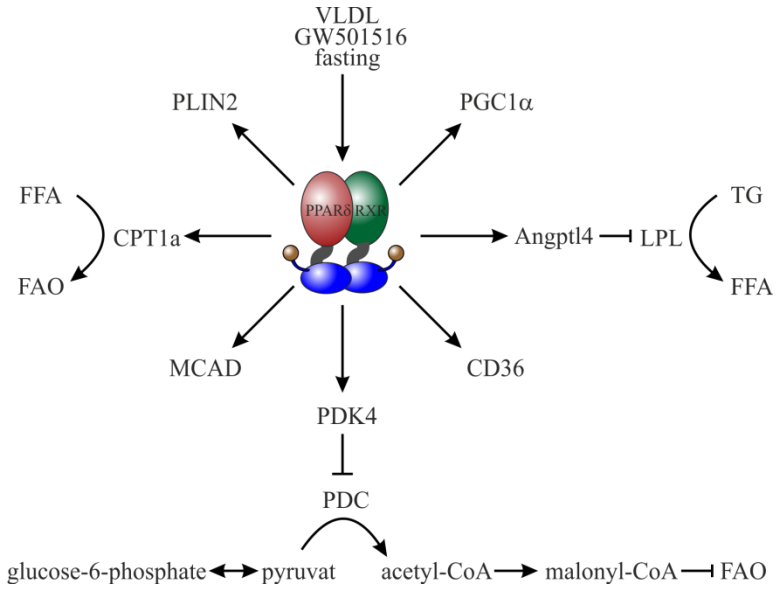

Figure 4: PPARδ signaling regulating lipid metabolism.

PPARδ can be activated by VLDL particles, agonist GW501516 or fasting and leads to an induction of PPARδ target genes involved in different metabolic pathways: fatty acid uptake (CD36), FAO (PDK4, MCAD, CPT1a), lipid droplet formation (PLIN2), lipolysis (Angptl4), and regulation of other transcription factors (PGC1α). PLIN2, perilipin 2; Angptl4, angiopoietin-like 4; LPL, lipoprotein lipase; TG, triglyceride; FFA, free fatty acids; CD36, cluster of differentiation 36; PDK4, pyruvate dehydrogenase kinase, isozyme 4; PDC, pyruvate dehydrogenase complex; FAO, fatty acid oxidation; MCAD, medium-chain acyl-CoA dehydrogenase; CPT1a, carnitine palmitoyltransferase 1a; PGC1α, peroxisome proliferator-activated receptor gamma co-activator 1α.

Summarizing, PPARδ binds different non-esterified and polyunsaturated fatty acids or eicosanoids, which causes transcriptional changes affecting lipid metabolism, FAO, and inflammation[118].

3.2.2. LXRα and ABCA1 - the regulators of cholesterol transport

LXRs are nuclear receptors with a major role in the regulation of cholesterol homeostasis[119], protecting cells from cholesterol overload[47]. LXRs can be activated by endogenous cholesterol derivatives oxysterols, such as 22(R)-hydroxycholesterol, 24(S)-hydroxycholesterol, but also by synthetic agonists, such as T0901317 or GW3965[120]. After the activation LXRs increase expression of genes associated with phagocytosis and cholesterol efflux in macrophages[121]. In addition, LXRs have been described to reduce ER stress acting anti-atherogenic in macrophages[122, 123]. LXRs are also described to act anti-bacterial protecting macrophages from apoptosis[124]. Besides, they control lipid, carbohydrate, and energy metabolism by decreasing dietary cholesterol absorption, increasing cholesterol excretion, as well as enhancing insulin sensitivity, but also insulin secretion[125]. These transcription factors attenuate NFκB-mediated cytokine expression and increase phagocytosis and RCT[125-127]. At the same time, they inhibit the expression of pro-inflammatory genes, such as iNOS, COX-2, and IL-6 after LPS treatment in murine but not human macrophages[127, 128]. In the latter system, they were reported to activate transcription of Toll-like receptor 4 gene, which initiates inflammatory signaling by LPS recognition[127]. Lipoprotein-associated phospholipase A_2 cleaves oxidized phospholipids generating pro-inflammatory and pro-atherogenic products[129]. Our laboratory has shown the up-regulation of cholesterol efflux to apoAI by phospholipase A_2-modified LDL activating LXR[130].

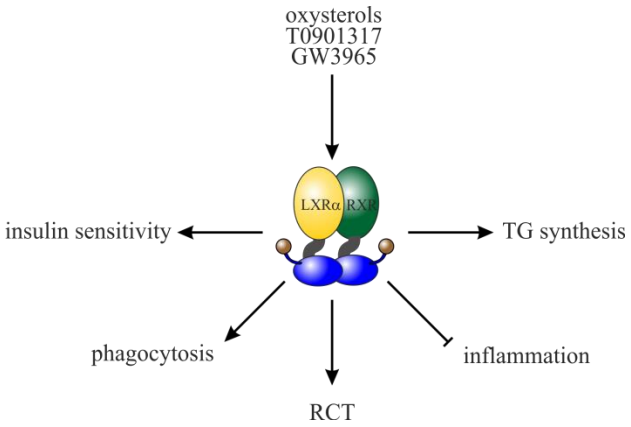

Figure 5: LXRα signaling regulating cholesterol transport.

LXRα can be activated by oxysterols, T0901317 or GW3965 and leads to an induction of TG synthesis, RCT, phagocytosis, and insulin sensitivity, but also to a reduction of inflammatory signaling. TG, triglyceride; RCT, reverse cholesterol transport.

Two different isoforms of LXRs are known: LXRα and LXRβ. Both share 77% sequence homology in their DBD and LBD but possess different expression pattern and functions in

metabolism[126]. LXRβ is ubiquitously expressed, whereas LXRα is mostly abundant in metabolically active tissues[131]. LXRα has been described to predominantly induce TG synthesis in the liver[132, 133]. The human LXRα gene, *NR1H3* is itself a target of LXRα forming autoregulating feedback loop[134, 135].

3.2.2.1. Structure of LXRα

Human LXRα consists of 447 amino acids (AA) possessing several post-translational modification sites for phosphorylation, acetylation, and sumoylation affecting its gene specificity. Two phosphorylation sites and at least one acetylation/sumoylation site of LXRα protein are known: phosphorylation on serine 198 in the hinge region possibly promoting cytoplasmic localization of LXRα[136], phosphorylation on threonine/serine 292/293[126], as well as acetylation on lysine 432 in AF-2 domain. Deacetylation on lysine 432 is mediated by silent information regulator T1 (SIRT1) and causes ubiquitination and degradation of the transcription factor[137]. Possible sumoylation is described on this site, too, allowing transrepression pathway by recruitment of NCoR-silencing mediator of retinoic acid and thyroid hormone receptor (SMRT) co-repressor complex at the pro-inflammatory gene promoters[138]. Besides, the *O*-linked *β-N*-acetylglucosamine (*O*-GlcNAc)-modified sites in the N-terminal region of LXRα protein are proposed in liver[139].

3.2.2.2. ATP-binding cassette transporter A1 (ABCA1)

In macrophages LXRs respond to elevated sterol concentrations and regulate the cholesterol efflux to HDL particles and RCT transferring cholesterol from peripheral tissues to the liver by the control of ATP-binding cassette transporter A1 (ABCA1), ABCG1 as well as apoE expression[131, 140-143]. ABCA1 plays a key role during atherosclerosis resolving atherogenic plaques by mediation of cholesterol efflux.

ABCA1 belongs to a superfamily of transporter proteins, which binds and hydrolyzes ATP to mediate the translocation of phospholipids to free apoAI-HDL at the plasma membrane[144, 145]. This transporter is abundantly expressed in liver, intestine, placenta, adipose, spleen, endothelium, adrenal gland and macrophages, and serves as the rate-limiting enzyme of RCT[146, 147]. The gene of ABCA1 contains 49 exons and expresses 220 kDa protein[148-150]. Its regulation occurs on both transcriptional and post-transcriptional levels[151]. After its synthesis, dimerized ABCA1 can be post-transcriptionally modified regulating its stability and is transferred to the plasma membrane[152]. Unlike fatty acids, cholesterol cannot be degraded to

acetyl-CoA, and should be transported from tissues to the liver by HDL particles[153, 154]. This regulation of RCT by LXRα and ABCA1 in human body is explained in Figure 6. The induction of cholesterol efflux by ABCA1 occurs directly by translocation of phospholipids and cholesterol to nascent HDL particles[145], and indirectly by changing of HDL phospholipid content forming a complex with apoAI[155]. The overproduction of apoAI is described to attenuate atherosclerosis in mice[64], which is confirmed by similar effect in humans[156, 157].

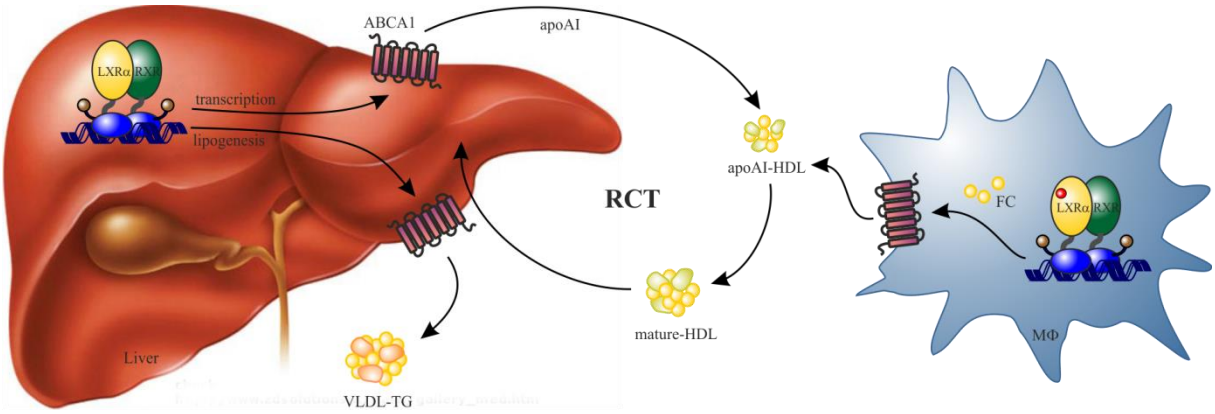

Figure 6: Regulation of RCT by ABCA1.

LXRα increases the expression of cholesterol transporter ABCA1 in liver and promotes the transport of apoAI to generate apoAI-HDL. In macrophages LXRα induces ABCA1 expression, too. ABCA1 transports free cholesterol to lipid-poor apoAI-HDL increasing RCT from macrophages. Mature HDL is transported to the liver (via SR-B1) where LXRα promotes the excretion of cholesterol to VLDL-TG and conversion to bile acids by secretion to the bile duct. apoAI, apolipoprotein AI; FC, free cholesterol; HDL, high-density lipoprotein; RCT, reverse cholesterol transport; VLDL, very low-density lipoprotein.

The free cholesterol accumulation inside the cells can be prevented by up-regulation of ABCA1 protein and elevated cholesterol efflux. Thus, *Abca1*$^{-/-}$ mice exhibit 23% more free cholesterol in isolated lipid rafts and show increased pro-inflammatory response after LPS stimulation than the WT mice[158, 159]. Additional study confirms these results showing an elevation of esterified cholesterol and pro-inflammatory response in macrophages in ABCA1 KO mice[160]. ABCA1-deficient mice reveal elevated numbers of circulating monocytes, which may contribute to increased atherosclerosis[161]. Combined deficiency of ABCA1 and ABCG1 leads to foam cell accumulation and development of atherosclerosis in mice[162]. On the contrary, the overexpression of ABCA1 reduces total cholesterol levels and atherosclerosis *in vivo*[163, 164]. Besides, ABCA1 weakens cholesterol interaction with phospholipids and destroys the formation of lipid rafts[165].

ABCG1 must be differently regulated as ABCA1. LXRα- and LXRβ-deficient mice show no increase in ABCG1 during the stimulation with endogenous LXR activator oxysterol[141]. Besides, the cholesterol efflux in human macrophages is described to be ABCA1-dependent, but ABCG1-independent[166, 167].

There is a link between the inflammation and ABCA1 regulation. Pro-atherogenic cytokines IFNγ and IL-1β, as well as TNFα are shown to down-regulate ABCA1 expression and its activity[168-170]. Bidirectional negative cross-talk between the transcription factors STAT1 and LXRα has an impact on ABCA1-mediated cholesterol efflux[171]. In human macrophages ABCA1 expression is reduced by C-reactive protein and cyclooxygenase-2, which are considered as endovascular inflammation markers[172, 173]. In contrast, Ma *et.al.* postulates the key role of ABCA1 not only in cholesterol efflux regulation, but also activating protein kinase A by cAMP, suppressing pro-inflammatory and enhancing anti-inflammatory cytokine production, like of IL-10 in murine macrophages. Anti-inflammatory cytokines IL-10 (via STAT3) and TGFβ are described to induce a transcription of ABCA1[174, 175]. These processes support the transition of macrophages toward M2 phenotype and facilitate the resolution of inflammation.

3.2.3. Regulation of cholesterol homeostasis by transcription factors

The clearance of apoptotic cells by macrophages delivers fatty acids and oxysterols inducing transcription factors PPARδ and LXRα. PPARδ and LXRα are involved in lipid metabolism regulating fatty acid oxidation and RCT in macrophages[67]. Both nuclear receptors enhance the release of IL-10, leading to attenuation of IL-12 and TNFα secretion and inhibition of inflammatory response[176, 177].

It has been described that PPARγ induces LXRα, which increases the ABCA1 expression and cholesterol efflux[178, 179]. In addition, PPARδ is shown to up-regulate the expression of ABCA1 and cholesterol efflux, too, in human macrophages, fibroblasts, and intestinal cells[101]. Besides, lipid accumulation and suppression of cholesterol efflux are demonstrated during the PPARδ activation in human THP-1 macrophages[180]. GW501516 has an anti-atherogenic impact in humans increasing HDL-cholesterol and decreasing LDL-cholesterol levels in the blood plasma[181]. In contrast, in murine macrophages no effects of either PPARδ depletion or ligands on cholesterol efflux are observed[86, 182]. However, other studies found benefitial

effects of PPARδ activation murine atherosclerotic models, investigating development of inflammatory atherosclerosis progress[94, 182, 183].

Increased ABCA1 expression and cholesterol efflux in THP-1 macrophages after LXR activation has been reported several times[166, 184, 185]. The stimulation with T0901317 shows anti-atherosclerotic effects *in vivo* in several independent studies[186, 187]. At the same time, massive TG accumulation in the liver and plasma during T0901317-treatment are found[188]. Deletion of LXR or ABCA1 in macrophages is reported to contribute to acceleration of atherosclerosis development[164, 189], whereas treatment with LXR agonist reduces this process[123]. The macrophages isolated from LXRα$^{-/-}$ mice show reduced ABCA1 mRNA expression in response to T0901317 compared to LXRβ$^{-/-}$ mice[190]. Deficiency of both LXRα and LXRβ leads to foam cell accumulation in aortic lesions[191].

Addressing ABCA1 as therapeutic approach, pathways increasing the expression of this transporter would promote cholesterol efflux, prevent foam cell formation, and inhibit atherosclerosis development[152].

3.3. AMP-activated protein kinase (AMPK)

AMP-activated protein kinase (AMPK) represents a main homeostasis factor in each cell and organism. It exhibits energy-producing, but also anti-inflammatory properties. Its intercalation into different pathways stimulated my interest to investigate its interaction with transcription factors regulating β-oxidation and cholesterol homeostasis, i.e. PPARδ and LXRα. In this section I introduce AMPK as a protein influencing important metabolic pathways.

3.3.1. AMPK structure

AMPK is a highly conserved heterotrimeric serine/threonine kinase, which is expressed in all eukaryotic cells regulating energy homeostasis of the whole body. AMPK serves as a sensor activating catabolic pathways and inhibiting ATP-consuming processes, such as lipid and protein biosynthesis or cell-cycle[192, 193]. AMPK heterotrimer consists of a catalytic α-subunit (63 kDa) and a regulatory β- and γ-subunits (38 and 35 kDa). The catalytic α-subunit exposes kinase activity and contains an auto-inhibitory domain, whereas the β-domain binds AMP and glycogen. AMPKα also contains a conserved threonine residue (Thr172 in rat α2 or Thr198 in human genome), which, when phosphorylated, increases catalytic activity about 6-

fold[194]. The N-terminus of γ-subunit consists of 4 CBS motifs binding AMP, or with lower affinity ATP, and acting cooperatively. There are 12 possible heterotrimetic combinations of AMPK consisting of different subunit isoforms: α1 or α2, β1 or β2, and γ1-3[195]. Mammalian AMPKγ has 3 AMP binding sites: one – non-exchangeable and two competing with magnesium-ATP[196]. The binding of the cellular AMP to the sites 3 (and 4) of the γ-subunit causes allosterical conformational changes in the whole AMPK protein[197, 198], but also protects phosphorylated Thr172 from the dephosphorylation by protein phosphatase 2C[200,201].

Thr172 can be phosphorylated in most cells by the tumor suppressor liver kinase B1 (LKB1) leading to AMPK activation[*199, 200*]. LKB1 is the major kinase phosphorylating AMPK in worms, flies, and mice[201]. Another prominent upstream kinase of AMPK is Ca^{2+}-activated calmodulin-dependent protein kinase kinase β, which also mediates Thr172 phosphorylation[202]. Physiological stress and related pathways, such as glucose starvation, metabolic stress, and hormones, can activate AMPK increasing AMP concentration[195]. A mutation of threonine to aspartic acid residue (T172D) mimics AMPK phosphorylation and increases its activity making AMPK almost insensitive to protein phosphatase treatment[203]. Besides, deletion of an auto-inhibitory domain (313-392 AA) inside the α-subunit increases the kinase activity[204].

3.3.2. AMPK activators

Besides endogenous factors, many synthetic activators can stimulate AMPK. The most investigated AMPK activators are 5-aminoimidazole-4-carboxamide ribonucleotide (AICAR), metformin, phenformin, berberine, salicylate, and A-769662.

AICAR is taken up by adenosine transporters into the cells[205], where it gets phosphorylated by adenosine kinase to the monophosphorylated ribotide 5-aminoimidazole-4-carboxamide ribonucleoside mimicking AMP, albeit 6-fold less potently than AMP itself[194]. AICAR acts anti-inflammatory inhibiting LPS-induced TNFα production in macrophages[206]. Reduction of adiposity is observed during AMPK activation by AICAR in male rats[207]. Some off-target effects of AICAR are shown including AMPK-independent activation of glycogen phosphorylase[208] and inhibition of fructose-1,6-bisphosphatase[209], blocking complex I of the respiratory chain[210], and finally leading to elevated AMP/ATP ratio[202]. Also AMPK-independent anti-inflammatory effects are ascribed to AICAR attenuating NFκB signaling[211].

Metformin is an oral biguanide anti-diabetic drug and is most widely used therapeutic for type 2 diabetes treatment improving insulin sensitivity[212]. Metformin use is also associated with a reduced risk of cancer development[213]. This drug significantly decreases TG and cholesterol content in human hepatoma cells[214]. Another biguanide AMPK activator, phenformin, inhibits glucagon-induced cAMP accumulation[215] and induces lactic acidosis[216]. Metformin and phenformin act both by inhibiting complex I of respiratory chain, indirectly activating AMPK by increased AMP concentration[217-219]. Both drugs show no effect on AMPK in cell-free assays[220].

Berberine is an isoquinolone alkaloid of plant origin and is used in traditional Chinese medicine[221]. It is reported to have anti-diabetic[222], anti-inflammatory[223], and anti-atherogenic properties[224-226]. It has been described to activate LXRα transcription inducing ABCA1 expression levels and cholesterol efflux without altering ABCG1 in THP-1 macrophages[225]. Berberine also acts indirectly on AMPK by inhibiting the respiratory chain and increasing the AMP amounts in the cell[217].

Salicylate and its derivatives are discovered as a plant hormones produced in case of fungal or bacterial infection[227], thus acting anti-inflammatory[228]. Salicylate has been recently found to allosterically activate AMPK, binding to the same site as A-769662[227].

An AMPK activator A-769662 is discovered during a high-throughput screen and is described to directly bind to AMPK at a site different from AMP in a reversible fashion with EC_{50}=800 nM[229]. Binding of A-769662 specifically requires AMPK β1-subunit and allosterically activates AMPK, at the same time inhibiting dephosphorylation of Thr172[227, 230] without displacing AMP from the γ-subunit[231]. A-769662 is shown to act directly on AMPK, without inducing neither cellular stress, nor toxicity, nor altering of the AMP/ATP ratio in primary rat hepatocytes[229]. The ACC phosphorylation seems to be AMPK-dependent during A-769662 stimulation. Importantly, hardly additional phosphorylation at Thr172 can be observed after treatment with A-769662 in primary mouse hepatocytes, muscle cells, and embryonic fibroblasts. In *ob/ob* mice, this activator leads to a reduction of weight gain, plasma glucose, and TG, as well as to attenuated expression of gluconeogenic enzymes phosphoenolpyruvate carboxykinase and glucose-6-phosphatase, and lipogenic enzyme fatty acid synthase[229].

3.3.3. AMPK regulates energy homeostasis

At the cellular level, AMPK plays a key role as an energy sensor and regulator inhibiting ATP-consuming pathways, e.g. fatty acid and cholesterol synthesis, as well as gluconeogenesis, and stimulating ATP-generating processes, such as fatty acid oxidation (FAO), lipolysis, and glycolysis[232, 233]. The phosphorylation target consensus sequence of AMPK substrate is XΦXXΦXXXΦXXβΦβXXXSXXXΦ[1] [234, 235]. There are many AMPK targets: ACC, 3-hydroxy-3-methylglutaryl-coenzyme A (HMG-CoA) reductase[196], glucose transporter 4[236], glycogen synthase[237, 238], creatine kinase[239], mechanistic target of rapamycin (mTOR) complex subunits tuberous sclerosis complex 2[240], as well as Raptor[241]. Inhibition of mTOR by AMPK leads to inability of cell to grow and proliferate[195, 242] indicating the role of AMPK as metabolic checkpoint[243,244]. AMPK causes efficient G2/M cell cycle arrest and therefore prevention of apoptosis[241]. In contrast, another study shows enhanced cell proliferation during the AMPK activation[243].

In lipid metabolism AMPK activation accomplishes the phosphorylation of ACC at Ser79 resulting in its inhibition[244]. The rate-limiting step for β-oxidation of long-chain fatty acids is their transport into the mitochondrial matrix via CPT1[245]. Malonyl-CoA is a product of ACC which attenuates the activity of CPT1. In addition to ACC, activated AMPK phosphorylates and activates malonyl-CoA decarboxylase[246]. Thus, the phosphorylation of both proteins by AMPK leads to CPT1 activation and finally to increased FAO in liver, heart, and skeletal muscle[247-249].

Anti-inflammatory effects attributed to AMPKα1 are suggested to involve NAD^+-dependent deacetylase sirtuin 1 (SIRT1) as a major mediator in macrophages. Here, AMPK inhibits LPS- and free fatty acid (FFA)-induced inflammation by NFκB inactivation through elevated SIRT1 activity[250, 251]. On the other hand, AMPK KD increases pro-inflammatory response in macrophages[251].

AMPK also changes metabolism of immune cells. Thus, AMPK increases the 6-phosphofructo-2-kinase activity in monocytes, elevating concentration of fructose-2,6-bisphosphate and allowing cells to generate ATP, even under hypoxic conditions[252]. Dendritic cells (DC) regulate innate and adaptive immunity switching to a mature state. This metabolic reprogramming is dependent also on AMPK, acting antagonizing on DC activation[253].

[1] Φ - hydrophobic residue (AA: M, L, F, I or V); β - basic residue (AA: R, K or H); S – phosphorylated S

Deletion of AMPKβ in mice results in reduced AMPK activity, ACC phosphorylation, and mitochondrial content, leading to attenuation of FAO in macrophages. In addition, inflammatory pathways and insulin resistance are activated in these animals[254]. The kinase Fyn is described to inhibit AMPK activation leading to attenuated FAO[255].

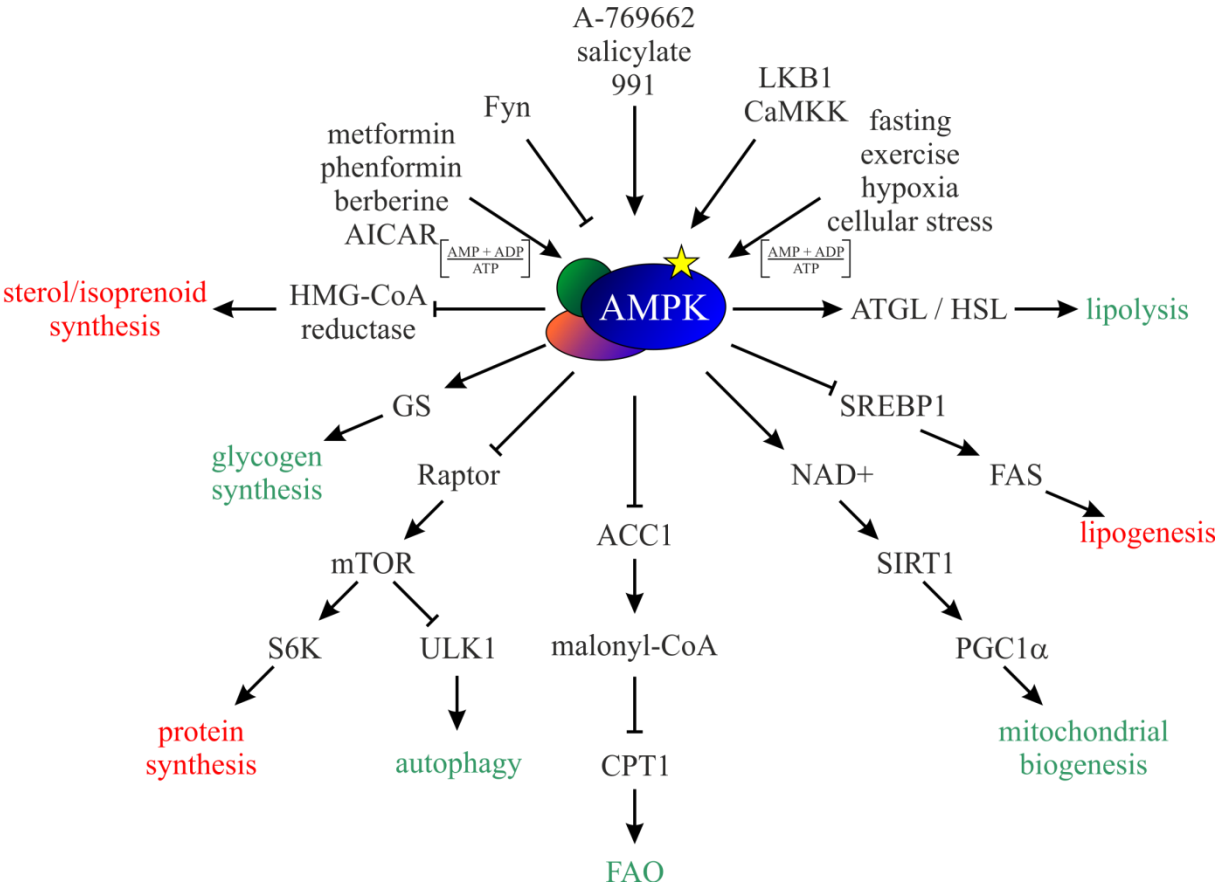

Figure 7: AMPK activation and signaling.

Pharmacological drugs, such as metformin, phenformin, berberine, or AICAR, but also endogenous metabolic pathways, e.g. fasting, exercise, hypoxia, or another cellular stress, can activate AMPK by inhibiting mitochondrial function and thus increasing AMP or ADP concentration. Upstream kinases LKB1 and CaMKK and drugs bind allosterically directly to AMPK stimulating its activity by promoting phosphorylation and by inhibiting dephosphorylation. Fyn kinase acts as AMPK antagonist impairing FAO pathway. Once activated, AMPK activates catabolic pathways (green text), such as lipolysis, FAO, autophagy, and glycogen synthesis, and inhibits anabolic processes (red text), such as lipogenesis, protein synthesis, sterol/isoprenoid synthesis. ACC, acetyl-CoA carboxylase; ATGL, adipose triglyceride lipase; CaMKK, Ca^{2+}/calmodulin-dependent protein kinase kinase; FAS, fatty acid synthase; GS, glycogen synthase; HSL, hormone-sensitive lipase; LKB, liver kinase B; NAD^{+}, nicotinamid adenine dinucleotide; PGC1α, peroxisome proliferator-activated receptor gamma, co-activator 1 alpha; S6K, S6 kinase; SIRT, situin; SREBP, sterol regulatory element-binding protein; ULK, unc-51 like autophagy activating kinase.

AMPK activation can lead to elevated glucose uptake in muscle[248], reduced gluconeogenesis in liver[256], increased FAO in muscle and liver[247], decreased fatty acid synthesis in liver and adipose tissue[194], and enhanced mitochondrial biogenesis[257]. Stimulated AMPK is also shown to reduce aortic lesions *in vivo*. Here, AMPK enhances an expression of mitochondrial transporter uncoupled protein-2 (UCP2), which is responsible for inhibition of oxidative stress and vascular inflammation[258], attenuating atherosclerotic plaque development[259]. As AMPK is proposed as a promising target for treatment of type 2 diabetes, the metabolic syndrome[260], but also inflammatory diseases such as atherosclerosis[254], we need better understanding of its molecular actions, particularly in the cells of the immune system.

3.4. Aims of the study

The metabolic syndrome and associated diseases like type 2 diabetes, obesity, hypertension, and atherosclerosis represent high health risks worldwide. Each of these syndromes is connected to impaired lipid metabolism resulting in increased cardiovascular dysfunction[229].

AMPK is a key regulator of fatty acid as well as glucose homeostasis and serves as an attractive target for treatment of mentioned diseases[261]. In skeletal muscle the AMPK-PPARδ interaction is previously described to increase training adaptation and stimulate PPARδ-dependent oxidative genes[262]. Additional study reports on the interaction between AMPK and PPARδ proposing the AMPK modulation by GW501516 via increase of AMP/ATP ratio in human skeletal muscle[263]. In conclusion, many studies are performed in skeletal muscle cells and adipocytes, which investigate the impact of AMPK and/or PPARδ on FAO and transport, but not much is known about their effects in other cells. The first part of my studies asks the question, if AMPK and PPARδ act together on lipid metabolism or have another impact in primary human macrophages. Therefore, overexpression of AMPKα1 with the simultaneous PPARδ activation in macrophages, isolation of the whole cell RNA, and a whole-genome microarray were performed. Subsequently, gene and pathway analysis, as well as validation followed.

Due to the increased consumption of dietary fats (cholesterol and fatty acids), the prevalence of type II diabetes mellitus and atherosclerosis in Western societies rises. A new approach for atherosclerosis therapy is needed. To better understand the pathogenesis of this disease, molecular mechanism should be explored. Two fundamental hallmarks of

atherosclerosis are known: cholesterol accumulation and inflammation[165]. Both can be prevented by one cholesterol transporter, ABCA1. Increase of ABCA1 expression might be a promising therapeutic drug for atherosclerosis treatment in the future. The second part of my studies consisted in analysis of ABCA1 regulation by AMPK, which leads to increased cholesterol efflux in human macrophages. In this setting, I investigated the AMPK effects on ABCA1 mRNA and protein expression levels, including the regulation of the mediator LXRα. To assure the involvement of LXRα, luciferase assays and ChIP experiments were performed. Using mass spectrometry (MS) method of stable isotope labeling by amino acids in cell culture (SILAC), I tried to find the post-translational modification of LXRα by AMPK.

4. Materials and methods

4.1. Materials

4.1.1. Chemicals, reagents, and kits

All chemicals were of the highest grade of purity. Used chemicals, reagents and kits are listed in Table 1 and 2.

Table 1: Chemicals and reagents

Chemical/reagent	Provider
2-Propanol	Carl Roth GmbH, Karlsruhe
5x Passive lysis buffer	Promega GmbH, Mannheim
Acid washed glass beads	Stratagene, Heidelberg
Agarose	PeqLab Biotechnologie GmbH, Erlangen
Ammonium persulfat (APS)	Merck, Darmstadt
Ampicillin/kanamycin	Carl Roth GmbH, Karlsruhe
Bovine serum albumin (BSA)	Sigma-Aldrich, Deisenhofen
β-Mercaptoethanol	Carl Roth GmbH, Karlsruhe
Calcium chloride	Sigma-Aldrich, Steinheim
CD14 microbeads (human)	Miltenyi Biotec GmbH, Bergisch-Gladbach
Coelentrazine	Promega GmbH, Mannheim
Columbia Agar	Hypha Diagnostica, Heidelberg
cOmplete, EDTA-free protease inhibitor cocktail tablets	Roche, Basel, Switzerland
Deoxynucleotide Solution Mix (dNTPs)	New England Biolabs, Frankfurt am Main
Diethyl pyrocarbonate (DEPC)	AppliChem GmbH, Darmstadt
Dimethylsulfoxide (DMSO)	Carl Roth GmbH, Karlsruhe
DNA sample buffer (6x)	Fermentas, St. Leon-Rot
DNAse 1	Promega GmbH, Mannheim
Ethanol	Sigma-Aldrich, Steinheim
Ethidiumbromid, UltraPure™ (10 mg/ml)	Invitrogen™, Darmstadt
Ethylenediaminetetraacetic acid (EDTA)	AppliChem GmbH, Darmstadt
GeneRuler™	Fermentas, St. Leon-Rot
Glycerin	Carl Roth GmbH, Karlsruhe

Glycine	Merck, Darmstadt
HEPES	Sigma-Aldrich, Steinheim
Hiperfect	Qiagen GmbH, Hilden
jetPEI® macrophage, transfection reagent	Polyplus transfection™, Darmstadt
JetPrime transfection reagent	PeqLab Biotechnologie GmbH, Erlangen
Lenti-X™ concentrator	Clontech, Saint-Germain-en-Laye
Lipofectamine™ 2000 Transfection Reagent	Invitrogen, Karlsruhe
Lithiumchlorid	Calbiochem/Merck, Darmstadt
Maxima SYBR Green qPCR master mixes	Thermo Fisher Scientific, Langenselbold
NEB-Puffer 1-4	New England Biolabs, Frankfurt am Main
Nonidet P-40 (nonyl phenoxylpolyethoxylethanol)	ICN Biomedicals GmbH, Eschwege
peqGOLD RNAPure™	PeqLab Biotechnologie GmbH, Erlangen
PfuUltra polymerase	Agilent Technologies, Böblingen
Potassium chloride (KCl)	Merck, Darmstadt
Potassium hydroxide (KOH)	Merck, Darmstadt
Protease inhibitor mix	Roche, Basel, Switzerland
Protease-Inhibitor-Mischung (25x), EDTA-free	Roche, Basel, Switzerland
Protein A/G PLUS-Agarose beads	Santa-Cruz Biotechnology, Heidelberg
Proteinase K	New England Biolabs, Frankfurt
Recombinant human MCSF	ImmunoTools GmbH, Friesoythe
Recombinant proteinase K	Roche, Basel, Switzerland
RNase A (100 µg/µl)	Qiagen GmbH, Hilden
Rotiphorese® Gel 30 (37.5:1); acrylamide bisacrylamid	Carl Roth GmbH, Karlsruhe
Salmon sperm DNA (10 g/l)	Invitrogen™, Darmstadt
Salzsäure (HCl)	Merck, Darmstadt
Sepharose Cl-4 beads	Sigma-Aldrich, Steinheim
Sodium chloride (NaCl)	Sigma-Aldrich, Steinheim
Sodium deoxycholate	Sigma-Aldrich, Deisenhofen

Sodium dodecyl sulfat (SDS)	Carl Roth GmbH, Karlsruhe
Sodium hydrogen carbonate	Merck, Darmstadt
Tetramethylethylendiamin (TEMED)	Merck, Darmstadt
Triglyceride reagent	Roche, Basel, Switzerland
Tris/HCl	AppliChem GmbH, Darmstadt
Triton-X 100	Sigma-Aldrich, Steinheim
Tween®-20	Merck, Darmstadt

Table 2: Used kits

Kit	Provider
Amplex red cholesterol assay kit	Invitrogen™, Darmstadt
DC Protein Assay Kit	Bio-Rad Laboratories GmbH, Munich
Maxima first strand cDNA synthesis kit	Fermentas, St. Leon-Rot
NucleoBond® Xtra Mini/Maxi kit	Machery-Nagel GmbH, Düren
QIAquick PCR purification kit	Qiagen GmbH, Hilden
RNeasy MinElute Cleanup Kit	Qiagen GmbH, Hilden
RNeasy total RNA cleanup kit	Qiagen GmbH, Hilden
Triglyceride determination kit	Roche, Basel, Switzerland

4.1.2. Media, solutions and buffers

Buffers and solutions were prepared with deionized water from a Millipore filter system. Growing media and buffers were sterile filtered and autoclaved for 20 min at 121°C and 2 bar. The cell culture media were kept at 4°C, whereas buffers at room temperature (RT).

Table 3: Growing media for cell and molecular biology

Medium	Provider
RPMI 1640	PAA Laboratories, Cölbe
RPMI 1640 – no phenol red	Gibco, Darmstadt
LB medium	Carl Roth, Karlsruhe
Macrophage SFM	Life Technologies™, Darmstadt
Modified Eagle Medium (MEM)	Gibco, Darmstadt
Lymphocyte separation media (Ficoll)	Biochrom AG, Berlin
Non-essential amino acids (NEAA)	PAA Laboratories, Cölbe

Sodium pyruvate (100x)	PAA Laboratories, Cölbe
Dulbecco´s Modified Eagle Medium (DMEM), 4.5 g/l or without glucose	Gibco, Darmstadt

Table 4: Buffers for cell biology and biochemistry

Buffer	**Composition**
Leukocyte rinsing buffer	2 mM EDTA in PBS
Leukocyte running buffer	2 mM EDTA 0.5% BSA (w/v) in PBS
NP-40 lysis buffer	50 mM Tris/HCl, pH 8 150 mM NaCl 5 mM EDTA 10 mM NaF 1 mM Na_3VO_4 0.5% NP-40 1 mM PMSF, 1x protease inhibitor cocktail
Renilla buffer	25 mM Tris/HCl, pH 7.5 100 mM NaCl 1 mM calcium chloride
Sample buffer 5x	500 mM Tris/HCl, pH 6.8 25% (v/v) glycerol 10% (w/v) SDS 50% (w/v) Bromphenol blue 50 mM DTT
SDS running buffer (WB) 10x	250 mM Tris 1.92 M glycine 35 mM SDS
SDS-PAGE separating gel (WB)	1.5 M Tris/HCl, pH 8.8 6.5-15% polyacrylamide 1% (w/v) SDS 1% APS 0.1% TEMED

SDS-PAGE stacking gel (WB)	0.5 M Tris/HCl, pH 6.8 4% polyacrylamide 1% (w/v) SDS 1% APS 0.1% TEMED
TAE 50x	2 M Tris/HCl, pH 8 50 mM EDTA 5,7% (w/v) acetic acid
TBS buffer (WB) 10x	100 mM Tris/HCl, pH 7.4 9% (w/v) NaCl
TBST buffer (WB) 1x	100 ml 10x TBS 0.1% (v/v) Tween 20 900 ml H_2O
Blocking buffer (WB)	5% (w/v) milk or BSA powder in 1xTBST
Blotting buffer (WB) 10x	250 mM Tris/HCl, pH 8.3 1,92 M glycine
Blotting buffer (WB) 1x	100 ml 10x blotting buffer 200 ml methanol 700 ml H_2O
Binding buffer	10 mM HEPES/NaOH, pH 7.4 150 mM NaCl 25 mM $CaCl_2$

Table 5: Solutions for cell culture and molecular biology

Solution	**Provider**
Ammonium persulfate (APS) (10% w/v)	Merck, Darmstadt
Biocoll separating solution	Biochrom AG/Merck, Darmstadt
Fetal calf serum (FCS)	PAA Laboratories, Cölbe
Formaldehyd	Sigma-Aldrich, Deisenhofen
L-Glutamin (200 mM)	PAA Laboratories, Pasching, Austria
Nonidet P-40	ICN Biomedicals GmbH, Eschwege
Penicillin/Streptomycin	PAA Laboratories, Cölbe

Phenylmethansulphonylfluorid (PMSF) solution in 2-propanol (200 mM)	Sigma-Aldrich, Deisenhofen
Potassium buffered saline (PBS)	Sigma-Aldrich, Deisenhofen
Triton X-100	Serva GmbH, Heidelberg
Trypsin, 0.05% with EDTA	PAA Laboratories, Cölbe

The chromatin immunoprecipitation (ChIP) experiment was performed using different self-made buffers which are listed in Table 6.

Table 6: Buffers for ChIP experiment

Buffer	Composition
Lysis buffer I	5 mM HEPES/KOH, pH 8 85 mM KCl 0.5% NP-40 fresh: 2 µl per 100 µl PI
Nuclear lysis buffer II = RIPA (also for IP)	10 mM Tris/HCl, pH 7.4 150 mM NaCl 1 mM EDTA 1% NP-40 1% (w/v) sodium deoxycholate 0.1% SDS fresh: 2 µl per 100 µl PI
Wash buffer I	20 mM Tris/HCl, pH 7.4 150 mM NaCl 2 mM EDTA 1% Triton-X 100 0.1% SDS
Wash buffer II	20 mM Tris/HCl, pH 7.4 500 mM NaCl 2 mM EDTA 1% Triton-X 100 0.1% SDS

Wash buffer III	10 mM Tris/HCl, pH 7.4 250 mM LiCl 1 mM EDTA 1% NP-40 1% sodium deoxycholate
Elution buffer, freshly made	100 mM sodium hydrogen carbonate 1% SDS
Reversion mix (42 µl per sample)	16 µl Tris/HCl (1 M), pH 6.8 16 µl NaCl (5 M) 8 µl EDTA (0.5 M) 10 µg / 0.1 µl RNase A (100 µg/µl) 20 µg / 2 µl Proteinase K

The measurement of samples using MS and SILAC occurred by collaboration partners. The media and buffers used here are listed in Table 7.

Table 7: Growing media and buffers for MS and SILAC experiments

Medium/buffer	Composition
Normal medium for SILAC experiment	Unlabeled DMEM (Silantes GmbH) 10% dialysed FCS 2 mM L-glutamine, 200 mg/l L-proline 2 g/l glucose, 1x penicillin/streptomycin 1x $^{12}C^{14}N$-R, 1x ^{12}C-K
SILAC medium	Unlabeled DMEM (Silantes GmbH) 10% dialysed FCS 2 mM L-glutamine, 200 mg/l L-proline 2 g/l glucose, 1x penicillin/streptomycin 1x $^{13}C^{15}N$-R, 1x ^{13}C-K
Fixing buffer	50% methanol in 10% acetic acid 100 mM ammonium acetat
Coomassie buffer	0.025% Coomassie dye in 10% acetic acid
Destaining buffer	10% acetic acid in millipore water
Ammonium bicarbonate (ABC) buffer	50 mM ammonium bicarbonate in chromatography grade H_2O

Chromatography buffer A	4% acetonitrile 0.1% formic acid in chromatography grade H_2O
Chromatography buffer B	80% acetonitrile 0.1% formic acid in chromatography grade H2O
Stage tip buffer A	0.5% formic acid in chromatography grade H2O
Stage tip buffer B	80% acetonitrile 0.5% formic acid in chromatography grade H2O

4.1.3. Oligonukleotides: siRNAs, quantitative PCR and sequencing primers

The siRNAs were purchased by Qiagen GmbH or Dharmacon at the end concentration of 10 pmol/µl. The names of siRNAs are listed in Table 8.

Table 8: siRNAs

siRNA	Provider
Hs_NR1H2_2 FlexiTube (LXRβ) siRNA	Qiagen GmbH, Hilden
Hs_NR1H2_3 FlexiTube (LXRβ) siRNA	Qiagen GmbH, Hilden
Hs_NR1H3_1 FlexiTube (LXRα) siRNA	Qiagen GmbH, Hilden
Hs_NR1H3_7 FlexiTube (LXRα) siRNA	Qiagen GmbH, Hilden
ON-TARGET plus Non-targeting pool (siControl)	Dharmacon, Schwerte
ON-TARGET plus Smartpool human ATF1 siRNA	Dharmacon, Schwerte
ON-TARGET plus Smartpool human PPARα siRNA	Dharmacon, Schwerte
ON-TARGET plus Smartpool human PPARδ siRNA	Dharmacon, Schwerte
ON-TARGET plus Smartpool human PPARγ siRNA	Dharmacon, Schwerte
Smartpool: siGENOME human PRKAA1 (AMPKα) siRNA	Dharmacon, Schwerte

Annealing temperature of primers for RT-PCR was set on 55°C for all primers. All primers were developed targeting human genome. The appropriate primer sequences are listed in Table 9.

Table 9: Primer sequences for RT-PCR

Name	Forward primer	Reverse primer
ABCA1	GCTTTCAATCATCCCCTGAA	TGACAGGCTTCACTCCACTG
ACAA2	GGCCAAGGTATTGCTGTCAT	TTGTGTCACCATGGCTTGAT
ACADVL	GTCCTTTGCTGTGGGAATGT	CAAGTGGTCTCCTCCACCAT
AMPK	GGAGCCTTGATGTGGTAGGA	TTTCATCCAGCCTTCCATTC
Angptl4	GCCTATAGCCTGCAGCTCAC	AGTACTGGCCGTTGAGGTTG
ATF1	GGGACTTCAGACATTAACCA	GTTTGTACGACCACCTGATT
βMG	TCCAAAGATTCAGGTTTACTCA	ATATTAAAAAGCAAGCAAGCAG
CHOP	TGGAAGCCTGGTATGAGGAC	AGGTGCTTGTGACCTCTGCT
CPT1a	TCGTCACCTCTTCTGCCTTT	ACACACCATAGCCGTCATCA
ETFDH	CTCAAACCTACGGGATTGGA	CCGAATGCTAGGATGGTGTT
FABP4	CATACTGGGCCAGGAATTTG	GTGGAAGTGACGCCTTTCAT
FABP5	TCAGCAGCTGGAAGGAAGAT	GCCATCAGCTGTGGTTTCTT
GAPDH	TGCACCACCAACTGCTTAGC	GGCATGGACTGTGGTCATGAG
MCAD	GCTGCAGGGTCCTGAGAAGTA	CTGCAGCCACTGGGATGATT
PDK4	CCTTTGGCTGGTTTTGGTTA	CCTGCTTGGGATACACCAGT
PLIN2	AAGAAAAATGGCATCCGTTG	CAATTTGCGGCTCTAGCTTC
PPARδ	TCACACAGTGGCTTCTGCTC	TCTACAGGGTGGTTCCCATC
SCD1	CGACGTGGCTTTTTCTTCTC	CAAGAAAGTGGCAACGAACA
SMPDL3A	CGAGTCGGAATTTGAGCTTC	GTGAGGCGGAGACAGAAGAC
ZNF366	TGAAGAAGACCCCCTCCTTT	TCTGCAGGGTGGTTATAGGG

Sequences of primers for PCR, ChIP, mutagenesis and sequencing are shown in Table 10 and 11.

Table 10: PCR, ChIP and site-directed mutagenesis primer

Primer name	Sequences in 5´→3´ direction
AMPK1-PCR-for	atgcgcagactcagttcctg
AMPK1-PCR-rev	CGAACAGAGAGAGACCGggcaactgccaaaggatcc
AMPK2-PCR-for	GAGGCAGCAGAGACCGatgcgcagactcagttcctg
AMPK2-PCR-rev	ggcaactgccaaaggatcc
FABP4-PCR-for	ATGTGTGATGCTTTTGTAGGTACCT
FABP4-PCR-rev	TGCTCTCTCATAAACTCTCGTGG
FABP5-PCR-for	ATGGCCACAGTTCAGCAGC
FABP5-PCR-rev	TTCTACTTTTTCATAGATCCGAGTACAG
LXRE in LXRα ChIP-for	ACGTGCTTTCTGCTGAGTGA[264]
LXRE in LXRα ChIP-rev	ACCGAGCGCAGAGGTTACTA[264]
LXRE in SMPDL3A ChIP-for	ACTCTGTGAGTCTTCACACCT
LXRE in SMPDL3A ChIP-rev	CTGAGAGGAGGCAGGAGAGTT
mutAMPK-for	CAGATGGTGAATTTTTAAGAGATAGTTGTGGCTCA-CCCAACTATGC
mutAMPK-rev	GCATAGTTGGGTGAGCCACAACTATCTCTTAAAAA-TTCACCATCTG
mutLXRα-K434Q-rev	CGTCTGCAGGACAAACAGCTCCCACCGCTG
mutLXRα-K434Q-rev	CAGCGGTGGGAGCTGTTTGTCCTGCAGACG
mutLXRα-K434R-for	CGTCTGCAGGACAAAAGACTCCCACCGCTGCTCTC
mutLXRα-K434R-rev	GAGAGCAGCGGTGGGAGTCTTTTGTCCTGCAGACG
mutLXRα-K86Q-for	CAAAAGCGGAAACAGGGGCCAGCCC
mutLXRα-K86Q-rev	GGGCTGGCCCCTGTTTCCGCTTTTG
mutLXRα-S197A-for	CCCCCAGGGCTGCCTCACCCCCCCAAATC
mutLXRα-S197A-rev	GATTTGGGGGGGTGAGGCAGCCCTGGGGG

Table 11: Sequencing primer

Primer name	Sequences in direction 5´→3´
pCDH-AMPK_seq	CTCCACGCTTTGCCTGACCCTGCTT
pGL3_seq1	CTAGCAAAATAGGCTGTCCCCAGTGC
pGL3_seq2	CCT TTCTTTATGTTTTTGGCGTCTTCC
LXR-K86Q_seq	GGCCCCTGTGCCTGACAT
LXR-S197A_seq	GGGCTTCCACTACAATGTTCTG
LXR-K434R/Q_seq	TTCGAGTTCTCCAGGGCC

4.1.4. Plasmids

Cloning vectors were purchased by several providers and are listed in Table 12.

Table 12: Plasmids

Plasmid name	Plasmid property	Provider
Myc-Flag-tagged human NR1H3	Expression vector	OriGene, Frankfurt am Main
pCDH-EF1-MCS-T2A-Puro	Cloning and expression lentivector	SBI System Biosciences, Heidelberg
pGL3-basic	Luciferase reporter vector	Promega GmbH, Mannheim

4.1.5. Self-cloned viral constructs

Some genes like AMPKα1, FABP4 and FABP5 were cloned into the mentioned plasmids (Table 12) using the primers shown in Table 10. The provided LXRα OE plasmid (Myc-Flag-tagged human NR1H3) contained the wildtype gene of LXRα. This and AMPKα1 genes were mutated resulting in new lentiviral constructs which are listed in Table 13.

Table 13: Lentiviral constructs

Target	Procedure
AMPKα1 wildtype OE	Cloning of catalytic AMPK subunit into pCDH-EF1
AMPKα1 mut (T172A) OE	Mutation of vector coding for AMPKα1$^{1-312}$
LXRα mut (K434R) OE	Mutation of vector coding for LXRα
FABP4 OE	Cloning of FABP4 gene into pCDH-EF1
FABP5 OE	Cloning of FABP5 gene into pCDH-EF1

4.1.6. Stimulants and inhibitors

During my dissertation different reagents as stimulants and inhibitors were used and are listed in Table 14.

Table 14: List of stimulants and inhibitors

Reagent	Target	Provider
A-769662	AMPK activator	LC Laboratories, Woburn, USA
Ex527	Selective SIRT1 inhibitor	Selleckchem, Munich
GW501516	PPARδ agonist	Axxora, Lörrach
GW9662	PPARα agonist	Cayman Chemical, Ann Arbor
Human plasma Apolipoprotein AI (apoAI)	Substrate of ABCA1	Merck Millipore, Darmstadt
Modified human acetylated LDL	Stimulant of LXRα	Intracel, Frederick, Maryland
Rosiglitazone	PPARγ agonist	Axxora, Lörrach
VLDL	Stimulant for foam cell formation	Self-made by human plasma ultra-centrifugation

4.1.7. Antibodies

Polyclonal primary antibodies (Table 15) were used in concentration of 1:500 / 1:1000 and 1:3000 in milk or BSA solution in TBST buffer. Secondary antibodies (Table 16) were diluted 1:10000 in milk in TBS buffer.

Table 15: Primary antibodies

Antibody specificity	Organism	Provider
ABCA1 (NB400-105)	rabbit	Novus Biologicals, Heford
AMPKα	rabbit	Cell Signaling, Leiden, The Netherlands
CPT1a	rabbit	Proteintech Europe, Manchester, UK
LXRα	rabbit	Active motif, La Hulpe, Belgium
LXRα	mouse	Abcam, Cambridge, UK
Nucleolin (C23, H-250)	rabbit	Santa Cruz, Heidelberg
PDK4	rabbit	Abcam, Cambridge, UK

pACC (Ser79)	rabbit	Cell Signaling, Leiden, The Netherlands
pAMPKα (Thr172)	rabbit	Cell Signaling, Leiden, The Netherlands
pRaptor (Ser792)	rabbit	Cell Signaling, Leiden, The Netherlands
Polyclonal IgG	rabbit	Merck Millipore, Darmstadt
Polymerase II (N20) X	rabbit	Santa Cruz, Heidelberg
PPARα (H-98) X	rabbit	Santa Cruz, Heidelberg
PPARδ (H-74) X	rabbit	Santa Cruz, Heidelberg
PPARγ (H-100) X	rabbit	Santa Cruz, Heidelberg
Tubulin	mouse	Sigma-Aldrich, Deisenhofen

Table 16: Secondary antibodies

Antibody	**Provider**
anti-mouse IRDye 680	LICOR Biosciences, Bad Homburg
anti-rabbit IRDye 680	LICOR Biosciences, Bad Homburg
anti-rabbit IRDye 800	LICOR Biosciences, Bad Homburg
anti-mouse IRDye 800	LICOR Biosciences, Bad Homburg

4.1.8. Bacteria

Escherichia coli strains were obtained by Agilent Technologies. The appropriate genotypes of XL1-Blue supercompetent cells and XL10-Gold ultracompetent cells are *rec*A1 *end*A1 *gyr*A96 *thi*-1 *hsd*R17 *sup*E44 *rel*A1 *lac* [F´ *pro*AB *lac*I^qZΔM15 Tn*10* (Tet^r)]; F^- *end*A1 *rec*A1; *lac*I^q Δ(*lac*Z)M15 and Tet^r Δ(*mcr*A)183 Δ(*mcr*CB-*hsd*SMR-*mrr*)173 *end*A1 *sup*E44 *thi*-1 *rec*A1 *gyr*A96 *rel*A1 *lac* Hte [F´ *pro*AB *lac*^{q}Z ΔM15 Tn10 (Tet^r) Amy Cam^r].

4.1.9. Cells

Cells were maintained in cell incubator at 37°C, 95% of relative humidity, and 5% CO_2 atmosphere. The whole cell culture work was performed under sterile conditions using a clean bench. Primary monocytes were isolated from human buffy coats of voluntary donors and differentiated by 100 nM TPA for 48 h into macrophages. Cells are listed in Table 17.

Table 17: Cells

Cell name	Cell type characterization
HEK293	Embryonic kidney cell line was generated by transformation with sheared adenovirus 5 DNA (ATCC®-Nummer: CRL-1573™)
HepG2	Human hepatocellular carcinoma cell line; has a rearranged chromosome 1 (ATCC®-Nummer: HB-8065™)
THP-1	Human acute myelomonocytic leukemia cell line; phagocytic suspension cells can differentiate into macrophages with 12-O-tetradecanoylphorbol-13-acetate (TPA) at a final concentration of 100 ng/ml over 48 h (ATCC®-Nummer: TIB-202™)
Primary human monocytes	Buffy coats were obtained from DRK-Blutspendedienst Baden-Württemberg-Hessen, Institut für Transfusionsmedizin und Immunhämatologie, Frankfurt am Main. Monocytes were isolated by Ficoll separation

4.1.10. Consumables

Plastic consumables were used in the cell culture, virology, and biochemistry laboratories and are listed in Table 18.

Table 18: Consumables

Consumable	Provider
BZO seal film	Biozym Scientific GmbH, Hessisch Oldendorf
Cell culture dishes	Sarstedt, Nürnbrecht
CryoTubes™ Nunc	Thermo Fisher Scientific, Langenselbold
Eppendorf cups (0.5 ml, 1.5 ml, 2 ml)	Eppendorf GmbH, Hamburg
Eppendorf cups (0.5 ml, 1.5 ml, 2 ml)	Eppendorf GmbH, Hamburg
Filter paper	Whatman GmbH, Dassel
Filter paper	Whatman, Dassel
Hard-Shell® 96-well PCR plates	Bio-Rad Laboratories GmbH, Munich
Leucosep tubes (15 ml, 50 ml)	Greiner Bio-One GmbH, Frickenhausen

Mr. Frosty 1°C freezing container	Nalgene™ Cryo, Darmstadt
Neubauer improved counting chamber	Labor Optik GmbH, Friedrichsdorf
Nitrocellulose membrane Hybond C extra	Amersham Bioschiences, Freiburg
PicoTip® nanospray emitters	New Objective, Woburn, USA
Pipet tips (10 µl, 100 µl, 1000 µl, 5000 µl)	Eppendorf GmbH, Hamburg
Pipette (5 ml, 10 ml, 25 ml)	Greiner Bio-One GmbH, Frickenhausen
Plastic material in cell culture	Greiner Bio-One, Frickenhausen
Sterile filter (0.22 µm, 0.45 µm)	Millipore GmbH, Schwalbach
Tissue culture dishes	Sarstedt AG&Co, Nürnbrecht
UVette® routine pack 220 nm-1.600 nm	Eppendorf GmbH, Hamburg
Whatman PROTRAN® nitrocellulose membrane	Whatman, Dassel

4.1.11. Instruments and software

During the dissertation certain instruments and software were used, which are listed in Table 19 and 20.

Table 19: Instruments

Instrument	Provider
Apollo-8 LB 912 multiplate reader	Bethold Technologies GmbH&Co.KG, Bad Wildbach
Autoclave Systec DX-200	Systec, Wettenberg
AutoMACS™ separator	Miltenyi Biotec GmbH, Bergisch-Gladbach
AxioVert 200M fluorescence microscope	Carl Zeiss Microlmaging GmbH, Jena
Bacteria clean bench Hera guard	Heraeus GmbH, Hanau
Bacteria incubator B5042	Heraeus GmbH, Hanau
BioSpectrometer kinetic	Eppendorf GmbH, Hamburg
Casy®TT cell counter	Schärfe System, Reutlingen
Centrifuges 5415 R and 5810 R	Eppendorf GmbH, Hamburg
CFX96™ or Connect™ real-time system	Bio-Rad Laboratories GmbH, Munich
FACS LSR II Fortessa mit Software FACSDiva™	Becton Dickinson Biosciences GmbH, Heidelberg
Galaxy mini microcentrifuge C1213	VWR international GmbH, Darmstadt

Gel electrophoresis chamber 40_1214	PeqLab Biotechnologie GmbH, Erlangen
HERAcell incubator	Heraeus, Hanau
HERAsafe clean bench	Heraeus, Hanau
Incubator Shaker Series Innova®44	New Brunswick scientific GmbH, Nürtingen
LabLine orbit shaker	Uniequip GmbH, Martinsried
LTQ Orbitrap XL™ ETD Hybrid Ion Trap-Orbitrap Mass Spectrometer	Thermo Fisher Scientific, Dreieich
Q Exactive™ Hybrid Quadrupole-Orbitrap Mass Spectrometer	Thermo Fisher Scientific, Bremen
Magnetic stirrer combimag RCH	IKA Labortechnik GmbH&Co. KG, Staufen
Magnetic stirrer MR3000	Heidolph Instruments GmbH & Co.KG, Schwabachne
Microscope Axiovert 200M	Zeiss, Göttingen
Mithras LB 940	Bethold Technologies GmbH&Co.KG, Bad Wildbach
NanoDrop ND-1000	PeqLab Biotechnologie GmbH, Erlangen
Odyssey infrared imaging system	Li-COR Biosciences GmbH, Bad Homburg
Optima™ L-90K ultracentrifuge	Beckman Coulter, Krefelt
PCR Mastercycler and vapo.protect pros	Eppendorf GmbH, Hamburg
pH-Meter Schott CG 842	Reiss Laborbedarf e.K, Mainz-Mombach
Pipetboy	Hirschmann Laborgeräte GmbH&Co.KG, Eberstadt
Plastibrand PD tip	Brand GmbH & Co.KG, Wertheim
RNA 2100 Bioanalyzer	Agilent Technologies, Böblingen
Rotating mixer RM5	Glaswarenfabrik Karl Hecht GmbH & Co.KG, Sondheim/Rhön
Scales MC1	Sartorius, Göttingen
Scales Mettler AE163	Gemini BV Labor, DG Apeldoorn, The Netherlands
Small shaker KM2 Akku	Edmund Bühler GmbH, Hechingen
Sonifier B250	Branson Ultrasonics, Danbury, USA
Thermomixer compact 5436	Eppendorf GmbH, Hamburg

Titramax 100 shaker for 96-well plates	Heidolph Instruments GmbH & Co.KG, Schwabach
Trans-blot SD blotting machine	Bio-Rad Laboratories GmbH, Munich
Trans-Blot Turbo™ transfer system	Bio-Rad Laboratories GmbH, Munich
UV-transilluminator gel documentation	Raytest, Straubenhardt
Water bath Julabo SW20C	Gemini BV Labor, DG Apeldoorn, The Netherlands

Table 20: Software

Software	Provider
Bio-Rad CFX manager	Bio-Rad Laboratories GmbH, Munich
Clone Manger Professional 9.2	Scientific&Educantional Software, Morrisville, USA
CorelDRAW Graphics Suite X5	Corel Cooperation, Ottawa, Canada
EndNote X2 and X5	Thomson Reuters Endnote, Carlsbad, USA
Li-COR Odyssey 2.1	Li-COR Biosciences GmbH, Bad Homburg
Microsoft Office 2003, 2007, and 2010	Microsoft Deutschland GmbH, Unterschleißheim
MikroWin 2000	Berthold Thechnologies GmbH&Co.KG, Bad Wildbach
ND-1000 V3.2.1	PeqLab Biotechnologie GmbH, Erlangen
Peaks 7.0	Peaks®, Waterloo, Canada
Photo Read V1.2.0.0	Berthold Thechnologies GmbH&Co.KG, Bad Wildbach
Prism 4	GraphPad Software, La Jolla, USA
SeqMan Pro (Lasergene 7)	DNASTAR®, Madison, USA

4.2. Methods

4.2.1. Cell biology

Monocytic leukemia cell line THP-1 was cultured in RPMI 1640 medium supplemented with 10% FCS. Cell density of this suspension cell line was kept between $2.5x10^5$ and $1x10^6$ cells per ml. Subcultivation was performed every second or third day by centrifugation for 5 min at 90 g. Supernatant containing dead cells and debris was removed, then cells were resuspended in medium and counted using Casy®TT cell counter.

Embryonic kidney cells HEK293 were cultured in DMEM supplemented with 10% heat-inactivated FCS. Hepatocellular carcinoma cell line HepG2 was kept in MEM containing 10% FCS, 1xNEAA and 1 mM sodium pyruvate solution. Both cell lines are adherent and were subcultivated when they reached 90% confluency by rinsing with phosphate buffered saline (PBS) and by dissociation using 0.05% trypsin and 0.02% EDTA in PBS for 2-5 min at 37°C. Enzymatic reaction was stopped by adding of appropriate medium to the cells. After centrifugation for 5 min at 500 g in tubes and aspiration of supernatant, cells were resuspended in appropriate medium and seeded in 1:3 to 1:10 ratios or counted using Neubauer improved counting chamber.

All media were supplemented with 2 mM L-glutamine, 100 U/ml penicillin and 100 µg/ml streptomycin. Standard culture conditions for all the cells were 5% CO_2 in a humidified incubator at 37°C.

4.2.1.1. Cryoconservation and recultivation of cells

For long-time storage cells were counted, centrifuged and resuspended in freezing medium (10% DMSO in FCS) with a density of $5x10^6$ to $1x10^7$ cells/ml. Cells were frozen in cryotubes at -80°C using freezing container “Mr. Frosty”. On the next day cells were transferred into liquid nitrogen tank.

For recultivation cell stocks were rapidly thawed in water bath at 37°C, immediately transferred into a tube with 9 ml of appropriate medium, centrifuged for 5 min at 500 g and placed into pre-warmed flask with growing medium. After maintenance in an incubator at 37°C overnight, medium was renewed and cells were subcultivated at least twice before usage. Cells were used for a maximum of 30 passages.

4.2.1.2. Isolation of CD14$^+$ human monocytes from blood by magnetic cell sorting and their differentiation

Human monocytes were isolated from buffy coats (DRK Blutspendedienst Baden-Württemberg Hessen) using Ficoll-Hypaque gradients as previously described[265]. In brief, two 50 ml Leukosep® tubes per buffy were layered with 15 ml lymphocyte separation media, blood cells were added followed by density gradient centrifugation for 35 min at 440 g, room temperature (RT), and break setting 2. After washing with leukocyte rinsing buffer and leukocyte running buffer, peripheral blood mononuclear cells were incubated with 70 µl magnetic CD14$^+$ microbeads per 7x10^7 cells for 15 min at 4°C. The reaction was stopped with leukocyte running buffer. After centrifugation for 10 min at 300 g and 4°C, CD14$^+$ cells were separated by positive selection with AutoMACS™ separator using program <possel D>. The eluted positive fraction was centrifuged at the same conditions and the pellet with CD14$^+$ cells was counted using Neubauer´s improved counting chamber. Monocytes were seeded at appropriate cell densities in macrophage serum-free medium (MSFM) containing 50 ng/ml recombinant human MCSF.

The differentiation into macrophages occurred by culturing monocytes for 6 days changing medium every second or third day where non-adherent cells were removed. Macrophages were used up to 6 days after isolation at cell densities between 60-90% confluency. After 6 days maintenance, macrophages were cultured in the same medium as THP-1 cells, RPMI medium supplemented with 10% FCS.

4.2.1.3. Lentiviral transduction

4.2.1.3.1. Lentiviral production in HEK293 cells

Cloned lentivector LF521A-1 encoding human truncated AMPKα1-subunit was transfected together with packaging vector pCMV-dR8 and the viral envelope plasmid pMD2G in 65-70% confluent 10 cm dishes with 3x10^6 HEK293 cells according to jetPrime transfection protocol (section 4.2.1.4). Supernatants containing lentiviral particles were harvested 72 h post-transfection, filtered and concentrated using Lenti™-X concentrator according to manufacturer´s protocol 1:20. Lentiviral supernatant was aliquoted and stored at -80°C.

4.2.1.3.2. Transduction of primary macrophages

$1x10^6$ $CD14^+$ human primary macrophages in 6-wells were transduced at day 6 after monocyte isolation by adding and centrifugation with 500 µl concentrated viral supernatant for 2 h at 2000 rpm (37°C, brake 2). Incubation occurred for additional 46 h at 37°C. After a medium change, macrophages were treated by different stimulants for 24 h.

4.2.1.4. Transient transfection

For overexpression (OE) experiments $6.5x10^6$ HepG2 cells were seeded in 15 cm dishes. Transfection with 20 µg Myc-Flag-tagged LXRα expression plasmid (OriGene) occurred on the next day using jetPrime transfection protocol. 4 h after transfection the medium was changed.

For KD experiments primary monocytes isolated as described in 4.2.1.2 were differentiated and seeded in 6-well plates at a density of $1x10^6$ cells per well with 80% confluency. For transfection with siRNA, ON-TARGETplus SMARTpool siRNAs or FlexiTube siRNAs and transfection reagent Hiperfect were used. Cells were transfected with 16.8 µl Hiperfect and 50 nM final concentration siRNA in 6-wells with volume of 500 µl. After 6 h-incubation 1 ml of the full medium was added. 72 h post-transfection, medium was changed and macrophages were treated with a stimulant for additional 24 h. KD efficiency was controlled by RT-PCR (section 4.2.2.3) in comparison to control medium-treated cells.

4.2.1.5. Cell staining, fixation, and fluorescence activated cell sorting (FACS) analysis

To determine the cell death, $5x10^5$ cells were detached, harvested by centrifugation at 500 g for 5 min at RT, and resuspended in 300 µl Annexin binding buffer. Cells were stained with Annexin V-FITC and propidium iodide (ratio 1:5) and incubated at 4°C for 15 min in the dark. Additional 250 µl binding buffer were added. Cells were vortexed and the cell death was verified by FACS analysis.

4.2.2. Molecular biology

4.2.2.1. RNA isolation

To isolate total RNA 1 ml peqGOLD RNAPure™ was added to each 6-well or 6 cm dish containing cells without medium. Cells were lysed by resuspension for 5 min and transferred

into 2 ml-tube. After addition of 200 µl chloroform, samples were vortexed for 15 sec and incubated for 5 min on ice. To separate aqueous phase containing RNA from the phenol and interphase, samples were centrifuged for 10 min at 12000 g and 4°C. After RNA precipitation and the addition of 500 µl 2-propanol to the aqueous phase, samples were overturned 10 times carefully and incubated on ice for 15 min. The precipitated (12000 g, 10 min, 4°C) RNA was washed twice with 75% ethanol in diethyl pyrocarbonate (DEPC)-H_2O. RNA pellets were dried at 70°C for 5 min and dissolved in 20 µl DEPC-H_2O by shaking at 60°C for 30 min. RNA concentration was determined using NanoDrop ND-1000 and optical density at 260 nm.

4.2.2.2. Reverse transcription

Reverse transcription of RNA to copy DNA (cDNA) was performed using Maxima first strand cDNA synthesis kit according to the manufacturer´s protocol. Briefly, each sample contained 1-2 µg RNA, 4 µl 5x reaction buffer, 2 µl reverse transcriptase, and nuclease-free H_2O was added to 20 µl. The preparation was incubated for 10 min at 25°C, 15 min at 50°C, and 5 min at 85°C for the inactivation of the transcriptase. The cDNA was diluted to final concentration of 10 µg/ml and stored at -20°C until use.

4.2.2.3. Quantitative real-time PCR (RT-PCR)

The expression analysis of individual mRNAs was performed by quantitative RT-PCR using Maxima SYBR Green qPCR Master Mixes. Each amplification sample contained 0.2 µl forward primer, 0.2 µl reverse primer (5 pmol/µl each), 8 µl Maxima SYBR Green qPCR master mixes, 2 µl cDNA and 2.6 µl distilled H_2O in each 96-well plate. The plate was briefly centrifuged and sealed with an optical adhesive BZO seal film. CFX96™ real-time system and the following RT-PCR thermal cycling program with repetition of 40 times were used.

Process	Temperature	Duration
Enzyme activation	95°C	15 min
Denaturation	95°C	15 sec
Annealing	55°C	30 sec
Elongation	72°C	30 sec

The specificity of amplification was performed using melting curve analysis of RT-PCR shown in following program:

Process	Temperature	Duration	
Denaturation	95°C	30 s	
Starting temperature	60°C	30 s	
Melting step	60°C + 0.5°C per cycle	10 s	80x

The mRNA expression was analyzed in duplicate for each gene and was normalized to glyceraldehyde 3-phosphate dehydrogenase (GAPDH) expression levels.

4.2.2.4. Microarray analysis

Primary macrophages were transduced with control (CV) or lentiviral particles as described in section 4.2.1.3 encoding the constitutively active AMPKα1 (AMPK OE) for 48 h. Additional treatment with 100 nM GW501516 occurred for 24 h. Total RNA isolation was performed by phenol-chloroform extraction (section 4.2.2.1) with some variations. The aqueous RNA-containing phase was purified with RNeasy total RNA cleanup kit and eluted in nuclease-free water. RNA quality was analyzed by the Agilent RNA 2100 bioanalyzer. The generated triplicates were stored at -80°C and sent later to Deutsches Krebsforschungszentrum in Heidelberg for further analysis.

Whole genome microarray was performed using the Illumina Sentric Human HT-12 v4 chip. Shortly, first and second strands of the RNA were synthesized; the cDNA was purified and transcribed. The formed cRNA was purified, quantified, hybridized, washed and scanned. Raw microarray data were normalized using the variance stabilization and normalization (VSN) method, and assigned to human gene symbols using R/Bioconductor[266] and the beadarray package[267]. Triplicates were contrasted using Limma[268] and differentially expressed genes were selected based on a 1.5-fold change and a Benjamini-Hochberg adjusted p-value smaller than 0.1. Functional annotation was performed using gene set enrichment analysis (GSEA)[269] against gene sets derived from the molecular signature database version 3.1, datasets c2, c3, and c6[269], from Pathway Commons[270] and from Genome Ontology via Ensembl, revision 70[271].

4.2.2.5. DNA amplification by polymerase chain reaction (PCR)

The DNA amplification was performed with the polymerase chain reaction (PCR) method. For this procedure the proofreading PfuUltra polymerase was used. All PCR samples were pipetted with 50 µl as the final volume.

10x Reaction buffer	5 µl
10x PCR-Enhancer solution	3 µl
10 mM dNTP mix	1 µl
10 µM Forward primer	1 µl
10 µM Reverse primer	1 µl
PfuUltra enzyme (2.5 Units/µl)	1 µl
100-250 ng Plasmid DNA	x µl
ddH_2O	fill to 50 µl

Samples were mixed and centrifuged. The PCR cycle protocol was repeated 30 times.

Process	Temperature	Duration
Enzyme activation	95°C	2-3 min
Denaturation	95°C	20 s
Annealing	55°C	20 s
Elongation	72°C	2-3 min
Elongation	72°C	5 min

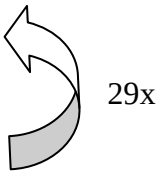

Amplified DNA was purified with PCR clean kit according the manufacturer´s protocol and stored at -20°C until use.

4.2.2.6. Digestion with restriction enzymes

Every DNA digestion analysis was performed in a volume of 25 µl:

Plasmid DNA (500 ng)	x µl
10x NEBuffer	2.5 µl
10x BSA	2.5 µl
Restriction endonuclease	1 µl (2-3 Units)
ddH_2O	fill to 25 µl

The preparation was incubated at the optimal temperature of the endonuclease (37°C) at least for 1 h. The linearized vector could be detected by gel electrophoresis (section 4.2.2.7).

4.2.2.7. Agarose gel electrophoresis

For detection of separated DNA fragments agarose gel electrophoresis was performed by the separation in gel electrophoresis chamber using appropriate 1-2% agarose gels. Agarose gel was prepared in 1xTAE buffer boiling up in a microwave oven and adding ethidium bromide 1:50. The gel was poured into the chamber and incubated till polymerization at RT. 1xTAE buffer was filled into the chamber and samples containing loading buffer were pipetted into the gel wells. To quantify the DNA fragment size a 100 bp or 1 kb marker was used. The electrophoresis run occurred till visible separation at 100 V. The DNA fragments were visualized by UV-transilluminator.

4.2.2.1. Site-directed mutagenesis

To exchange one or more bp inside a reading frame, the mutagenesis procedure was used. The preparation was pipetted like during PCR preparation (section 4.2.2.5) using 10 ng plasmid DNA and 125 ng of each primer. Mutagenesis protocol was repeated 19 times.

Process	Temperature	Duration
Enzyme activation	95°C	1 min
Denaturation	95°C	50 s
Annealing	60°C	50 s
Elongation	68°C	1 min/kb
Elongation	68°C	7 min

18x

The digestion with restriction nuclease DpnI (10 U/µl) occurred to eliminate parental supercoiled double strand DNA for at least 1 h at 37°C.

The DNA sequencing was performed by the company SeqLab/Microsynth using 1.2 µg plasmid and 30 pmol primer in volume of 15 µl to confirm the authenticity of the mutation and to ensure no other mutations.

4.2.3. Microbiology

4.2.3.1. Transformation of *Escherichia coli*

Competent *Escherichia coli* bacteria were transformed with plasmid DNA by a heat-shock. Therefore, 50 µl of bacteria glycerol stocks were thawed on ice and 2 µl β-mercaptoethanol were added to increase the transformation efficiency. After incubation on ice for 10 min, 50-100 ng of DNA were added followed by next incubation on ice for 30 min. After a heat-shock for 30 sec at 42°C, bacteria were incubated on ice for 5 min. For initial growth, 450 µl SOC medium were added followed by 1 h-incubation at 37°C, shaking at 250 rpm. 200 µl of growth culture were inoculated on a LB agar plate containing 100 µg/ml ampicillin and incubated at 37°C overnight to select positive, plasmid-carrying bacteria clones.

4.2.3.2. Bacterial culture and plasmid preparation

For long-time storage 500 µl of bacteria stock were resuspended with 500 µl of 7% DMSO solution and stored at -80°C. To culture plasmid-containing bacteria again, small part of frozen culture was scraped and put into 2 ml LB medium containing 100 µg/ml ampicillin/kanamycin shaking at 37°C overnight. Transformation as described in section 4.2.3.1 followed.

For plasmid preparation single bacteria clones were picked from the LB agar plate, transferred into 2 ml LB medium with 100 µg/ml ampicillin/kanamycin and cultured at 37°C shaking the tubes at 250 rpm overnight. After 8 h the bacterial culture was transferred into 200 ml LB medium containing 100 µg/ml of appropriate antibiotic and shaken at 37°C overnight. The plasmid preparation was performed according to the manufacturer´s protocol using the NucleoBond® Xtra Maxi kit. DNA was dissolved in RNAse-free water and DNA content was measured using the NanoDrop ND-1000.

4.2.4. Biochemistry

4.2.4.1. Protein isolation

For protein isolation, monolayers containing 2-3x10^6 cells were washed with PBS and harvested by centrifugation for 5 min at 500 g in 100 µl NP-40 lysis buffer including phosphatase inhibitors (PI). The lysates were sonicated 3x0.6 sec. After the centrifugation at the maximal velocity for 10 min, the protein concentration in cleared supernatant was measured using the Lowry method (section 4.2.4.2).

4.2.4.2. Determination of protein concentration (Lowry)

For protein determination a standard dilution series of bovine serum albumin was prepared in still water (0.5 to 2 mg/ml). The protein concentrations were determined by the DC Protein Assay Kit, based on the Lowry method[272]. 2 µl of each standard dilution and sample were pipetted in duplicates into a 96-well plate. 25 µl reagent A and 200 µl reagent B were added to each well and incubated shaking for 15 min at RT. The extinction was measured at 750 nm using Apollo-8 LB 912 photometer.

4.2.4.3. Western analysis

After protein isolation and protein measurement, 5xSDS sample buffer was added to 80-100 µg protein for denaturation for 5 min at 95°C. Depending on their size, proteins were separated on a 7.5, 10 or 15% SDS polyacrylamide gel using 1xSDS running buffer and the Mini-PROTEAN 3 cell system. Separated proteins were transferred onto a nitrocellulose membrane by semi-dry blotting using Trans-Blot Turbo™ transfer system (100 mA, 25 V, 90 min). To minimize unspecific binding, membranes were blocked with 5% milk in TBS or 5% BSA in TBS considering thereafter used antibody, for 1 h at RT. Membranes were incubated with primary antibodies in 5% milk in TBST or 5% BSA in TBST at indicated concentrations at 4°C overnight. For protein detection, membranes were washed 3 times with TBST for 5 min, incubated with IRDye-conjugated secondary antibodies 1:10000 in 5% milk in TBST or 5% BSA in TBST for 45 min at RT and washed with TBST 3 times again. Proteins were visualized and densitometrically analyzed using the chemiluminescence or the infrared imaging system and Li-COR Odyssey 2.1 software.

4.2.4.4. ATP assay

$5x10^5$ THP-1 macrophages were not or treated with 5 µg/ml oligomycin and 20 mM deoxyglucose for 3 h or with A-769662 for 24 h, whereupon each sample contained 1 ml minimal RPMI medium. Afterwards, cells were pelleted for 30 sec at maximal speed and 100 µl of 1xPassive lysis buffer were added to the pellet. ATP standard samples were prepared in dilution buffer (Sigma). Luminescence during 20 sec of ATP standards and cell lysates was determined in doublets. The measurement occurred very fast to capture the current ATP content of the cells. Protein concentration of each sample was determined.

4.2.4.5. Immunoprecipitation (IP)

At least $6.5x10^6$ HepG2 cells were seeded in 15 cm dishes, transfected with 20 µg LXRα OE plasmid the next day (section 4.2.1.4) using jetPrime and stimulated after 24 h by A-769662 for 6 h. Cells were harvested as described in section 4.2.4.1 in RIPA buffer including PI by scraping with a rubber policeman. After sonication 2 times with 3x0.6 sec (amplitude 20%) on ice, lysates were clarified by centrifugation for 15 min at 12000 g and 4°C. Protein concentration was determined as previously described in 4.3.2 (section 4.2.4.2) where 800 µg-1 mg protein were used for following immunoprecipitation. Agarose A/G beads were washed with RIPA buffer and added to lysates for pre-clearing. After 2 h-rotation at 4°C, supernatants of the mixes (1 min, 2000 g, 4°C) were collected and incubated with 10 µg antibody at 4°C overnight.

Agarose A/G beads were blocked before using them with the lysates to avoid unspecific binding. The beads were once rinsed with RIPA buffer and blocked with 5% of 10% BSA solution and 0.5% of salmon sperm DNA (10 mg/ml) rotating at 4°C overnight.

The next day blocked beads were added to the protein lysates and rotated for 1 h at 4°C for connection of protein-antibody complexes to the beads. After a short centrifugation for 1 min at 1000 rpm and 4°C, pellets containing bead-antibody-protein complexes were washed 3 times with 1 ml cold RIPA buffer, overturned 3 times and centrifuged for 1 min at 1000 rpm and 4°C. After the last centrifugation step, 50 µl dithiothreitol (DTT)-free 1xSDS-sample buffer was added to the beads and shaken for 10 min at 95°C. Samples were spun for 1 min at 13200 rpm and their supernatants were loaded on a 10% gel to separate the proteins. 1/3 of the IP samples were loaded onto second 10% gel proceeding as in section 4.2.4.3 to blot the membrane and identify the target protein. The gel was fixed with fixing buffer for 30 min, stained with Coomassie for the next 30 min and destained overnight. The appropriate protein bands were cut out of the first gel and provided for the mass spectrometry analysis.

4.2.4.6. Stable isotope labeling by amino acids in cell culture (SILAC)

To show the differences in abundance of LXRα protein post-translational modification without and during the AMPK activation, the specific mass spectrometry (MS)-based method SILAC was used. First, the half of HepG2 cells got labeled with heavy AA by special SILAC medium incorporating Lys-6 and Arg-10 only, but no unlabeled Lys and Arg. All other AA were not labeled with heavy isotopes. The other half of the cells was grown in normal

medium. Then, IP for the LXRα protein from the lysates was performed and the LXRα protein was cut out of the SDS gel whereupon further MS and data analysis followed. The peptide preparation, its measurement and data analysis were performed by collaboration partners.

4.2.4.6.1. Sample preparation

$4x10^4$ HepG2 cells were washed with PBS and cultivated in normal or SILAC medium for 48 h in 6-wells. Further 5 cell cycles (each cycle lasts about 2 days) a medium exchange occurred. To avoid cell confluency of 100%, cells were transferred into 6 cm dishes and later into 10 cm and 15 cm dishes and cultivated in an appropriate normal or SILAC medium. After 7 passages 4 different samples were prepared transfecting with LXRα OE plasmid (section 4.2.1.4) using jetPrime and later stimulating with DMSO or 250 µM A-769662 for 6 h: unlabeled and untreated cells (a); unlabeled and A-769662-treated cells (b); labeled and untreated cells (c); labeled and A-769662-treated cells (d). IP preparation (section 4.2.4.5) of each sample followed whereupon the protein A/G beads of the samples (a) and (d), and of the samples (b) and (c) were mixed to form 2 IPs which were loaded onto a Coomassie Blue stained gel. The bands presumably containing the protein LXRα (55 kDa) were cut out and divided into 4 pieces.

4.2.4.6.2. Protein digestion and peptide purification

The gel pieces were destained by 50% acetonitrile and 50% 50 mM ammonium bicarbonate (ABC) buffer, reduced with 10 mM DTT in 50 mM ABC buffer, washed in 100% acetonitrile (ACN), and alkylated with 55 mM iodo acetamide in ABC buffer. Subsequently, samples were washed with ABC buffer, 70% ACN, and finally digested with a) 15 µl trypsin (10 ng/µl ABC) or b) 15 µl thermolysin (100 ng/µl ABC). Limited digestion was stopped after 15 min by acidifying with 10% trifluoroacetic acid (final concentration 0.1%) and adding 100 µl of stage tip buffer A for desalting on 3 disc stage tips. The other part of the samples was digested overnight.

After the loading of peptides onto stage tips and their purification from salts using stage tip buffer A, they were eluted with stage tip buffer B into MS microtiter plates (Nerbe). They were dried for 10 min in speed vacuum until ACN completely evaporated. After the adding of 50 mM citric acid the microtiter plate was sealed, shaken for 30 min, and stored at -20°C until use.

4.2.4.6.3. Mass spectrometry (MS) measurement

Two different types of equipment for MS were used: LTQ Orbitrap XL™ ETD Hybrid Ion Trap-Orbitrap mass spectrometer[2] (Thermo Fisher Scientific, Dreieich) and Q Exactive™ Hybrid Quadrupole-Orbitrap mass spectrometer[3] (Thermo Fisher Scientific, Bremen). The gradient time accounted 90 min whereupon a dynamic Top10 method was chosen, which picked the most abundant 10 precursor masses for fragmentation in case of signal/noise ratio higher than 1000[2] and 6700[3]. Doubly, triply, and quadruple[2] or 2-6[3] charged precursor ions, respectively were allowed for fragmentation. In front of the LTQ Obritrap mass spectrometer an Agilent 1200 chromatography system was installed. 6 µl sample were injected via the 8 µl sample loop and loaded to the precolumn at a flow rate 5 µl/min using 1% ACN and 0.1% formic acid in water. The Agilent Zorbax (300 µM internal diameter 5 µM C18) bead columns were washed for 10 min before the elution. After the purification of peptides, they were separated on an in-house prepared column with Reprosil-Pur 3 µm beads (Dr. Maisch, Amerbruch, Germany), packed into a 75 µm ID PicoTip® nanospray emitter of 15 cm length using linear gradient of chromatography buffer B from 5% to 63% within 60 min and ionized at 2.6 keV. Finally the column was washed with 95% chromatography buffer B and re-equilibrated to 5% for 10 min. The eluted peptides were sprayed at 2.6keV tension directly from the tip of the emitter using a liquid junction ionization interface. To collect the optimal amount of ions for detection, an injection time of 160 msec was allowed for MS and 150 msec for MS-MS.

The procedure using Q Exactive mass spectrometer occurred in the same way except of Thermo Ultimate 3000 UPLC System installed in front of spectrometer. Besides, the peptides were separated on an in-house prepared column: 75 µm ID and 20 cm length with Reprosil-Saphir 2.2 µm beads. The sample loading was performed at a flow rate of 25 µl/min.

4.2.4.6.4. Data analysis

The data was analyzed and subsequently quantified with the software Peaks 7.0; first the software processed the data for search against the Uniprot Human database. The following parameters were set for the search: the mass accuracy was limited to 8 ppm for MS and 0.02 Da for MS-MS data. Each peptide was allowed to have 3 missed cleavages and maximum 3 variable modifications. The following modifications were allowed in the Peaks

[2] LTQ Orbitrap XL™ ETD Hybrid Ion Trap-Orbitrap mass spectrometer
[3] Q Exactive™ Hybrid Quadrupole-Orbitrap mass spectrometer

Search: oxidation of Met, carbamidomethylation of Cys, deamidation of Asn and Asp, methylation and dimethylation of Arg and Lys, acetylation, butyrylation and propionylation of Lys, SILAC Arg-10 and SILAC Lys-6, as well as phosphorylation of Ser/Thr/Tyr. The data was quantified using MS detectable peak pairs with the SILAC typical distances of 6 or 10 Da respectively.

4.2.4.7. Chromatin IP (ChIP)

Before the beginning of ChIP procedure protein A sepharose CL-4B beads were blocked by washing with lysis buffer II twice in 15 ml tube centrifugating for 5 min at 1200 g at 4°C. After addition of lysis buffer II, 1 g/l BSA and 0.4 g/l salmon sperm DNA to avoid unspecific binding, the samples were rotated at 4°C overnight. Blocked sepharose beads were stored for months at 4°C.

Dependent on the cell line, 8-16x10^6 cells were seeded in 15 cm dishes and stimulated by A-769662 for 4 h To cross-link the proteins to DNA, 1% formaldehyde was added to the cell monolayer shaking for 10 min at RT. This reaction was stopped by adding of 0.125 M glycine and shaking for additional 5 min. Cells were washed twice with ice-cold PBS and harvested by scraping and following centrifugation for 5 min, 1200 g at 4°C in 15 ml tubes. Cell pellets could be shock-frozen in liquid nitrogen and stored at -80°C until further use.

After thawing the pellets on ice, cells were resuspended 10x in lysis buffer I (1 ml per 2.5x10^7 cells) with PI. After the incubation on ice for 20 min, suspension was centrifuged for 5 min at 1200 g and 4°C. The pelleted cell nuclei were resuspended in the same volume of lysis buffer II as lysis buffer I with PI and incubated at least for 10 min on ice. Nuclei suspension was aliquoted with maximal volume of 500 µl in 1.5 ml tubes and sonicated using glass beads and 20 pulses with 15% amplitude (1 min: 2 sec pulse; 1 sec pause) to shred the whole genome DNA. The lysates were cleared by centrifugation for 15 min at 1200 g and at 4°C and soluble chromatin of each sample was pooled. The lysates were analyzed by agarose gel electrophoresis to determine DNA fragmentation. For pre-clearing 50% slurry of the beads and lysis buffer II (100 µl per 1 ml sample) was added to chromatin samples and rotated for 45 min at 4°C. After the centrifugation for 1 min, at 2000 g and 4°C, soluble chromatin was immunoprecipitated with 4 µg antibody rotating at 4°C overnight.

Blocked protein A/G agarose beads, as described in section 4.2.4.5, were added to the samples to form bead-antibody-protein-DNA complexes and incubated for 1 h by rotation at 4°C. Washing steps with 1 ml each followed by inverting three times and centrifugation for 1 min at 100 g and 4°C: 1x wash buffer (WB) I, 1x WB II, 2x WB III. The last two wash steps were performed with TE (pH 7.4) at RT. The elution of protein-DNA complexes occurred with freshly made elution buffer incubating the samples twice for 15 min by vigorous shaking and pooling the supernatants of each sample. To reverse crosslinks between DNA and proteins, 42 µl reversion mix were added to each tube and incubated at 65°C overnight. On the next day, DNA was purified using QIAquick PCR purification kit according to manufacturer´s protocol. Briefly, samples were incubated for 30 min in 5x volume precipitation buffer, DNA was bound on provided column and eluted twice with 40 µl water. The eluted DNA served as a template for further RT-PCR runs.

4.2.4.8. Triglyceride measurement

Human very-low density lipoprotein (VLDL) was isolated from the EDTA-plasma samples of healthy volunteers by sequential ultracentrifugation at 32000 rpm and 22°C overnight. Primary macrophages were pretreated with 100 nM GW501516 and/or 250 µM A-769662 for 48 h. After the medium change cells were loaded with 20 µg/ml VLDL for additional 24 h. Triglyceride (TG) content was determined using TG determination kit according to the manufacturer´s instructions and normalized to protein content.

4.2.4.9. Cholesterol efflux assay

Foam cell formation was induced by stimulation with 50 µg/ml acetylated LDL (acLDL) for 8 h. After the medium change, macrophages were incubated with 250 µM A-769662 for 24 h. After the medium exchange to phenol-free RPMI cholesterol efflux was induced by human recombinant 10 µg/ml apolipoprotien AI (apoAI) for 16 h. Cholesterol was detected at 590 nm using high-sensitive fluorescence method Amplex red cholesterol assay kit according to manufacturer´s protocol.

4.2.4.10. Luciferase assay

For luciferase reporter assay $1x10^4$ cells were seeded in each well of 96-well plate. Next day cells were transfected with jetPrime as described in section 4.2.1.4 with Firefly/Renilla ratio of 1:50. 24 h post-transfection, medium was changed and stimulation with A-769662 or T0901317 occurred for 24 h. Cells were harvested with 1xPassive lysis buffer shaking for

15 min at RT. 10 µl of each cell lysate was placed into a new transparent 96-well plate for the measurement of Renilla luciferase activity; 20 µl – for the measurement of Firefly luciferase activity. Renilla substrate Coelentranzine was prepared making a 1:100 dilution in Renilla buffer. During the measurement 50 µl of luciferase substrate was added to each well. The fluorescence was detected in triplicates using Mithras LB 940. The results were analyzed counting the ratio of Firefly activity / Renilla activity values and normalizing to control/untreated samples.

4.2.5. Statistical analysis

All data in bar graphs are presented as mean values ± standard error of the mean (SEM) and each experiment was performed at least three times. Statistical significance was determined by unpaired student's *t*-test or the one-way analysis of variance (ANOVA). Differences were considered significant at */#/$, $p \leq 0.05$; **/##/$$, $p \leq 0.01$; ***/###/$$$, $p \leq 0.001$.

5. Results

Macrophages are one of the major cell types which regulate human immunity. Deregulation of macrophages lipid metabolism contributes to different relevant diseases such as metabolic syndrome or atherosclerosis. The possibility to treat and heal those diseases relies on fundamental research. This is the reason, why I concentrated on the pathways regulating fatty acid and cholesterol metabolism in human macrophages in my studies.

5.1. AMPK and PPARδ interact and regulate lipid metabolism in primary human macrophages

Previous studies reveal the interaction of AMPK and PPARδ promoting exercise endurance and fatty acid oxidative metabolism in murine muscle cells[262]. The aim of this project was to investigate the effects of AMPK and PPARδ activation and its interaction in primary human macrophages by establishing AMPKα1 overexpressing system and analyzing AMPK- and PPARδ-dependent changes of the transcriptome.

5.1.1. Establishing of AMPKα1 knock-down and overexpression in human macrophages

As AMPK is an enzyme regulating the energy homeostasis in the whole body, it was interesting to identify its role in human macrophages. To investigate the function of AMPK, it was knocked down using MISSION® shRNA plasmid in THP-1 cells. THP-1 cells which were transduced with scrambled control shRNA (CV) served as control cells. Stable THP-1 AMPKα1 KD (α1 KD) cell line was generated using puromycin selection. AMPKα1 mRNA and protein expression of differentiated macrophages were analyzed by RT-PCR or Western analysis. Transduction and the KD of AMPKα1 were successful showing 93% reduction of AMPKα1 mRNA expression compared to CV-transduced THP-1 macrophages (Figure 8 A). Western blot shows no detectable total AMPK expression in KD cells (Figure 8 B). Since the antibody recognizes both α1 and α2, this confirms the negligible expression of α2 isoform, consistent with literature data[251]. The phosphorylation of AMPK substrate ACC indicates an activity of AMPK which was abolished in AMPKα1 KD THP-1 cells.

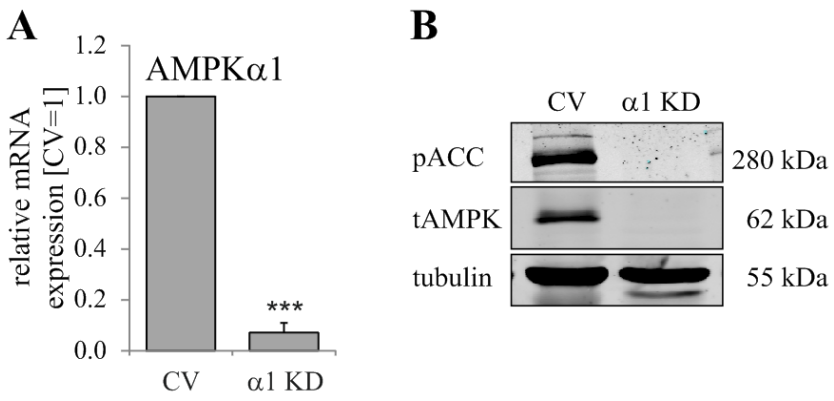

Figure 8: Verification of AMPKα1 KD in human THP-1 MΦ.

500 µl of control (CV) or AMPKα1 KD (α1 KD) lentiviral particles were added to $2x10^6$ THP-1 cells and incubated for 24 h. Following selection by puromycin, THP-1 monocytes were differentiated to macrophages by 100 nM TPA-treatment for 48 h. **A** AMPKα1 mRNA expression was quantified by RT-PCR and is shown relative to GAPDH. Statistics were performed using unpaired student´s *t*-test. Data are means ± SEM (***, $p \leq 0.001$; n = 3). **B** Western analysis of total AMPK and phospho-ACC protein expression in whole cell lysates. Tubulin served as loading control. Blot is representative of at least three independent experiments.

To further investigate the role of AMPK and to avoid off-target effects associated with pharmacological AMPK activation, I developed a new AMPK OE construct using pPS-EF1-LCS-T2A plasmid. First, PCR of AMPKα1 (PRKAA1) was performed where THP-1 cDNA served as a template. Using applied Clone-it™ enzyme free lentivector system, the construct was recombined into the target vector (sections 4.2.2.5-4.2.3.2). Previous studies have already shown increased AMPK-specific activity using truncated AMPKα1 OE[214, 273], because the whole catalytic subunit (1-392 AA) contains auto-inhibitory domain blocking AMPK activity. As a mutation T198D (T172D according to murine genome) leads to predominantly phosphorylated/activated AMPK state[203], I decided to generate truncated and mutated AMPKα1-subunit (1-334 AA) using a site-directed mutagenesis at the site T198D to create constitutively active AMPK. After sequencing the correct bacterial clones were identified and their plasmid DNA was amplified. The plasmid was used for transient transfection of HEK293 cells to produce lentiviral particles for transduction of human macrophages as described in section 4.2.1.3.2.

Initial experiments showed low transduction efficiency using standard protocols. So, additional optimization steps were necessary. First, I tried to improve the transduction by use of polybrene which was reported to enhance viral transfer[274]. During these experiments the concentration 6 µg/ml of polybrene was used. Stimulation with polybrene did not lead to any increase of transduction efficiency. Furthermore, the transduction of blood-dervied monocytes

did not provide positive results. The differentiation of monocytes to macrophages turned out to be necessary. Finally, the improvement of the transduction efficiency could be achieved by post-transductional centrifugation of the cells at 500 g and 37°C, for 1 h 40 minutes and a second transduction with viral supernatant. Such an effect was already described using an adenovirus[275].

Primary MCSF-differentiated macrophages were transduced by control (CV) or AMPKα1-conding lentiviral particles (AMPKα1 OE) for 48 h. With the antibody against total AMPK, AMPKα1-subunit containing 334 AA could be identified at the size of 38/40 kDa showing double bands (Figure 9). The upper band with 40 kDa represents AMPKα1-subunit, whereas additional bands may represent some degradation products.

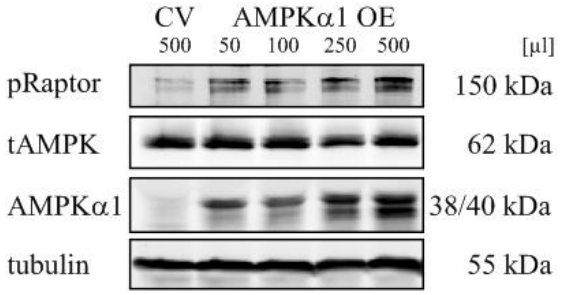

Figure 9: Dose-dependent transduction efficiency of primary MΦ with AMPKα1 OE construct.
Primary macrophages were transduced with control (CV) or AMPKα1-containing lentiviral particles (AMPKα1 OE) for 48 h. Cell lysates were analyzed by Western blotting. Tubulin served as a loading control. Blot is representative of at least three independent experiments.

According to the blot shown in Figure 9, the expression of endogenous AMPK doesn´t change, whereas the AMPKα1 expression increases with higher dose of lentiviral particles. Using following equation: $\frac{(\boldsymbol{band}\,[\mathbf{40}\boldsymbol{kDa}]+\boldsymbol{band}\,[\mathbf{62}\boldsymbol{kDa}])}{\boldsymbol{band}\,[\mathbf{62}\boldsymbol{kDa}]}$, the OE degree could be calculated giving values of 1.14, 1.17, 1.28 and 1.44 after transduction with respectively 50, 100, 250 or 500 µl AMPKα1. This outcome indicates 500 µl as the best volume for primary macrophage transduction resulting in enhanced AMPKα1 OE. The phosphorylation of Raptor reflects the AMPK activity increasing also dose-dependent in AMPKα1 OE macrophages. For the following experiments I used the optimal volume of 500 µl to perform the lentiviral transduction of primary cells.

5.1.2. Microarray analysis: AMPK and PPARδ co-activation increase β-oxidation gene expression

5.1.2.1. Microarray setup

Microarray is a useful tool for identification of novel mRNA patterns to understand cellular pathways. To analyze the genome-wide RNA expression changes of primary human macrophages, PPARδ activation by 100 nM GW501516 followed after the AMPKα1 OE. For an identification of novel genes regulated by both proteins, I prepared microarray samples for the whole genome expression profiling as described in section 4.2.2.4 (Figure 10) in triplicates.

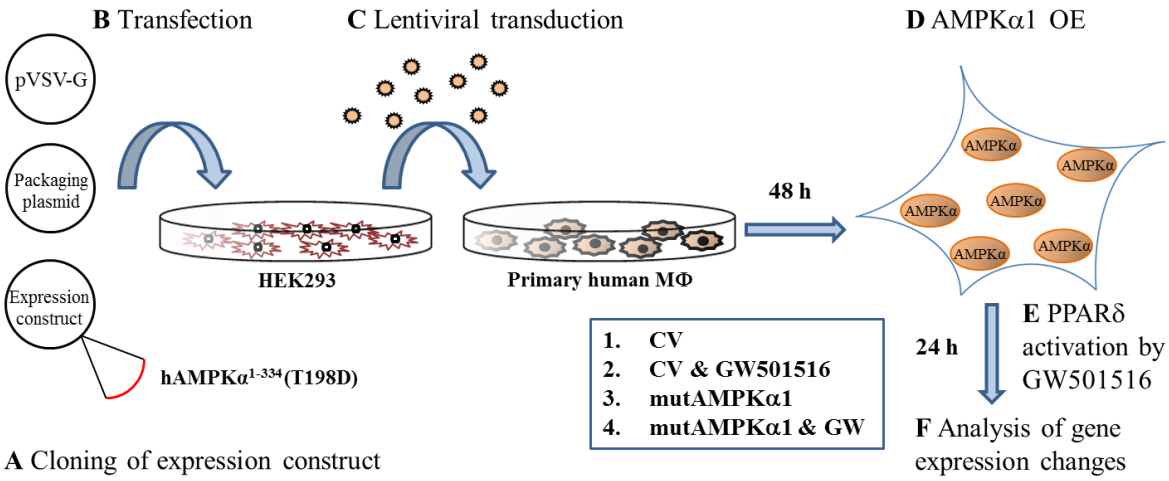

Figure 10: Experimental steps before the microarray analysis.

A The T198D mutated AMPKα1 construct (mutAMPKα1) was cloned into an expression vector. **B** Transfection of HEK293 cells with vectors encoding for viral envelope proteins, packaging and non-coding DNA (CV)/mutAMPKα1 plasmids provided production of lentiviral particles, 500 µl of which were used to transduce MCSF-differentiated macrophages for 48 h (**C,D**). **E** After OE of mutated AMPKα1 (AMPKα1 OE), cells were stimulated or not with 100 nM GW501516 for 24 h and harvested for RNA isolation. **F** Microarray analysis was performed using HT-12 v4 expression BeadChip kit.

The microarray was performed in collaboration with a bioinformatics group of German cancer research center (DKFZ) in Heidelberg, which specializes in expression profiling. Illumina human HT-12 v4 expression BeadChip kit was used allowing high reproducibility, yield, and low sample input of 50-100 ng of total RNA. Samples were hybridized and sequenced.

5.1.2.2. Microarray analysis – results

Results of the microarray profiling are publicly available (EMBL-EBI Array Express accession number E-MTAB-2524). Genes, which are up- or down-regulated by AMPK and/or PPARδ, are summarized in Figure 11. Further analysis was performed by collaborators of the laboratory of Prof. Müller in Marburg which is described in section 4.2.2.4.

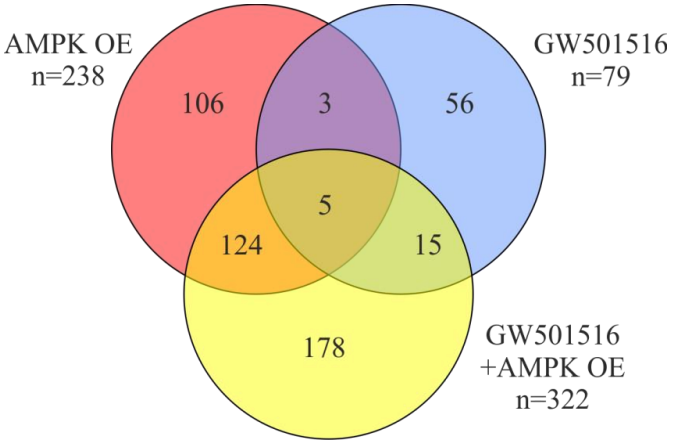

Figure 11: Number of genes regulated by AMPK and PPARδ activation in primary human MΦ.
Primary macrophages were transduced with CV or mutAMPKα1 (AMPK OE) lentiviral particles for 48 h and stimulated or not with 100 nM GW501516 for additional 24 h. Total RNA was isolated and microarray using HT-12 v4 expression BeadChip kit was performed in triplicates. Venn diagram shows the numbers of genes regulated by AMPK OE (**red**), GW501516 (**blue**), and co-stimulation (**yellow**). The numbers shown in overlapping spaces represent commonly regulated genes. The analysis was performed with Limma setting, adjusted p-value < 0.1 and the fold change >1.5.

In this setting mutAMPKα1 OE (AMPK OE) regulates 238 genes (107 up and 131 down) using $\log_2$(fold change)≥0.58 as the cutoff value. PPARδ activation up-regulates 46 and down-regulates 33 genes. Using this cutoff, 8 genes (3 up and 5 down) are commonly regulated by AMPK and PPARδ. Co-stimulation alters 322 genes (128 up and 194 down) at all. Testing the cooperativity of the AMPK and PPARδ gene regulation, no synergistic effect was found, which was defined as ≥50% difference in intensity after co-activation of AMPK and PPARδ compared with single stimulations.

Gene set enrichment analysis (GSEA) is a method to interpret gene expression data finding enriched pathways. Using this method, gene sets and groups with common biological function and regulation can be found[269]. Table 21 shows the list of 20 mostly regulated pathways according to normalized enrichment score (NES). The normalization occurred towards the size of the gene set[269]. The p-value shows how significant the result is. Comparing combined

AMPK/PPARδ activation with untreated samples revealed fatty acid oxidative metabolism dominating the list of up-regulated pathways.

Table 21: Major regulated pathways by GSEA

Gene set	p-value	NES
Fatty acid β-oxidation	0.047	2.21
Pyruvate metabolism and TCA cycle	0.074	2.14
Kinesin binding	0.060	2.13
TCA cycle and respiratory electron transport	0.052	2.12
Ion transport by P-type ATPases	0.120	2.06
ATP biosynthetic process	0.099	2.05
Pyruvate metabolism	0.150	2.01
TCA cycle	0.195	1.99
Oxidative stress response	0.191	1.97
Pyruvate metabolic process	0.209	1.97
STAT3 targets	0.183	1.96
PPAR signaling pathway	0.184	1.96
FFA oxidation	0.198	1.96
Hydrolase activity, acting on acid anhydrides, catalyzing transmembrane movement of substances	0.225	1.94
Cellular aromatic compound metabolic process	0.250	1.91
ER organization	0.253	1.91
Estrogen metabolic process	0.300	1.88
Regulation of fatty acid beta oxidation	0.339	1.83

GSEA, gene set enrichment analysis; NES, normalized enrichment score

The list of most highly induced genes following AMPK/PPARδ co-activation is shown in Table 22. This list includes FAO-associated genes PDK4, CPT1a, acetyl-CoA acyltransferase 2 (ACAA2), long-chain fatty acid elongase 6 (ELOVL6) and acyl-CoA dehydrogenase (ACADVL). PLIN2 is a common PPARδ target gene and is also present in

this list. All of these genes represent the type II ligand-induced stimulation of PPARδ transcriptional response according to induction by GW501516[89].

Table 22: 20 most highly induced genes upon combined AMPK/PPARδ activation

Gene symbol	Gene name	log_2(fold change), GW+AMPK OE vs. CV
PDK4	pyruvate dehydrogenase kinase, isozyme 4	2.11
CPT1a	carnitine palmitoyltransferase 1A (liver)	1.48
FABP4	fatty acid binding protein 4, adipocyte	1.30
PLIN2	perilipin 2	1.08
ACAA2	acetyl-CoA acyltransferase 2	1.03
UCHL1	ubiquitin carboxyl-terminal esterase L1 (ubiquitin thiolesterase)	0.96
RNF128	ring finger protein 128, E3 ubiquitin protein ligase	0.96
DHRS9	dehydrogenase/reductase (SDR family) member 9	0.95
ELOVL6	ELOVL fatty acid elongase 6	0.91
FAM160B1	family with sequence similarity 160, member B1	0.91
IMPA2	inositol(myo)-1(or 4)-monophosphatase 2	0.87
ANKDD1A	ankyrin repeat and death domain containing 1A	0.84
SPINK1	serine peptidase inhibitor, Kazal type 1	0.83
ACADVL	acyl-CoA dehydrogenase, very long chain	0.82
ZNF366	zinc finger protein 366	0.81
HPSE	heparanase	0.81
SEMA3E	semaphorin 3E	0.79
CDH23	cadherin-related 23	0.79
NBL1	neuroblastoma, suppression of tumorigenicity 1	0.79
CD36	CD36 molecule (thrombospondin receptor)	0.76

5.1.2.3. Microarray validation

To validate and confirm the microarray results, I performed quantitative PCR. The same samples as in the microarray were used and several targets from the Table 22 were chosen for the validation. As demonstrated in Figure 12, RT-PCR experiments show the same effects on FAO-associated gene expression as indicated by the microarray data.

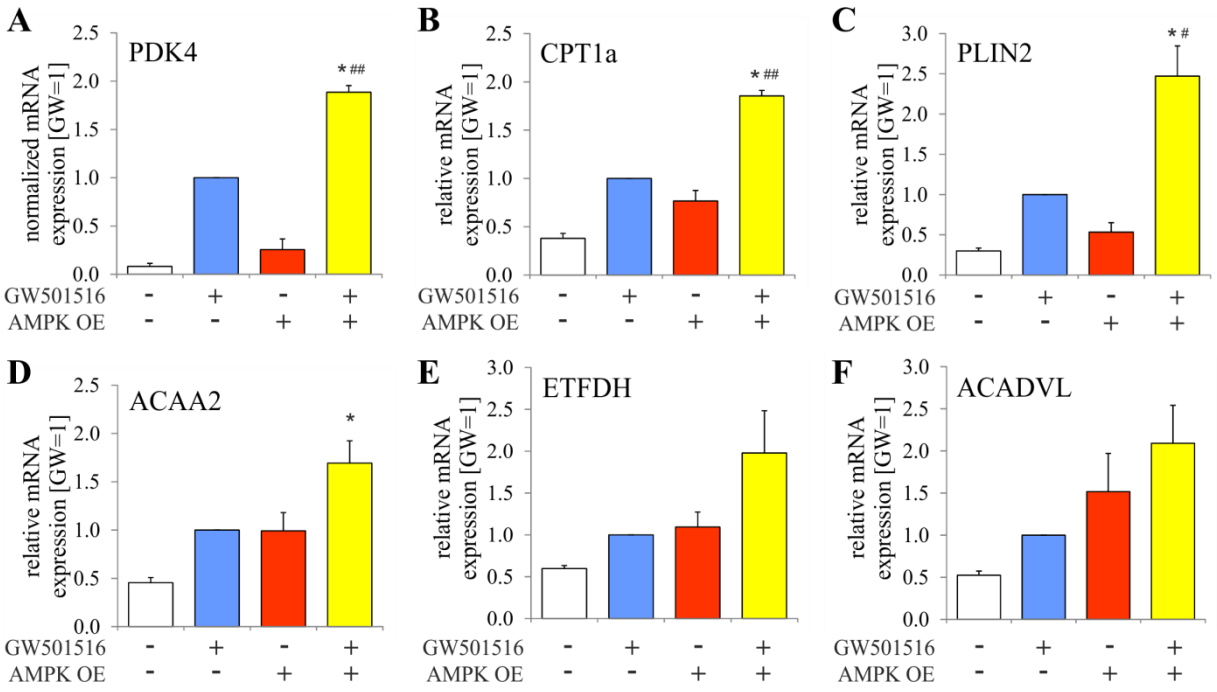

Figure 12: Microarray validation.

The treatments of primary macrophages were performed as in Figure 11 and the colors reflect the same stimulations. mRNA expression levels of PDK4, CPT1a, PLIN2, ACAA2, ETFDH and ACADVL relative to GAPDH were normalized to GW501516 treatment. Statistics were performed using one-way ANOVA. All data are means ± SEM (*, $p \leq 0.05$ vs. GW501516; #, $p \leq 0.05$ vs. AMPK OE, ##, $p \leq 0.01$vs. AMPK OE; n = 3).

The colors reflect the same treatment used during the microarray analysis (Figure 11) and the bars show mRNA expression relative to GAPDH mRNA and normalized to GW501516 treatment. FAO-associated genes are increased by single treatments and additionally enhanced after combined activation of AMPK and PPARδ. The genes PDK4, CPT1a, and PLIN2 exhibit significantly higher gene expression after a co-treatment in comparison to single activation by AMPK OE or GW501516, whereas the expression of ACAA2 significantly increases only in comparison to PPARδ activation (Figure 12 A-D). Other FAO genes ACADVL and ETFDH show a tendency of the elevation after the co-treatment without reaching any significance (Figure 12 E, F).

5.1.2.4. Confirmation of microarray analysis by AMPK activation

As the results should be confirmed, further experiments with the same experimental procedure were needed. Although the effects of overexpressing mutated AMPKα1 were good, I had sometimes problems to generate active transducing lentiviral particles. The reason for this could be either HEK293 cells or medium. The lentiviral generation was also expensive, so I decided to use an AMPK activator to confirm the results of AMPK OE in primary macrophages. I chose A-769662 out of several AMPK activators because of its description as a direct and "specific pharmacological AMPK activator" acting at low concentrations[231].

First, the optimal concentration and time period of A-769662 treatment were of interest. MCSF-differentiated primary macrophages were stimulated with 250 µM and 500 µM A-769662 for 24 h to identify the changes of AMPK phosphorylation and/or its activation following ACC phosphorylation.

As shown by Western analysis (Figure 13), the total AMPK protein amount and its phosphorylated form are almost not affected by the A-769662 binding, whereas the phosphorylation of ACC increases, especially during the treatment with the concentration of 500 µM A-769662.

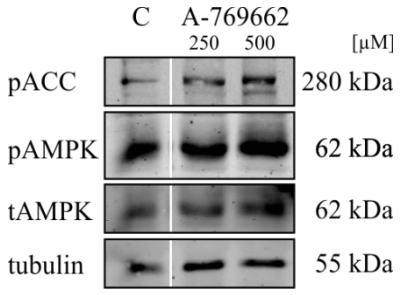

Figure 13: A-769662 stimulation leads to ACC phosphorylation in primary macrophages.
Primary macrophages were treated with 250 or 500 µM A-769662 for 24 h. Western analysis of AMPK and phosphorylated ACC was performed. Tubulin served as a loading control. Blot is representative of at least three independent experiments.

To determine the best time for A-769662 treatment, I performed kinetics experiments and found the greatest effects on gene expression after 24 h.

Further, I raised the question, if the microarray results could be confirmed by allosteric AMPK activation instead of AMPKα1 OE. The first three most affected target genes of the microarray were chosen for RT-PCR analysis. As shown in Figure 14, treatment with A-769662 enhanced the mRNA expression of the PPARδ target genes PDK4 (A), CPT1a (B),

and PLIN2 (C) to a similar extent over the GW501516-stimulation as the exposure of cells to AMPK OE shown in Figure 12. The gene expression increases from 1.5 to 3-fold.

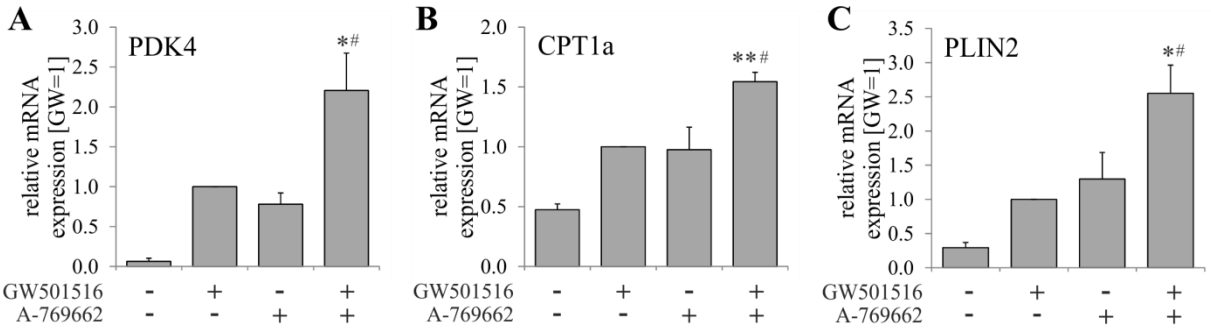

Figure 14: AMPK activation using A-769662 induces expression of PPARδ target genes.
Primary macrophages were stimulated with 500 µM A-769662 and/or 100 nM GW501516 for 24 h. mRNA expression levels of PDK4 (**A**), CPT1a (**B**), and PLIN2 (**C**) were normalized to GAPDH. Statistical analyses were performed using one-way ANOVA. All data are means ± SEM (*, $p \leq 0.05$ vs. GW501516, **, $p \leq 0.01$vs. GW501516; #, $p \leq 0.05$ vs. A-769662; n = 3).

To confirm the mRNA results of additively regulated genes affecting β-oxidation, I analyzed the protein levels of FAO-associated targets PDK4 and CPT1a in primary human macrophages.

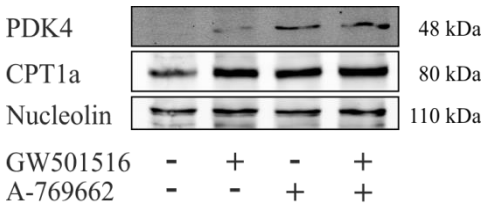

Figure 15: PDK4 and CPT1a protein amounts increase during AMPK and PPARδ activation.
Primary macrophages were stimulated with 500 µM A-769662 and 100 nM GW501516 for 24 h. Western analysis of PDK4 and CPT1a was performed. Nucleolin served as a loading control. Blot is representative of at least three independent experiments.

Western analysis shows an increase of protein expression of PDK4 and CPT1a in response to GW501516 and/or A-769662 compared to control cells (Figure 15). An increase of PDK4 and CPT1a protein levels can be observed in co-activated macrophages in comparison to single GW501516-treated cells. The elevation of protein amount is not that high as the increase of the mRNA expression level. The reason for this phenomenon will be discussed in section 6.2.

5.1.2.5. AMPK activation by A-769662 and its effects in macrophages

The inhibition of protein synthesis by AMPK has been reported via mTOR blocking p70S6 kinase activation[242]. Determining the optimal concentration of 500 µM and treatment duration of 24 h, I also tested cellular effects of A-769662 compound. An interesting question was, if A-769662 appears toxic in primary human macrophages. This approach was implemented determining cell death using FACS analysis as described in section 4.2.1.5 (Figure 16).

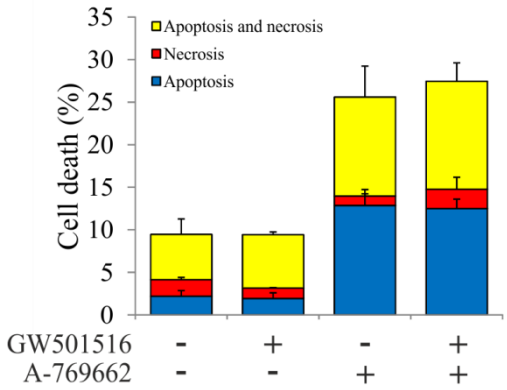

Figure 16: A-769662 treatment causes cell death in human MΦ.

Primary macrophages were treated with 100 nM GW501516 and/or 500 µM A-769662 for 24 h. Cells were harvested, stained with annexin V and propidium iodid in binding buffer for 15 min at 4°C, and analyzed by FACS LSR II Fortessa using software FACSDiva™. Colors indicate the kind of cell death: apoptosis (**blue**), necrosis (**red**), or both (**yellow**).

Annexin V binds to phosphatidylserine identifying apoptotic cells; whereas propidium iondide intercalates with nucleic acids revealing necrotic cells. Using this method, different kinds of cell death can be visualized. PPARδ agonist GW501516 does not have any effect on the cell death in human macrophages. In contrast, A-769662 elevates apoptosis almost 5-fold (Figure 16, blue) in comparison to DMSO- or GW501516-treated macrophages. This effect does not increase in combined activation by GW501516 and A-769662, indicating A-769662 as the sole factor causing macrophage apoptosis under given conditions.

Furthermore, it was interesting to know, whether A-769662 influences intracellular ATP levels in my experimental setting. As a positive control, the cells were treated with an ATP synthase inhibitor oligomycin A (Ol), uncoupling the oxidative phosphorylation, and glycolysis inhibitor deoxyglucose (D) to deplete cellular ATP levels[276]. Both were described as AMPK-dependent inhibitors[277]. Another sample of primary macrophages was stimulated with 500 µM A-769662 for 24 h (Figure 17).

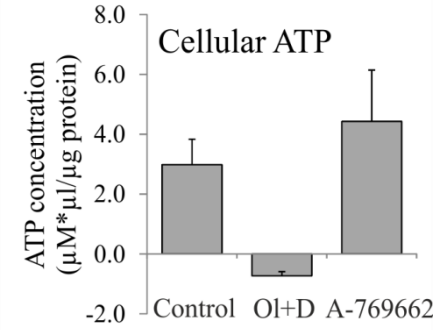

Figure 17: AMPK activation by A-769662 does not cause ATP repletion of primary MΦ.
Primary macrophages were treated with 5 µg/ml oligomycin A (Ol) and 20 mM deoxyglucose (D) for 3 h or with 500 µM A-769662 for 24 h. ATP concentration was measured and normalized to protein amount. Data are means ± SEM.

As shown in Figure 17, oligomycin A and deoxyglucose treatment (Ol+D) completely depleted cellular ATP in primary macrophages within 3 h. Additional samples stimulated with A-769662 show no effect on cellular ATP concentration. No sign of A-769662 toxicity can be observed by this experiment.

5.1.2.6. PPARδ-dependent regulation of angiopoietin-like 4 (Angptl4) and TG degradation

The TG content can be regulated by chylomicron and VLDL uptake on one side and hydrolysis of VLDL triglycerides to FFA by LPL on the other[278]. As PPARδ serves as one of the major regulators of lipid metabolism, it controls cellular TG content through regulation of Angptl4 and FAO gene expression. Angptl4 serves as LPL inhibitor preventing TG hydrolysis on VLDL particles. Previous studies have shown that VLDL-induced TG accumulation is significantly reduced by PPARδ activation reducing LPL activity in THP-1 macrophages[279, 280]. Figure 18 shows the mRNA expression levels of Angptl4 in untreated or GW501516-treated THP-1 and primary human macrophages.

Angptl4 is significantly induced in the THP-1 cell line consistent with previous findings[279], but not in primary macrophages during PPARδ activation. As Angptl4 is hardly expressed in GW501516-stimulated primary human macrophages, PPARδ control of TG accumulation may be predominantly due to the FAO activity.

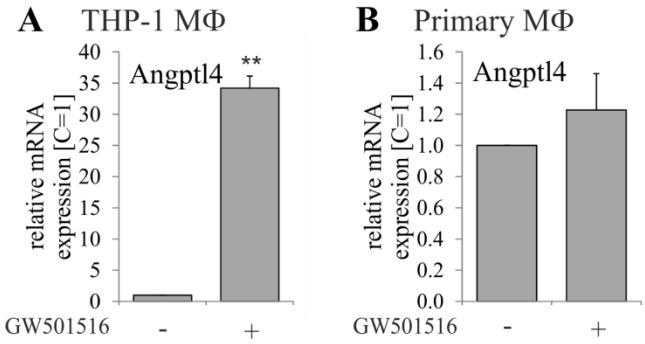

Figure 18: Angptl4 mRNA expression in GW501516-stimulated human MΦ.

THP-1 or primary macrophages were treated with 100 nM GW501516 for 24 h. Angptl4 mRNA expression was normalized to GAPDH expression level. Statistical analysis was performed using unpaired student´s *t*-test. Data are means ± SEM (**, $p \leq 0.01$; n = 3).

As PPARδ activation has no effect on LPL in primary macrophages, only FAO-associated gene expression leads to a change of cellular TG content (Figure 18). To confirm the results of AMPK/PPARδ co-activation, measurement of the TG content in primary macrophages after the stimulations with GW501516 and A-769662, followed by additional treatment with VLDL for 24 h, was performed. The results were normalized to VLDL-stimulated foam cells (Figure 19).

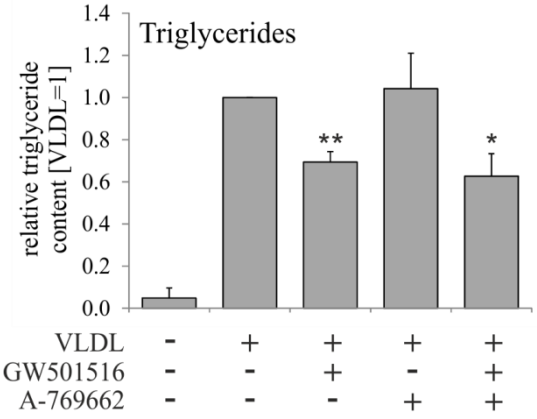

Figure 19: PPARδ activation increases TG degradation in foam cells.

Primary macrophages were treated with 100 nM GW501516 and/or 250 µM A-769662 for 48 h. VLDL (20 µg/ml) stimulation occurred for additional 24 h. TG content was normalized by protein concentration. Statistical analyses were performed using unpaired student´s *t*-test. Data are means ± SEM (*, $p \leq 0.05$ vs. VLDL, **, $p \leq 0.01$ vs. VLDL; n = 6).

The stimulation with VLDL leads to cellular TG accumulation leading to foam cell formation shown in Figure 19. Relative triglyceride content achieves here 10-fold increase in VLDL-treated macrophages. Additional treatment with GW501516 significantly reduces TG

content. During the measurement, no decrease of TG could be observed after the AMPK activation. Figure 14 shows increased FAO gene expression after the co-stimulation with A-769662 and GW501516. Interestingly, co-activated macrophages show no stronger reduction of TG content compared to single PPARδ activation and VLDL-treatment.

5.1.2.7. AMPK action on PPARδ target genes is PPARδ-dependent

Further question I addressed in this project was how AMPK and PPARδ are involved into the activation of PPARδ target genes. For this approach a silencing of PPARδ by specific siRNA and stimulation of primary macrophages with A-769662 or GW501516 were performed (Figure 20).

Figure 20 shows that PPARδ silencing (siPPARδ) achieves a 72% KD compared to siControl (siC) treatment (A) and elevates the basal expression of PPARδ target genes PDK4 (B), CPT1a (C), PLIN2 (D), ACAA2 (E), ETFDH (F), ACADM (G), and ACADVL (H). As expected, PPARδ activation by GW501516 leads to increased mRNA expression levels of these genes in siC macrophages.

It has been reported that ligand-free PPARδ represses its target gene expression[86]. This phenomenon can be observed in this experiment, too. Non-stimulated PPARδ KD leads to an elevation of PPARδ target gene mRNA compared to non-stimulated siC macrophages (Figure 20 B-H). Interestingly, PPARδ target genes do not respond to GW501516 or to A-769662 stimulation in siPPARδ macrophages indicating the AMPK action through PPARδ.

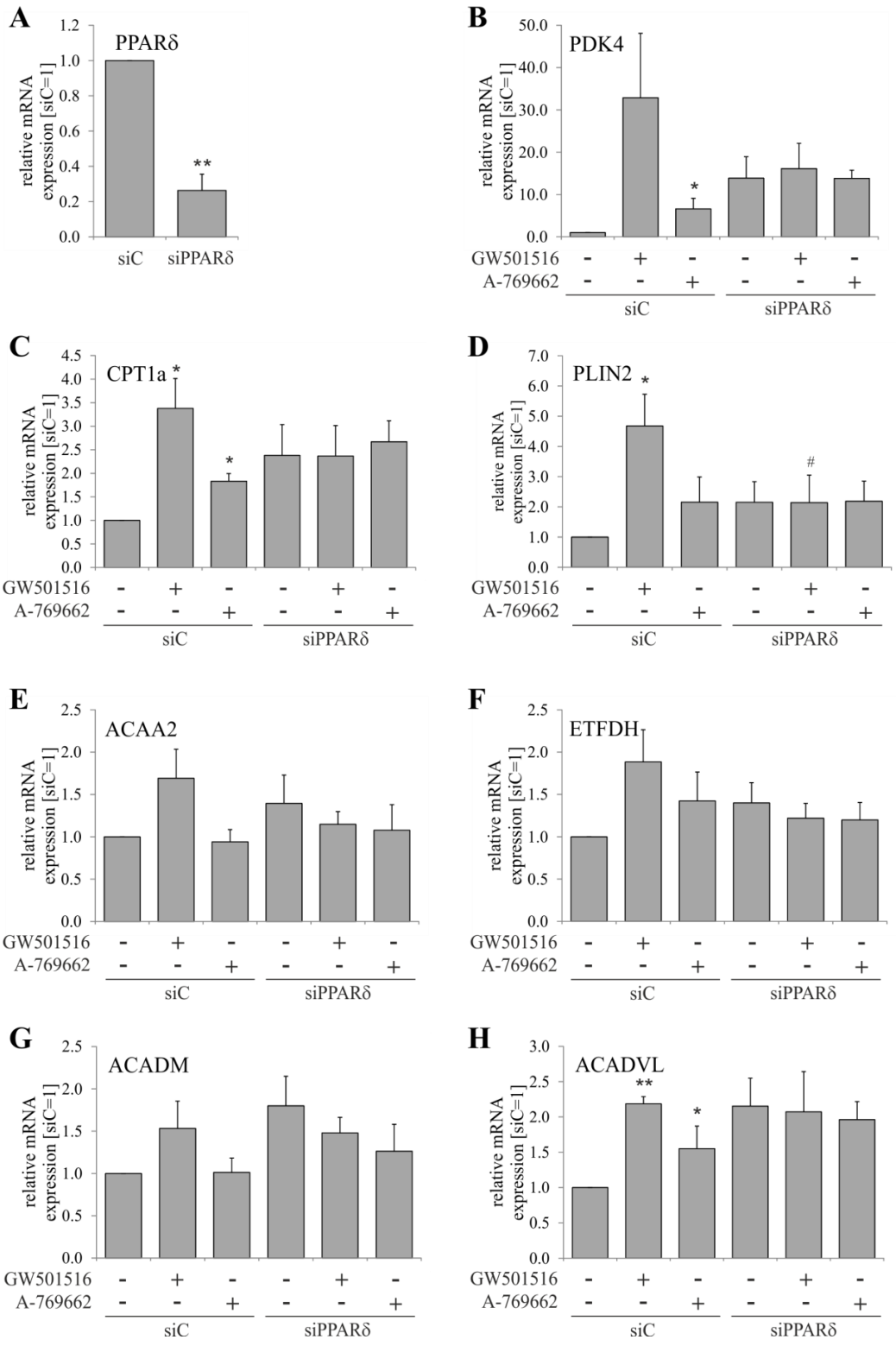

Figure 20: AMPK activates PPARδ target genes through PPARδ.

Primary macrophages were transfected with 50 nM scrambled control (siC) or PPARδ siRNA (siPPARδ) for 72 h and treated with 100 nM GW501516 or 500 µM A-769662 for additional 24 h. mRNA levels of PPARδ (**A**), PDK4 (**B**), CPT1a (**C**), PLIN2 (**D**), ACAA2 (**E**), ETFDH (**F**), ACADM (**G**), and ACADVL (**H**) were normalized to GAPDH expression. Statistics were performed using unpaired student´s *t*-test. All data are means ± SEM (*, $p \leq 0.05$ vs. siC, **, $p \leq 0.01$ vs. siC; #, $p \leq 0.05$ vs. siC+GW; n = 3).

5.2. AMPK regulates ABCA1 via dephosphorylation of the transcription factor LXRα

Previous studies of our laboratory indicated that AMPK influences ABCA1 expression during the monocyte-to-macrophage differentiation[281]. There was no evidence of this effect in literature at that moment. In this project I concentrated on the mechanism of ABCA1 regulation by AMPK in human macrophages.

5.2.1. AMPK OE or activation increases ABCA1 expression and cholesterol efflux in human macrophages

First, previous findings of our laboratory should be confirmed. To test the changes of ABCA1 expression, primary human macrophages overexpressing truncated AMPKα1 subunit or A-769662-treated for 24 h were analyzed. ABCA1 mRNA and protein expression levels were determined and shown in Figure 21.

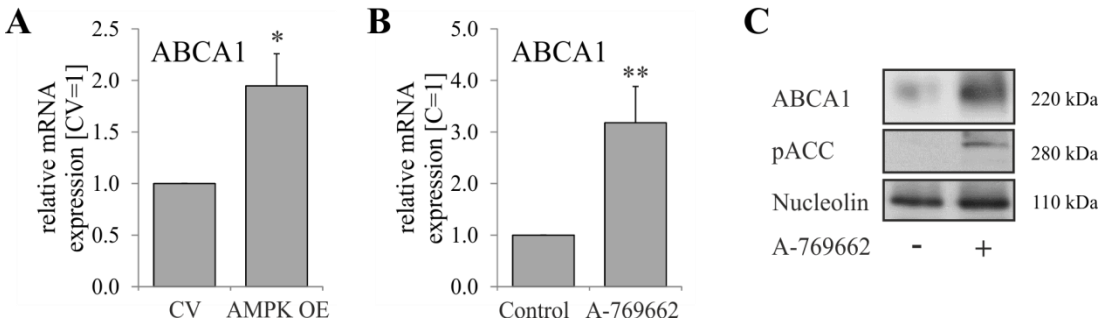

Figure 21: AMPK up-regulates ABCA1 expression in primary human MΦ.

A Primary macrophages were transduced with control (CV) or AMPKα1-containing lentiviral particles (AMPK OE) for 48 h as in Figure 10 A-D. **B** Primary macrophages were stimulated with 500 µM A-769662 for 24 h. mRNA expression of ABCA1 was normalized to GAPDH expression levels. Statistical analyses were performed using unpaired student´s *t*-test. Data are means ± SEM (*, $p \leq 0.05$ vs. CV, **, $p \leq 0.01$ vs. C; $n = 4$). **C** Primary macrophages were treated as in **B** and cell lysates were analyzed on Western blot. Nucleolin served as a loading control. Blot is representative of at least three independent experiments.

AMPKα1 OE leads to a significant 2-fold up-regulation of ABCA1 mRNA (Figure 21 A). Almost 3-fold increase of ABCA1 mRNA can be observed after the AMPK activation by A-769662 (Figure 21 B). Also ABCA1 protein expression is increased in A-769662-treated cells as shown in Figure 21 C. The enhanced phosphorylation of ACC confirms increased AMPK activity.

Furthermore, the AMPK-dependency of ABCA1 regulation was checked by AMPKα1 KD (Figure 8). THP-1 monocytes were stably transduced with control (CV) or AMPKα1 KD lentiviral particles and were differentiated into macrophages and stimulated with A-769662 (Figure 22).

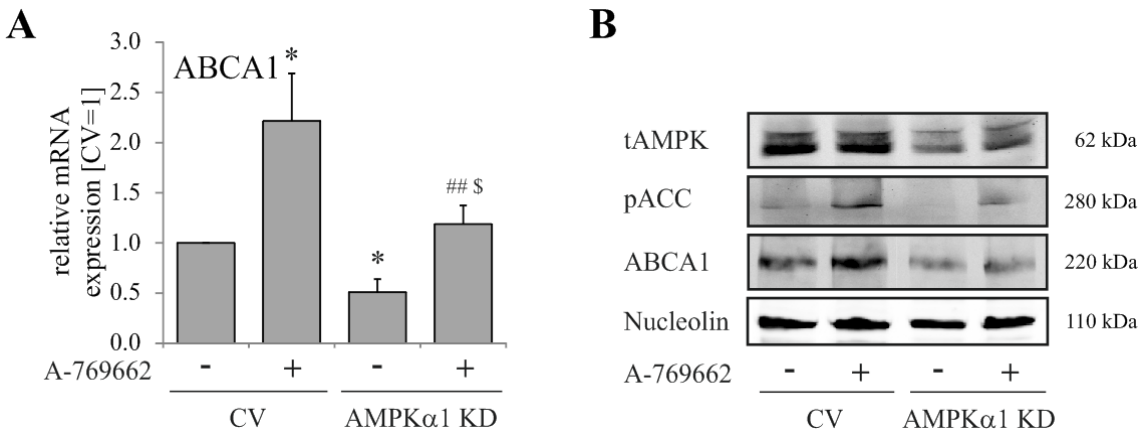

Figure 22: AMPKα1 KD affects ABCA1 mRNA and protein expression levels.

THP-1 monocytes were transduced with 500 µl control (CV) or AMPKα1 KD lentiviral particles and incubated for 24 h. Following selection by puromycin, THP-1 monocytes were differentiated to macrophages by 100 nM TPA-treatment for 48 h and treated with 500 µM A-769662 for additional 24 h. **A** ABCA1 mRNA levels are shown relative to GAPDH. Statistics were performed using unpaired student´s *t*-test. All data are means ± SEM (*, $p \leq 0.05$ vs. CV; ##, $p \leq 0.01$ vs. CV+A-769662; $, $p \leq 0.05$ vs. AMPK KD; n = 4). **B** Cell lysates were analyzed using Western blot. Nucleolin served as a loading control. Blot is representative of at least three independent experiments.

AMPK activation by A-769662 significantly increases ABCA1 mRNA in CV THP-1 macrophages (Figure 22 A). AMPKα1 KD significantly reduces the ABCA1 gene expression, which can be restored by A-769662. AMPK activation shows also here a significant effect compared to non-treated AMPKα1 KD macrophages.

The protein level of ABCA1 elevates in A-769662-treated cells showing higher ACC phosphorylation (pACC) compared to CV indicating increased AMPK activity (Figure 22 B). AMPKα1 KD causes a reduction of total AMPK, pACC, and ABCA1 proteins indicating ABCA1 regulation by AMPKα1. The ABCA1 protein levels of A-769662-stimulated AMPKα1 KD macrophages are due to mRNA expression.

Cellular cholesterol efflux capacity is dependent on ABCA1 expression level[50]. The interesting question was, if the increased ABCA1 expression by AMPK also results in increased activity, transferring cholesterol out of the cell and loading apoAI. The detailed

protocol of cholesterol assay can be found in section 4.2.4.9. Shortly, THP-1 macrophages were loaded with acLDL first, stimulated with A-769662, and treated with a cholesterol acceptor apoAI (Figure 23).

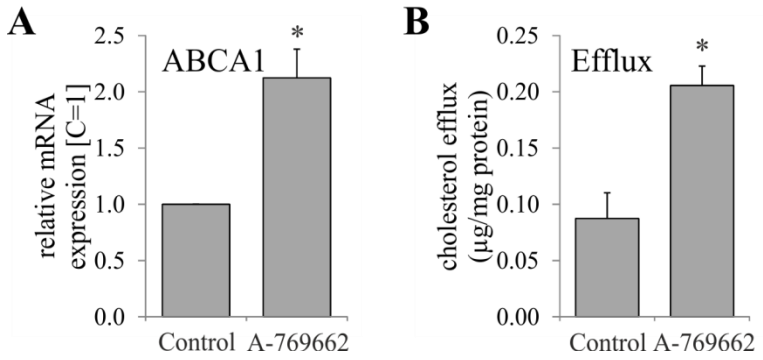

Figure 23: AMPK activation increases ABCA1 activity elevating cholesterol efflux in human MΦ.
A THP-1 macrophages were stimulated with DMSO (Control) or 500 µM A-769662 for 24 h. ABCA1 mRNA was normalized to GAPDH expression (n = 4). **B** THP-1 macrophages were pre-treated with 50 µg/ml acLDL for 8 h, stimulated with DMSO or 250 µM A-769662 for 24 h and treated with 10 µg/ml apoAI for additional 16 h. The fluorescence of cholesterol derivate was measured at 590 nm and normalized to protein concentration of each sample (n = 5). Statistical analyses were performed using unpaired student´s *t*-test. Data are means ± SEM (*, $p \leq 0.05$).

Figure 23 A demonstrates a 2-fold increase of ABCA1 mRNA after AMPK stimulation in THP-1 macrophages. Results of cholesterol efflux shown in B confirm the mRNA and protein findings in primary cells revealing a significantly higher activity of ABCA1 during the AMPK activation in human macrophages.

5.2.2. ABCA1 regulation occurs not via PPARs but through LXRα

Since AMPK influences PPARδ activity and ABCA1 was shown to be regulated by PPARδ in some cellular systems[89, 102, 282], the major question appeared, if PPARδ or other PPAR subtypes are involved in the mechanism of ABCA1 regulation. Besides, some other publications indicate the participation of PPARs in ABCA1 regulatory mechanism[81, 101, 180]. To question the involvement of PPARs, silencing of PPAR subtypes in primary human macrophages was performed. Besides, appropriate activation of PPAR was monitored using the compound GW7647 as PPARα agonist, whereas Rosiglitazone served to activate PPARγ.

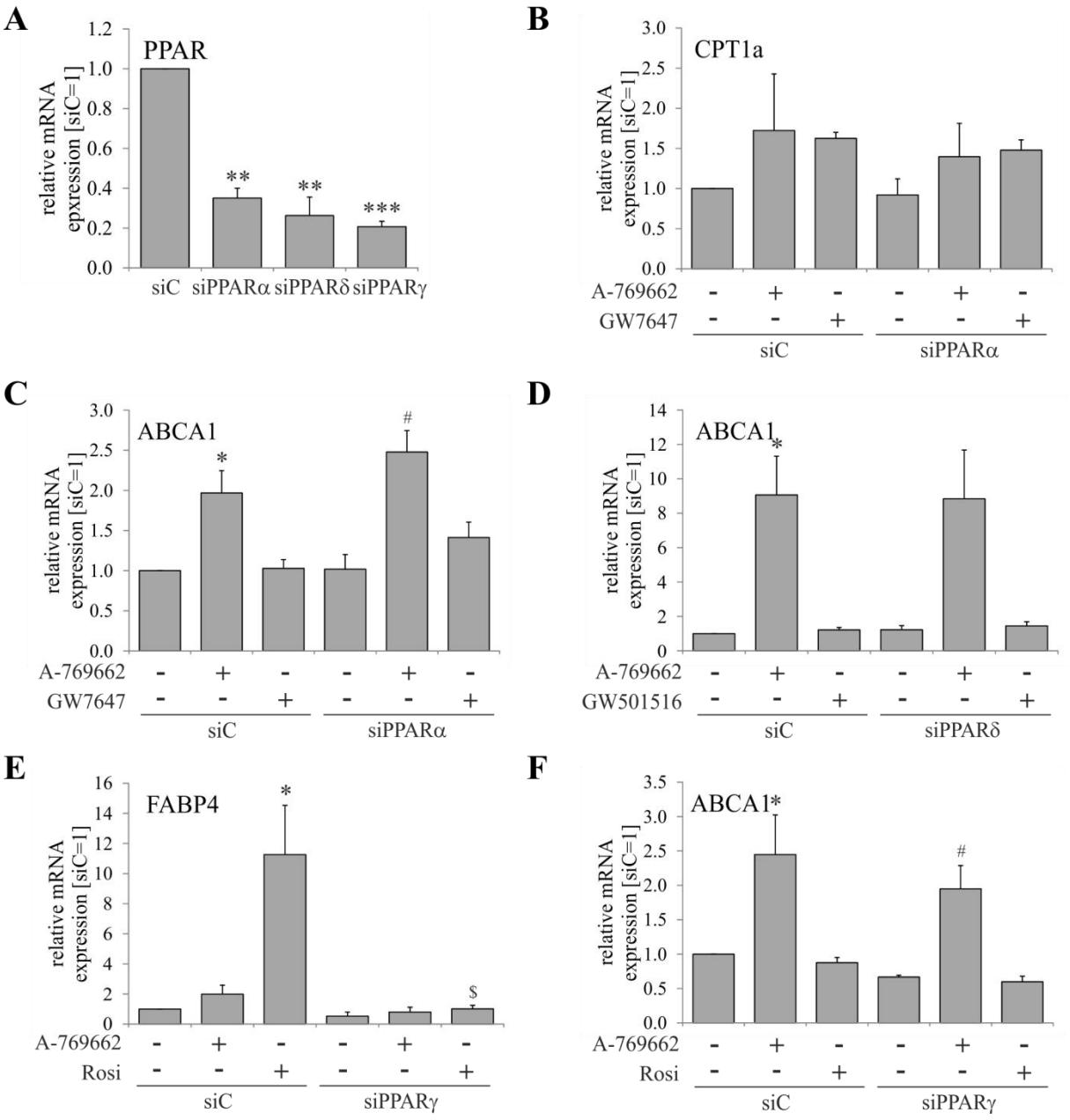

Figure 24: ABCA1 expression is not regulated by PPARα, PPARδ or PPARγ in human MΦ.

Primary macrophages were transfected with 50 nM of scrambled control siRNA (siC) or PPARα (siPPARα), PPARδ (siPPARδ), and PPARγ (siPPARγ) siRNAs for 72 h (**A**) and stimulated with 500 µM A-769662 or particular PPAR activator for additional 24 h (**B-F**). 100 nM GW7647, 100 nM GW501516, and 1 µM Rosiglitazone (Rosi) were used. mRNA levels of PPARα, PPARδ, PPARγ (**A**), CPT1a (**B**), FABP4 (**E**), and ABCA1 (**C, D, F**) are shown relative to GAPDH expression. Statistical analyses were performed using unpaired student´s *t*-test. All data are means ± SEM (*, $p \leq 0.05$ vs. siC, **, $p \leq 0.01$ vs. siC, ***, $p \leq 0.001$ vs. siC; #, $p \leq 0.05$ vs. siPPAR; $, $p \leq 0.05$ vs. siC+Rosi; $n \geq 3$).

Figure 24 A shows significant silencing of each PPAR subtype by siRNAs in primary macrophages. The mRNA of CPT1a and FABP4 serve as positive controls for functional PPARα and PPARγ activation (B, E). PPARδ-dependent genes have already been shown in

Figure 20. In case of FABP4, Rosiglitazone significantly increases its expression 11-fold in primary macrophages treated with siControl (siC). PPARγ KD abolishes this effect showing unchanged expression levels after Rosiglitazone stimulation. The RT-PCR results of ABCA1 mRNA expression levels (C, D, F) indicate no regulation by any of PPARs, where neither activation nor silencing of PPARs affect ABCA1 mRNA. AMPK activation up-regulates ABCA1 in siC as well as in PPAR KD cells.

Some publications indicate the involvement of LXRα in the regulation of ABCA1 protein[190, 283]. I wanted to find out, if ABCA1 regulation is really LXRα-dependent using LXRα KD and simultaneous AMPK activation in primary macrophages (Figure 25).

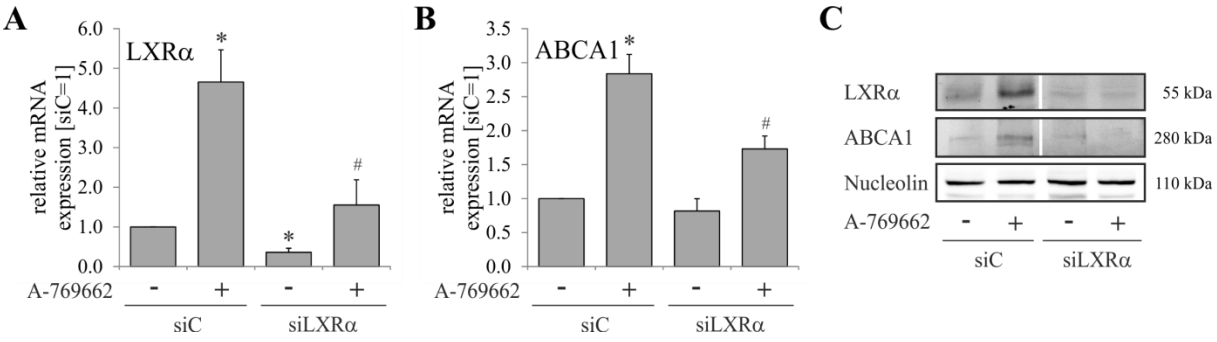

Figure 25: LXRα silencing causes a reduction of ABCA1 mRNA and protein in primary MΦ.

Primary macrophages were transfected with 50 nM of scrambled control siRNA (siC) or LXRα siRNA (siLXRα) for 72 h and stimulated with 500 µM A-769662 for additional 24 h. mRNA levels of LXRα (**A**) and ABCA1 (**B**) are shown relative to GAPDH expression. Statistics were performed using unpaired student´s *t*-test. All data are means ± SEM (*, $p \leq 0.05$ vs. siC; #, $p \leq 0.05$ vs. siC+A-769662; n = 3). **C** Cell lysates were analyzed using Western blot. Nucleolin served as a loading control. Blot is representative of at least three independent experiments.

AMPK activation by A-769662 induces the LXRα and ABCA1 expression on mRNA, but also protein levels (Figure 25 A-C). LXRα KD (siLXRα) leads to significantly reduced LXRα expression levels (A, C). The LXRα mRNA and protein induction by A-769662 is present in siC macrophages but is significantly reduced in siLXRα cells (A), which is also reflected by protein levels (C). Also ABCA1 mRNA drops during A-769662-treatment in LXRα KD primary macrophages compared to siC cells, whereas silencing of LXRα alone does not affect the expression of ABCA1 (B). Western blot reflects the results of mRNA expression levels (C).

Some reports indicate LXRα regulation by PPARs[184, 284]. To investigate, if LXRα induction is PPAR-dependent or not, LXRα mRNA expression in PPAR KD macrophages was checked (Figure 26). Here, RT-PCR of LXRα in PPAR KD cells (Figure 24) was performed.

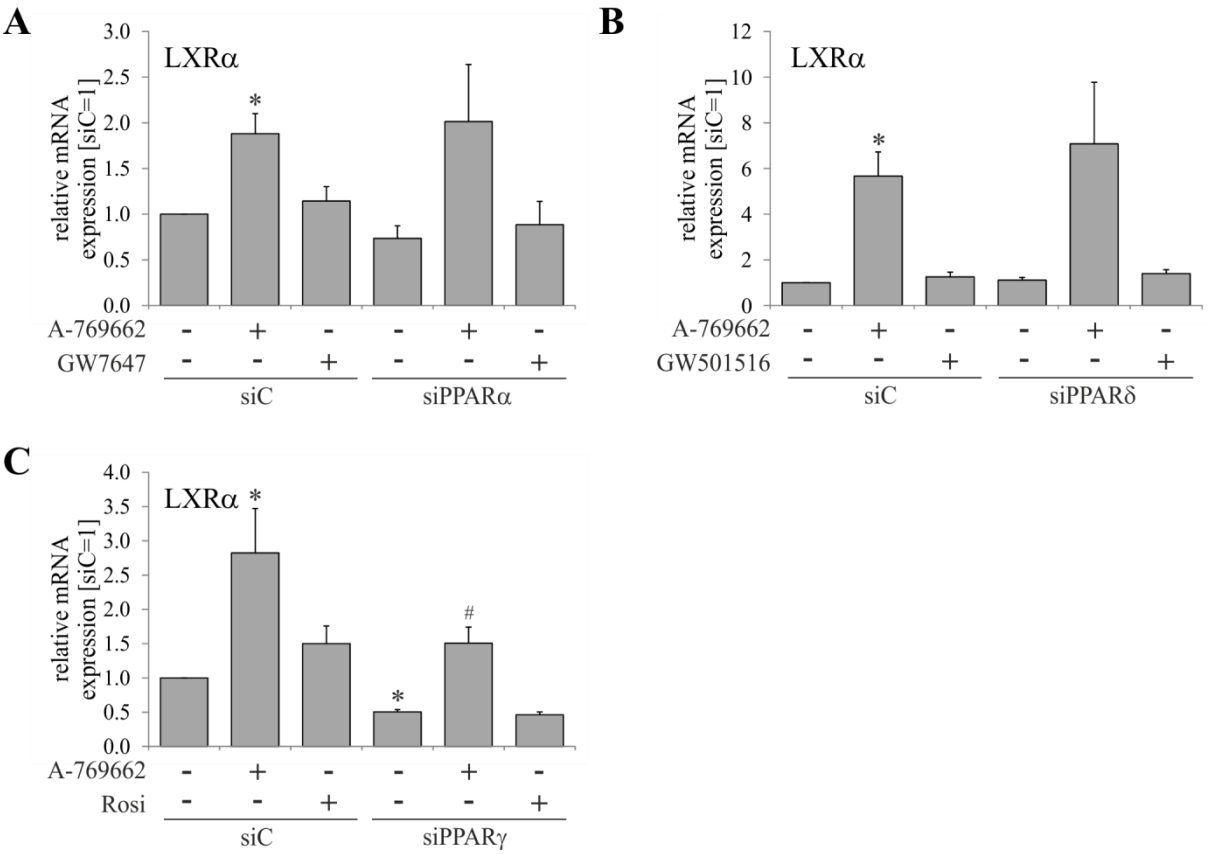

Figure 26: LXRα mRNA expression is not dependent on PPARα and PPARδ, but on PPARγ.

The experimental procedure was performed as in Figure 24. mRNA levels of LXRα are shown relative to GAPDH expression. Statistical analyses were performed using unpaired student´s *t*-test. All data are means ± SEM (*, $p \leq 0.05$ vs. siC; #, $p \leq 0.05$ vs. siC+A-769662; n = 3).

The PPAR activators GW7647, GW501516, and Rosiglitazone do not affect gene expression of LXRα shown in Figure 26. LXRα mRNA expression seems to be neither PPARα- nor PPARδ-dependent (A, B), whereas PPARγ KD significantly reduces LXRα mRNA (C). Also the induction by A-769662 treatment is significantly down-regulated in PPARγ-silenced primary macrophages indicating LXRα transcription dependency on PPARγ.

A recent report described ABCA1 regulation by AMPK dependent on LXRβ and ATF1[285]. Thus, both transcription factors were silenced to look, if ABCA1 expression is really LXRβ- or ATF1-mediated in MCSF-differentiated macrophages (Figure 27 and Figure 28).

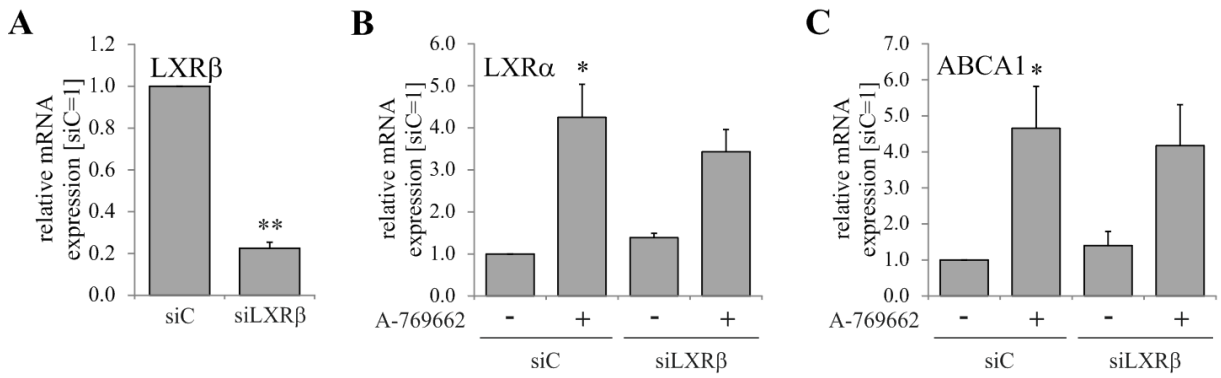

Figure 27: LXRα and ABCA1 are not regulated by LXRβ in primary MCSF-differentiated MΦ.
Primary macrophages were transfected with 50 nM of scrambled control siRNA (siC) or LXRβ siRNA (siLXRβ) for 72 h and stimulated with 500 µM A-769662 for additional 24 h. mRNA levels of LXRβ (**A**), LXRα (**B**), and ABCA1 (**C**) are shown relative to GAPDH expression. Statistics were performed using unpaired student´s *t*-test. All data are means ± SEM (**, $p \leq 0.01$ vs. siC; n = 3).

Figure 27 A shows significant down-regulation of LXRβ mRNA expression by siRNA. This treatment does not have any effect on LXRα or ABCA1 mRNA (B, C).

Figure 28 reveals the effect of ATF1 KD in primary macrophages. Significant silencing of ATF1 (A) does not influence the mRNA levels of LXRα or ABCA1 (B, C). The significant increase of both mRNAs after an A-769662 treatment remains unchanged in ATF1-silenced primary macrophages.

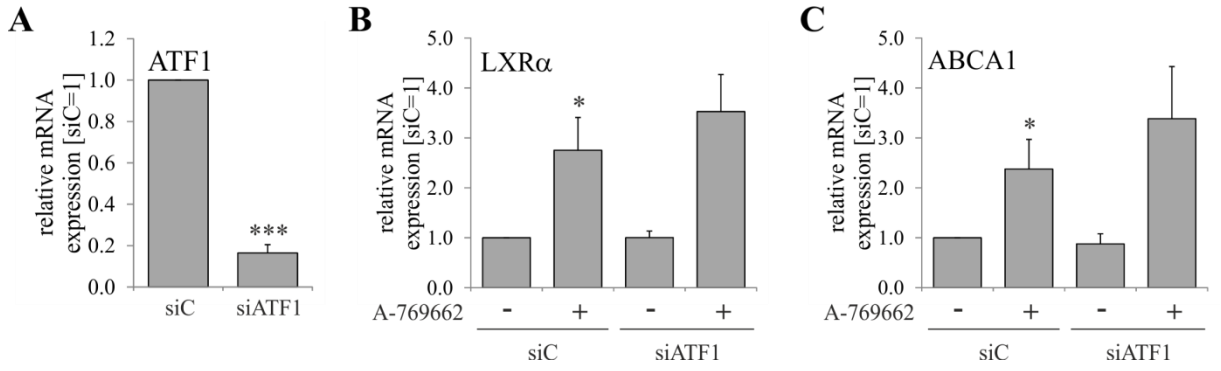

Figure 28: Neither LXRα nor ABCA1 are ATF1-dependent in primary MCSF-differentiated MΦ.
Primary macrophages were transfected with 50 nM of scrambled control siRNA (siC) or ATF1 siRNA (siATF1) for 72 h and stimulated with 500 µM A-769662 for additional 24 h. mRNA levels of ATF1 (**A**), LXRα (**B**), and ABCA1 (**C**) are shown relative to GAPDH expression. Statistics were performed using unpaired student´s *t*-test. All data are means ± SEM (*, $p \leq 0.05$ vs. siC, ***, $p \leq 0.001$ vs. siC; n = 3).

Furthermore, I wanted to prove the ABCA1 dependence on LXRα using a reporter system. The used luciferase pGL3 constructs were kindly provided by the group of A. J. Brown (The

University of New South Wales in Sydney, Australia). These include a regulatory region (-922 to +113 bp) of *Abca1* promoter[286]. The region prior the start codon contains LXRE site (-62 to -47 bp) where LXR protein can bind to induce transcriptional activation. One construct (mutABCA1) contained mutated LXRE site with 5 exchanged bp (CTTTG**TGT**GATAGTAAC**TA**CT → CTTTG**ACC**GATAGTAAC**CT**CT), so that the LXR-binding cannot occur (Figure 29 A). In this experiment, the concentration of 250 µM A-769662 have been chosen to avoid additional cell stress and apoptosis, already caused during the transfection by jetPrime.

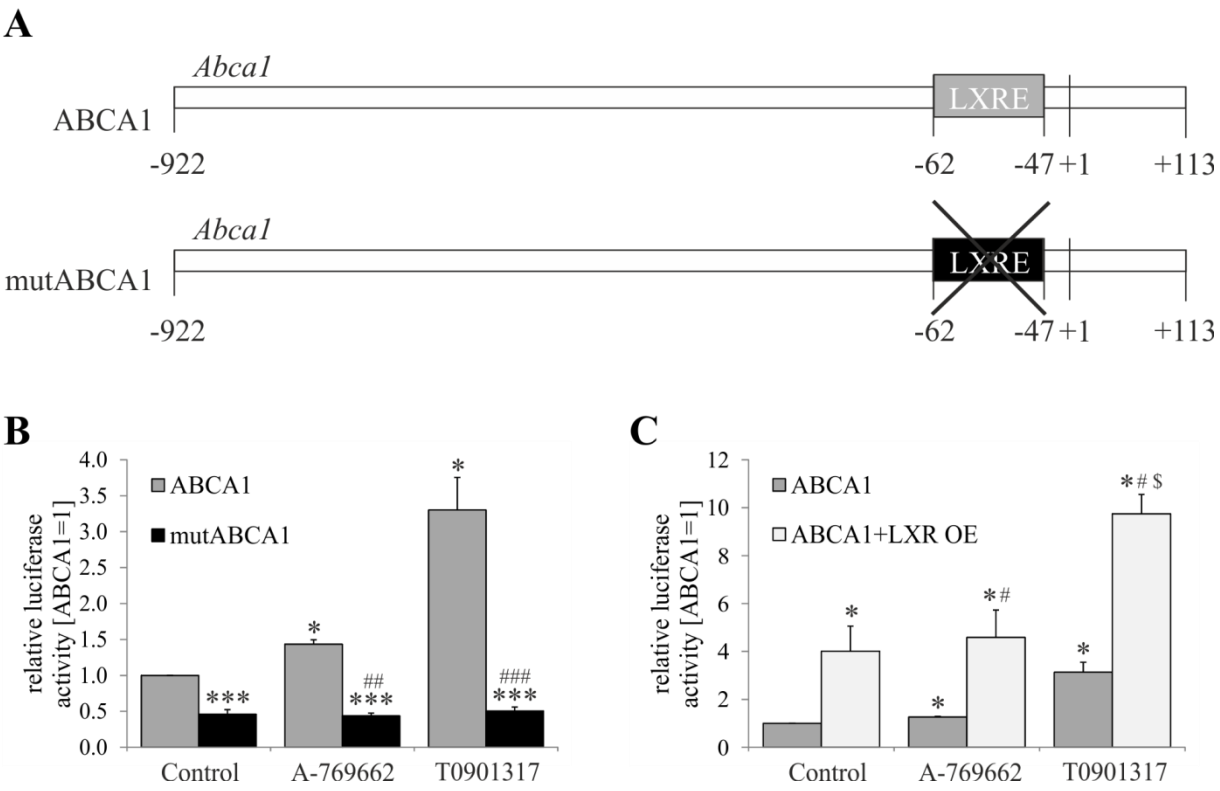

Figure 29: LXRE of *Abca1* gene is essential for ABCA1 expression by LXRα.

A Luciferase constructs containing wild-type (ABCA1) or mutated *Abca1* promoter region (mutABCA1). The second construct includes CTTTG**TGT**GATAGTAAC**TA**CT → CTTTG**ACC**GATAGTAAC**CT**CT mutation in LXRE site. **B** HepG2 cells were transfected with constructs ABCA1 and mutABCA1 for 24 h and stimulated with 250 µM A-769662 or 1 µM T0901317 for additional 24 h. **C** ABCA1 construct was transfected with control or LXRα OE plasmid for 24 h into HepG2 cells. Treatment with 250 µM A-769662 or 1 µM T0701317 for additional 24 h followed. Statistical analyses were performed using unpaired student´s *t*-test. All data are means ± SEM (*, $p \leq 0.05$ vs. ABCA1, ***, $p \leq 0.001$ vs. ABCA1; #, $p \leq 0.05$ vs. ABCA1 with same treatment, ##, $p \leq 0.01$ vs. ABCA1 with same treatment, ###, $p \leq 0.001$ vs. ABCA1 with same treatment; $, $p \leq 0.05$ vs. LXRα OE; n = 3).

The transfection of HepG2 cells with shown constructs leads to different results. ABCA1 construct including WT LXRE site can be expressed. The LXR agonist T0901317 serving as positive control, but also A-769662 significantly increases reporter activity (B). In contrast, mutated LXRE site of *Abca1* inhibits the LXRα-binding causing significant reduction of luciferase activity. Both stimulations cannot restore the luciferase activity in transfected HepG2 with a mutated luciferase construct showing the dependence of LXR binding on LXRE site in the *Abca1* promoter.

The transfection with additional LXRα OE plasmid besides the ABCA1 construct significantly increases the luciferase activity in untreated and A-769662- or T0901317-treated cells (Figure 29 C). Whereas T0901317 causes significant reporter activation in LXRα OE cells, the difference between the untreated and A-769662-treated LXRα OE cells is not significant. The value of luciferase activity in AMPK-activated LXRα OE cells is too variable to get significance compared to non-treated ABCA1+LXR OE cells. Taken together, the results in Figure 29 confirm the LXRα-dependency of ABCA1 expression in human cells.

LXR heterodimerizes with RXR and binds to a consensus sequence DR4 in the ABCA1 proximal promoter region, which is highly conserved between murine and human genes to induce ABCA1 transcription[287, 288]. In Figure 25 and Figure 27 I can confirm the results in primary macrophages that only LXRα, but not LXRβ, binds to the *Abca1* promoter[283]. During my study, the AMPK effect on LXRα binding to DR4 sequence can be shown by ChIP experiment described in section 4.2.4.7. Two different polyclonal antibodies were used: IgG and LXRα. IgG was applied as a negative control. As sphingomyelin phoshodiesterase acid-like 3A (SMPDL3A) is described as a LXRα target gene[289], it serves as a positive control in this experiment. Furthermore, AMPK silencing was used to prove AMPK-dependent LXRα binding to the *Abca1* promoter region.

Figure 30 shows a direct interaction between LXRα protein and LXRE site of the *SMPDL3A* and *Abca1* promoter sequences. LXRα antibody binds more than 3-fold (A) and 5-fold (B) stronger to the LXRE site as IgG does in CV-transduced THP-1 macrophages. During AMPK activation by A-769662 and AMPK silencing, IgG binding remains unchanged (A, B). The binding of LXRα increases by A-769662 treatment and drops significantly in AMPK KD cells. The effect of AMPK activation can partly be observed, but is still reduced

during the AMPK silencing in THP-1 macrophages indicating regulation of LXRα-mediated genes by AMPK.

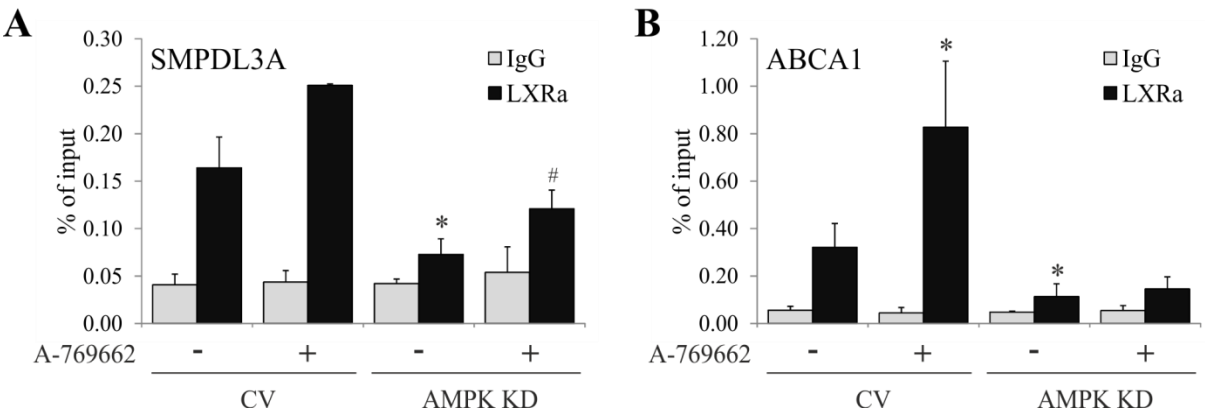

Figure 30: LXRα binding to LXRE in *Abca1* promoter mediates ABCA1 expression by AMPK.
ChIP analysis of LXRα binding to SMPDL3A (A) and ABCA1 (B) LXRE promoter site in CV or AMPKα1 KD THP-1 macrophages treated with 500 µM A-769662 for 6 h. Statistical analyses were performed using unpaired student´s *t*-test. All data are means ± SEM (*, $p \leq 0.05$ vs. LXRα in CV; #, $p \leq 0.05$ vs. LXRα in A-769662-stimulated CV; n = 3).

These results prove the AMPK-dependent ABCA1 regulation by LXRα protein, which binds to the LXRE site of *Abca1* promoter.

5.2.3. AMPK may regulate ABCA1 by dephosphorylation of LXRα

MS is a powerful technique to analyze modifications of proteins measuring ionized peptides. I attempted to identify the post-translational LXRα modifications during AMPK activation and to determine how AMPK alters LXRα to regulate ABCA1 expression. As the LXRα OE was difficult to perform in primary macrophages, I chose HepG2 cells as a suitable system to overexpress this protein in large amounts. Thus, LXRα-overexpressing HepG2 cells were treated with DMSO or A-769662 for 6 h. After IP using LXRα antibody, the band corresponding to LXRα protein (55 kDa) was identified in the Western blot, cut out of the gel and analyzed by MS. Quantification was performed by integration of the MS signal in a label-free approach. In addition we and our collaboration partners used the method of SILAC to robustly quantify the changes of post-translational modifications of LXRα protein. The method is described in detail in section 4.2.4.6 and visualized in Figure 31.

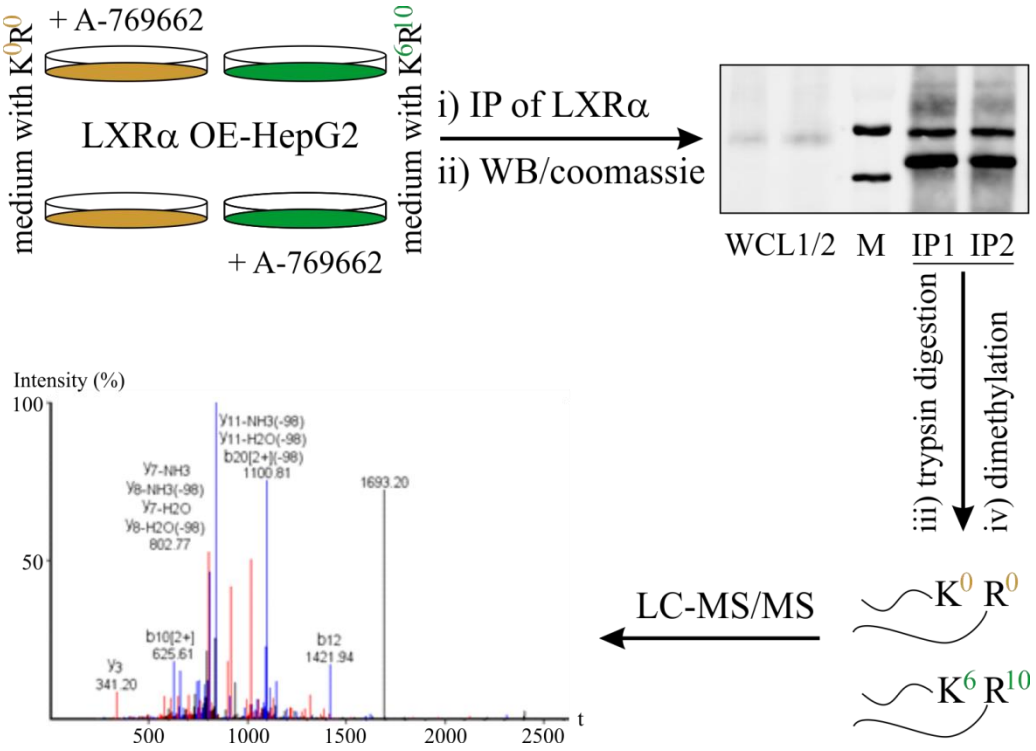

Figure 31: Visualization of the SILAC method.

LXRα-overexpressing HepG2 cells were cultivated either in normal (orange) or in SILAC medium (green) for 7 passages and stimulated with either DMSO or 250 µM A-769662 for 6 h. Cells were harvested for IP and IP of LXRα followed whereas two mixtures were prepared as described in section 4.2.4.6. After identification of LXRα protein by Western blot, the LXRα band was cut out of the Coomassie-stained gel, trypsinized, and analyzed by LC-MS/MS. Peptide fragmentation induces the formation of N-terminal (b, blue) and C-terminal (y, red) ions as shown in Figure 32.

First, I incubated the HepG2 cells in normal (label-free) or SILAC medium for 7 passages. Both conditions contained DMSO- and A-769662-treated cells for 6 h. After the IP of LXRα, samples of DMSO-treated cells grown in normal medium and of A-769662-treated cells grown in SILAC medium were mixed. In the reverse experiment samples of DMSO-treated cells grown in SILAC medium and of A-769662-treated cells grown in normal medium were put together for later quantification as described in section 4.2.4.6. Finally, LXRα protein could be definitely identified in the gel lysates by MS. During the peptide fragmentation, fragment ions are formed based on different energy contents, which determine observed breakings of -C-C-, -C-N-, and -N-C- bonds. Figure 32 shows the nomenclature of peptide fragmentation describing the most common MS-MS fragmentation events and the resulting ions.

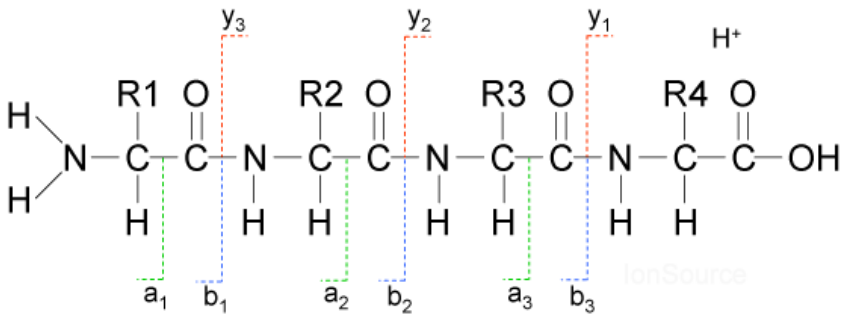

Figure 32: Peptide fragmentation nomenclature in mass spectra.

The formed ions by fragmentation in low energy collisions are a (green dotted line), b (blue dotted line) and y (red dotted line). The a ions describe the -C-C- bond and are low abundant. The b ions extend from the N-terminus, and y ions – from the C-terminus of a peptide[290].

The statistical breakage of all peptide bonds and simultaneous detection of the resulting charred peptide fragment ions results in the observed spectrum (Figure 33). However, some peptide bonds break more easily than others and the fragments are thus observed more abundantly than others.

The MS measurement determines the precise mass of the peptides thereby the MS-MS analysis shows the distances of contained peptide ions and recognizes light and heavy AA. The combination of both datasets allows the definitive peptide identification. Our collaboration partners used LTQ Orbitrap XL™ ETD Hybrid Ion Trap-Orbitrap mass spectrometer which gives precise MS data. Later, another Q Exactive™ Hybrid Quadrupole-Orbitrap mass spectrometer was used to generate MS-MS spectra of SILAC samples with higher mass accuracy in order to analyze post-translational modifications more precisely.

The fragmentation of the first sample containing cell lysates cultivated in normal medium and A-769662-stimulated lysates incubated in SILAC medium is shown in Figure 33. Each blue dot indicates a peptide fragment of trypsinized LXRα sample. As dots lay on one correlation line, homogenous distribution reveals well performed SILAC experiment. Constant intensity indicates very well coverage of the structure, preparation, and performance of both IP and MS, which is an important requirement for the concluding statement.

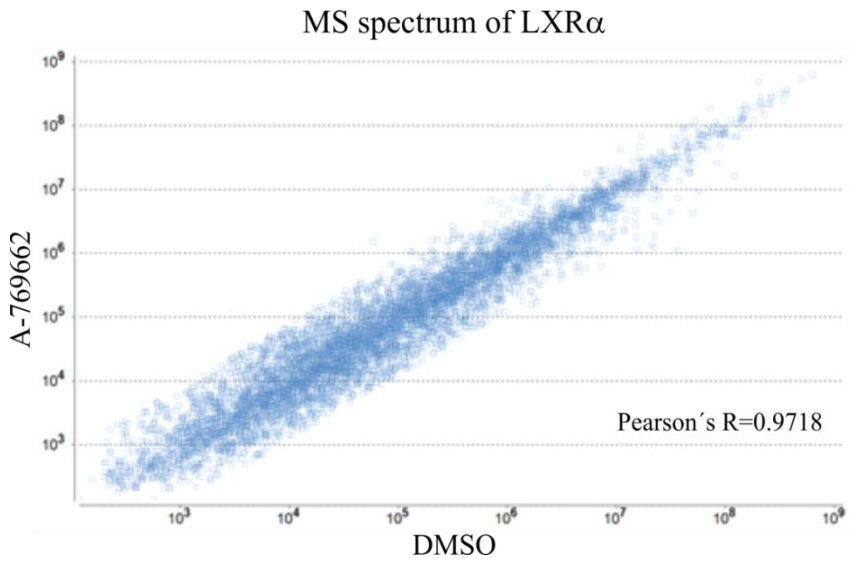

Figure 33: DMSO- and A-769662-treated peptides of LXRα protein steady spread in MS.
HepG2 cells were incubated in normal or SILAC medium for 7 passages. IP, SILAC, and MS were performed as described in sections 4.2.4.5 and 4.2.4.6. The graph serves as an example for the distribution and good coverage during MS measurement.

The digestion of LXRα with different enzymes (trypsin and thermolysin), used in our setting, provides different peptides. Trypsin digests C-terminal to Arg and Lys, whereas thermolysin preferentially cleaves N-terminal to aromatic sites of Ile, Leu, Val, Ala, Met, and Phe. Although the trypsin digestion reached a very good protein coverage, it shows a phosphorylation at either Ser197 or Ser198, but the MS-MS spectrum did not deliver enough information to differentiate between these two sites because of very little peptide fragments from the N-terminal positions of the peptide. In contrast, the thermolysin-generated peptide has the two serines in the middle of the peptide sequence and thus gives an unequivocal answer to the localization. Furthermore, the thermolysin peptide pool suggests other sites of phosphorylation on the same peptide sequence.

The software Peaks 7.0 with quantification tool can calculate the ratio of each peptide of DMSO- and A-769662-treated LXRα protein. These ratios give information about the peptide amount of control sample in comparison to the peptide formation of AMPK-activated LXRα. Table 23 summarizes the results of both the SILAC labeling experiment and label-free quantification of non-labeled samples for a peptide encompassing Ser197 or Ser198 phosphorylation (+79.97), Met213 oxidation (+15.99), Lys216 SILAC labeling (+6.02), Gln201 deamidation (+0.98), and Arg195 SILAC labeling (+10.01). Importantly, the phosphorylation of Ser197 or Ser198 could not be distinguished by the used tools. But a tendency lies at Ser198 because of completely convered y-type ion series shown in Figure 35.

Table 23: Label-free and SILAC results indicate reduction of phosphorylation at Ser197/Ser198 in LXRα protein during AMPK activation.

Peptide	Digestion by	control: activated[a]
R.AS**S(+79.97)**PPQILPQLSPEQLGMIEK.L	trypsin	1 : 0.488
R.AS**S(+79.97)**PPQILPQLSPEQLGMIEK.L	trypsin	1 : 0.805
R.AS**S(+79.97)**PPQILPQLSPEQLGMIEK.L	trypsin	1 : 0.691
R.AS**S(+79.97)**PPQILPQLSPEQLGMIEK.L	trypsin	1 : 0.455
R.AS**S(+79.97)**PPQILPQLSPEQLGMIEK.L	trypsin	1 : 0.350
R.AS**S(+79.97)**PPQILPQLSPEQLGMIEK.L	trypsin	1 : 0.363
R.AS**S(+79.97)**PPQILPQLSPEQLGM(+15.99)IEK.L	trypsin	1 : 0.431
R.AS**S(+79.97)**PPQILPQLSPEQLGM(+15.99)IEK.L	trypsin	1 : 0.439
R.AS**S(+79.97)**PPQILPQLSPEQLGMIEK.L	trypsin[b]	1 : 1.095
R.AS**S(+79.97)**PPQILPQLSPEQLGM(+15.99)IEK.L	trypsin[b]	1 : 1.258
R.AS**S(+79.97)**PPQILPQLSPE(+21.98)QLGMIEK.L	trypsin[b]	1 : 1.592
R.AS**S(+79.97)**PPQILPQLSPEQLGMIEK(+6.02).L	trypsin[b]	1 : 1.161
R.AS**S(+79.97)**PPQILPQLSPEQLGMIEK.L	trypsin[b]	1 : 0.802
R.AS**S(+79.97)**PPQILPQLSPEQLGM(+15.99)IEK.L	trypsin[b]	1 : 0.695
R.A**S(+79.97)**SPPQILPQLSPEQLGMIEK.L	trypsin[b]	1 : 1.472
H.ATSLPPRAS**S(+79.97)**PPQ.I	thermolysin[b]	1 : 0.426
K.LKRQEEEQAHATSLPPRAS**S(+79.97)**PPQ.I	thermolysin[b]	1 : 0.800
K.LKRQEEEQAHATSLPPRA**S(+79.97)**SPPQ(+0.98)ILPQ.L	thermolysin[b]	1 : 0.425
H.ATSLPPR(+10.01)A**S(+79.97)**SPPQ.I	thermolysin[b]	1 : 0.329
H.ATSLPPR(+10.01)A**S(+79.97)**SPPQ.I	thermolysin[b]	1 : 0.318
H.ATSLPPRA**S(+79.97)**SPPQ.I	thermolysin[b]	1 : 0.441
H.ATSLPPRA**S(+79.97)**SPPQ.I	thermolysin[b]	1 : 0.542
H.ATSLPPRA**S(+79.97)**SPPQ.I	thermolysin[b]	1 : 0.426
H.ATSLPPRA**S(+79.97)**SPPQ.I	thermolysin[b]	1 : 0.522
Mean values of Ser197/Ser198(+79.97)	**trypsin**	**1 : 0.806**
Mean values of Ser197/Ser198(+79.97)	**thermolysin**	**1 : 0.470**

[a]certain peptide incidence ratio of DMSO- (control) and A-769662-treated (activated) samples
[b]SILAC samples

The results of the MS experiments strongly indicate a phosphorylation at Ser198 residue (Figure 35) and possible phosphorylation at Ser197 (data not shown) which attenuates during the AMPK activation by A-769662. The numbers of <1 in "ratio of peptide" column in Table 23 reveal this fact which gets stronger looking at the number of >1 in "ratio of whole protein" column. Thus, AMPK activation probably leads to dephosphorylation of LXRα protein increasing its activity. Previously described LXRα acetylations were not found.

The spectrum shown in Figure 34 reveals fragmentation of LXRα protein digested by thermolysin. The b (blue) and y (red) ions are visible.

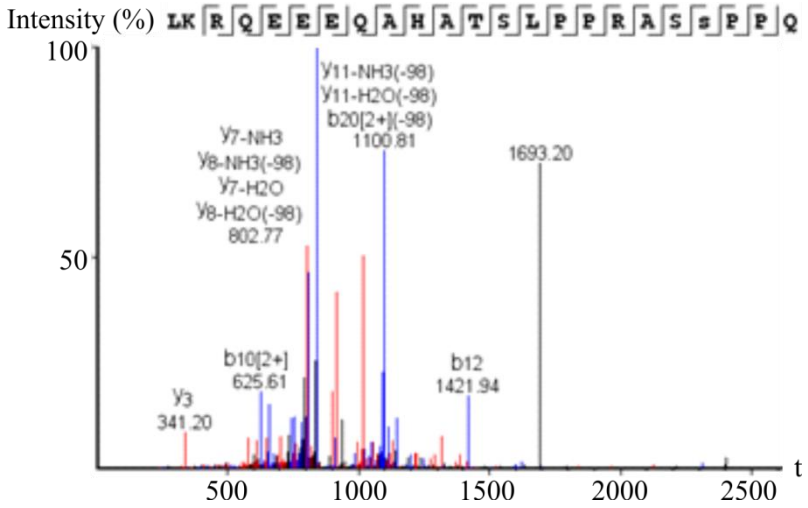

Figure 34: Spectrum of peptide fragmentation.

One of the phosphorylated peptides observed after the measurement of thermolysin digested LXRα protein analyzed by Q Exactive™ Hybrid Quadrupole-Orbitrap mass spectrometer. The formed ions by fragmentation exhibit energy which can be determined by the intensity and peak area. In red the y-type fragment ions and in blue the b-type fragment ions are shown. The x-axis indicates the m/z value for the fragment ion, the y-axis the relative intensity.

Figure 35 shows a corresponding ion fragmentation table of the above spectrum. It reveals all fragment ions covered of the thermolysin-generated peptide. The numbers reflect the accurate mass by two peak areas as shown in Figure 34. The spectrum clearly indicates the phosphorylation site at Ser198 in LXRα by its completely convered y-type ion series at this site (y, y-H_2O, y-NH_3).

#	Immonium	b	b+H2O	b-NH3	b (2+)	Sequence	y	y-H2O	y-NH3	y (2+)	#
1	86.10	114.09	96.08	97.06	57.55	L					23
2	101.11	242.19	224.18	225.16	121.59	K	2524.19	2506.18	2507.17	1262.60	22
3	129.11	398.29	380.48	380.48	199.64	R	2396.10	2378.09	2379.07	1198.24	21
4	101.07	526.51	508.62	509.46	264.13	Q	2240.00	2221.99	2222.97	1121.21	20
5	102.06	655.49	637.19	638.36	328.19	E	2111.94	2093.93	2094.91	1056.76	19
6	102.06	784.63	766.66	766.66	392.37	E	1982.90	1964.70	1965.87	991.67	18
7	102.06	913.62	895.79	895.79	456.56	E	1853.85	1835.05	1837.08	927.43	17
8	101.07	1041.45	1023.52	1024.73	521.78	Q	1724.81	1706.80	1707.78	862.91	16
9	44.05	1112.65	1095.03	1095.03	556.92	A	1596.75	1578.74	1579.73	798.88	15
10	110.07	1249.75	1231.72	1232.92	625.61	H	1525.65	1507.71	1508.63	763.42	14
11	44.05	1321.38	1302.96	1302.96	660.91	A	1388.55	1370.51	1371.63	694.83	13
12	74.06	1421.94	1403.78	1404.57	711.36	T	1317.60	1300.04	1300.04	658.73	12
13	60.04	1508.63	1490.74	1491.72	755.10	S	1216.48	1198.24	1199.55	608.26	11
14	86.10	1621.76	1603.74	1605.58	811.50	L	1129.46	111.33	1112.65	564.82	10
15	70.07	1718.88	1700.87	1701.81	859.94	P	1016.50	998.39	999.43	509.46	9
16	70.07	1815.94	1797.92	1798.91	908.25	P	919.40	901.39	902.38	460.49	8
17	129.11	1972.04	1954.03	1955.01	986.87	R	822.35	803.75	804.97	411.68	7
18	44.05	2043.07	2025.06	2026.05	1022.46	A	666.42	648.24	649.69	334.37	6
19	60.04	2130.11	2112.09	2113.08	1065.60	S	594.44	577.94	578.57	298.11	5
20	140.01	2297.10	2279.09	2280.08	1149.06	S(+79.97)	508.62	490.73	490.73	254.59	4
21	70.07	2394.16	2376.15	2377.13	1198.24	P	341.20	323.20	324.14	171.09	3
22	70.07	2491.21	2473.20	2474.18	1246.10	P	244.07	226.12	227.10	122.56	2
23	101.07					Q	147.08	129.07	130.05	74.04	1

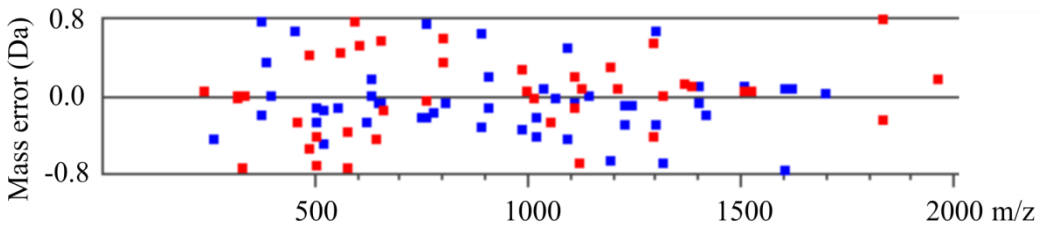

Figure 35: Spectrum of the peptide LKRQEEEQAHATSLPPRASS(+79.97)PPQ during MS.
MS was performed using Q Exactive™ Hybrid Quadrupole-Orbitrap mass spectrometer after a thermolysin digestion. The b-type fragment ions (blue) and the y-type fragment ions (red) show a complete coverage of the found phosphorylation site. x-axis shows the peptide mass; y-axis – mass error due to calculated fragment mass.

The green boxed numbers belong to the b- and y-type ion series and cover the phosphorylation site at Ser198 with high confidence. The thermolysin digestion shows a phosphorylation (+79.97) at Ser198. The y-type series seem to be confident which is indicated by the red colored numbers revealing a complete coverage of the phosphorylation site. The graph below shows mass error of MS-MS fragments in relation to their nominal mass for b-type (blue) and y-type (red) ions (x-axis). Most of the fragments are located in the area of ±0.8 indicating not big spreading of the mass variance (y-axis).

There is also an evidence for other post-translational modifications of LXRα protein by AMPK activation, such as phosphorylation of Ser99 or Arg195. But these interesting and new findings are not confirmed and should be proven by additional MS experiments.

6. Discussion

Transcription factors like PPARδ and LXRα connect metabolism and inflammation serving as promising targets for the treatment of different metabolic diseases, such as diabetes and atherosclerosis. Results of my dissertation further strengthen the connection between metabolism and immunity, suggesting AMPK as a key regulator of PPARδ- and LXRα-dependent pathways in human macrophages.

In the first part of my study I investigated by analyzing the transcriptome of primary human macrophages, if AMPK and PPARδ synergize to promote an anti-diabetic macrophage phenotype. Simultaneous activation of AMPK and PPARδ leads to higher expression of FAO-associated genes compared to single treatments acting through PPARδ.

Furthermore, I was able to show a novel signaling pathway from AMPK to ABCA1 via LXRα in primary human macrophages. Here, the AMPK activation increases the LXRα expression levels and activity, which enhances the mRNA and protein expression of ABCA1 elevating cholesterol efflux. These findings indicate a promising possibility to treat atherosclerotic progress in humans.

6.1. AMPKα1 OE and usage of A-769662 as AMPK activator

First, I overexpressed constitutively active AMPKα1 in macrophages by lentiviral transduction. In this construct, the residue Thr198 is mutated to aspartate, which mimics phosphorylation and enables permanent AMPK activity[203]. Using no polybrene, but centrifugation during macrophage transduction, I could improve the transduction efficiency of primary cells (Figure 9). Optimizing the lentiviral transduction new approaches can be tried out in the future. Additional study suggests to use VSV-G pseudotyped-based lentiviral vectors which seem not to interfere with macrophage differentiation[291].

To confirm the AMPK action, a THP-1 cell line including AMPK KD was generated. Verification shows a down-regulation to only 7% presence of AMPK mRNA, whereas no detection of AMPK protein in silenced cells occurred (Figure 8). Both OE and KD of AMPK can indicate a significance of my following experimental results.

A-769662 was recently found to directly and reversibly activate AMPK[229]. But macrophage treatment with A-769662 seems to induce apoptosis (from 3% to 13%) as shown by FACS analysis in Figure 16. These results contrast with those observing AMPK as

inhibitor of apoptosis and suggest an off-target effect of A-769662 at concentration applied[241]. Another study is in accordance with my findings showing an off-target effect of A-769662 inhibiting 26S proteasome[292], which possibly could lead to protein accumulation and to apoptosis. In contrast, Figure 17 indicates no cytotoxic effect of A-769662 revealing no ATP depletion in human macrophages. Thus, following investigations were performed using this AMPK activator as the only direct AMPK-activating chemical available at the moment. The stimulation with A-769662 in primary macrophages results in almost no phosphorylation of endogenous AMPK (Figure 13). This phenomenon is observed also by Sanders *et.al*. and Göransson *et.al*. describing the interaction between A-769662 and AMPK[198, 231]. The AMPKβ1-subunit is significant for A-769662 binding and allosteric AMPK activation. Here, A-769662 activates AMPK inhibiting Thr172 dephopshorylation on Ser108. This site is supposed to be responsible also for endogenous stimulation of AMPK[198]. A-769662 acts independently of AMPK upstream kinases binding to a large hydrophobic cavity[231, 293]. The AMPK phosphorylation seems to be cell type-specific. AMPKα1 OE and A-769662 were not used at the same time in my experiments, because previous study already reported the inability of A-769662 to phosphorylate truncated (auto-inhibitory domain-lacking) protein[198, 231]. Thus, there would be no benefit on AMPK activation.

6.2. AMPK/PPARδ co-activation in human MΦ

Previous human studies show an elevation of PPARδ expression after exercise training[294, 295], where the exercise induces AMPK activation indicating an interaction between both proteins in the human system. Exercise training leads to a reduction of lipid accumulation, increase of FAO, and enhancement of insulin action[296]. To test the AMPK-PPARδ interaction in macrophages a microarray was performed following activation of both proteins. The microarray results reveal lipid metabolism as a major affected pathway induced by combined activation of AMPK and PPARδ (Table 21). The most highly induced genes, such as PDK4, CPT1a, PLIN2, ACAA2, ACADVL, FABP4, and CD36 shown in Table 22 are involved in fatty acid metabolism of primary macrophages.

Figure 36 shows the possible interaction between AMPK and PPARδ and their associated, common regulated pathways leading to additional increase of FAO in human macrophages. FABP4 provides the transport of free LCFA to facilitate acyl-CoA formation (not shown).

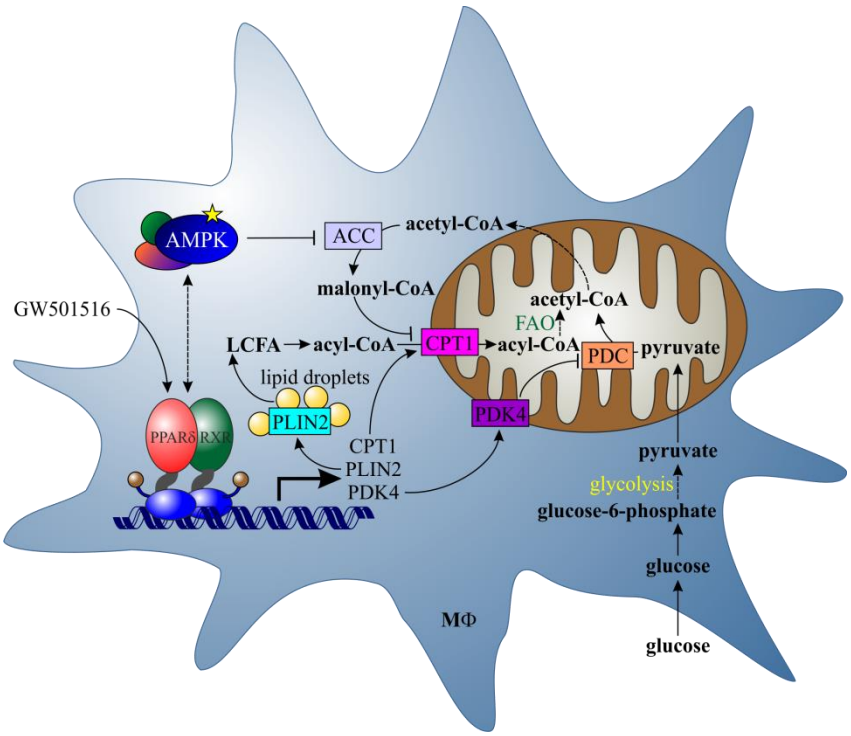

Figure 36: Co-activation of AMPK and PPARδ in human MΦ.

PPARδ activation by GW501516 induces transcription of FAO-associated genes, e.g. CPT1, PDK4, PLIN2, which stimulate fatty acid transfer into the mitochondrium (CPT1), stabilize lipid droplets providing LCFA (PLIN2), and inhibit pyruvate processing to acetyl-CoA (PDK4) after their translation. Glucose transported into macrophages undergoes glycolysis resulting in pyruvate and finally converts into acetyl-CoA in mitochondrium. AMPK activation increases CPT1 activity by ACC inhibition blocking malonyl-CoA production and interacts with PPARδ stimulating FAO-associated genes. Thus, simultaneous co-activation of AMPK and PPARδ additively increase FAO pathway. ACC, acetyl-CoA carboxylase; AMPK, AMP-activated protein kinase; CPT1, carnitine palmitoyltransferase 1; FAO, fatty acid oxidation; LCFA, long-chain fatty acids; MΦ, macrophage; PDC, pyruvate dehydrogenase complex; PDK4, pyruvate dehydrogenase kinase 4; PLIN2, perilipin 2; PPAR, peroxisome proliferator-activated receptor; RXR, retinoid X receptor.

As a consequence of increased PDK4 expression and activity, e.g. by GW501516, macrophages down-regulate glucose metabolism through inhibition of pyruvate dehydrogenase complex (PDC) thus, increasing the substrate availability of acetyl-CoA for FAO[297] (Figure 12, Figure 36). Confirming our observations, Adhikary *et.al.* shows "fatty acid metabolism" and "lipid, fatty, and steroid metabolism" as most enriched biological processes after performing genome-wide identification of PPARδ target genes together with ChIP-Seq experiments[89]. In addition, GW501516 treatment of human skeletal muscle cells results in elevation of PDK4, CPT1a, CD36, and FAO activity[102]. PDK4, FABP4, and SCD1 are described being influenced by both AMPK and PPARδ[262]. In contrast to that study, no

synergistic effects of combined AMPK and PPARδ could be observed in primary macrophages during my studies.

ChIP experiments in fibroblasts, hepatocytes and pancreatic β-cells reveal cell type-specific differences in PPARδ target gene modulation[73]. Therefore, the PPARδ effects in primary human macrophages shown here are likely cell type-specific. This specificity may partly be to the cell-type specific pattern of PPARδ transcriptional co-activators. Thus, Gan *et.al*. e.g. propose a synergistic co-activation of transcription factor myocyte enhancer factor 2 (MEF 2) by PPARδ and AMPK in muscle[298]. The co-factor and target of MEF2 is PGC1α[299]. Another study confirms these results showing the involvement of PGC1α in AMPK-PPARδ complex in human skeletal muscle cells[263]. Importantly, PGC1α and PPARδ interact, but their expression regulation is altered in obese individuals[300]. This co-activator may be required for the full activation of PPARδ to induce transcription of target genes[85, 107, 301]. In human embryonic kidney cells no direct interaction between Flag-PGC1α and AMPK is found proposing AMPK-independent binding of PGC1α to PPARδ[262]. Further IP experiments are needed to investigate the possibility of AMPK-PGC1α-PPARδ interaction in human macrophages although only small amounts of PGC1α are detected in these cells[302]. Investigations on PGC1α-lacking mice reveal a reduced FAO elevation during PPARδ activation[301] leading to hypothesis of PPARδ-PGC1α interaction[296]. LDL-receptor$^{-/-}$ mice with macrophage-specific deletion of PGC1α show increase of atherosclerosis revealing anti-atherosclerotic properties of this nuclear receptor co-activator[303]. Thus, the cell-specific composition of PPARδ co-activators, such as PGC1α, may contribute to cell type-specific outcome of the PPARδ down-regulation, i.e. de-repression vs. de-activation.

PDK4 was also identified as up-regulated gene in a microarray performed in murine muscle cells during AMPK and PPARδ activation[262] and is elevated during and after exercise[304], which on its part decreases ATP concentration and increases AMPK activity inside the cells. So, it is not surprising to find *PDK4* as the strongest regulated by combined activation of AMPK and PPARδ in primary macrophages (Table 22). High glucose levels are described to reduce mRNA of PDK4[305] implying a possible effect by inhibited AMPK. Indeed, an additional study reveals synergistic stimulation of PDK4 expression and glucose oxidation reduction by activated AMPK and fatty acids in primary cardiomyocytes. This study also proposes the AMPK-dependent regulation of ligand-activated PPARδ[306]. AMPK

may increase PDK4 mRNA also in adipocytes[307], an effect which I can confirm in my study in macrophages (Figure 12, Figure 14, Figure 15).

In murine RAW 264.7 macrophages and skeletal muscle cells increased CPT1a expression can be observed during the GW501516 treatment[79, 107]. Figure 14 shows the CPT1a induction in PPARδ-activated human macrophages to the extent comparable to these studies. Investigations in our laboratory observed FAO-dependency on CPT1a expression showing reduction of β-oxidation in CPT1a KD macrophages[308]. The small increase of protein amount in comparison to mRNA levels of PDK4 and CPT1a (Figure 15) may be explained by AMPK-dependent inhibition of mTOR pathway causing attenuated protein translation. Another study detected significant changes of mRNA levels of FAO genes after GW501516 treatment in skeletal muscle, but no functional activity of them, finding unchanged running performance[262]. This fact indicates the possibility of different regulation of transcription and protein functionality.

An interesting question was: if increased mRNA and protein expression levels would also enhance PDK4 and CPT1a activity in primary macrophages. The activity of both could be shown by a measurement of cellular oxygen consumption rate (OCR) and an extracellular acidification rate (ECAR) using a Seahorse extracellular flux analyzer. The OCR provides a value of mitochondrial respiration, whereas ECAR refelcts proton excretion as readout of cellular glycolysis. According to biosafety aspects, it was not possible to use AMPKα1-transduced primary macrophages for Seahorse measurements. On the other side, multiple tests with A-769662 did not show any reliable results because of no measurable OCR or ECAR, whereas GW501516 treatment lead to increased oxygen consumption (data not shown). These data cannot be explained to this moment. No publication mentions this phenomenon or the use of A-769662 during a Seahorse experiment. So, further investigations are needed to clarify these findings. To indirectly investigate the activity of PPARδ targets, another assay was chosen measuring TG amounts inside the cells (sections 5.1.2.6 and 6.3).

Analyzing microarray data, further genes showing enhanced expression besides *PDK4* and *CPT1A* were identified. *UCHL1* was strongly affected especially by AMPK. This finding is novel and is not reported yet. UCHL1 exhibits ubiquitin hydrolase and ligase activities. It is the most abundant protein in brain lysates (1-2%) regulating the timing and the pattern of ubiquitination. Mutations in the *UCHL1* gene lead to neurodegenerative diseases[309]. Interestingly, the OE of UCHL1 protein was shown to attenuate neuritic plaque formation and

improve memory deficits in Alzheimer´s disease transgenic mouse model[310]. Therefore, UCHL1 serves as a promising target to treat neurodegenerative diseases. The microarray data of my study reveals AMPK as one of the main UCHL1 regulators raising the interest for further experiments.

IMPA2 is identified as a target gene of AMPK and PPARδ (Table 22) confirming the previous reports showing PPARδ-dependence of IMPA2 expression[311]. IMPA2 is not well investigated at all and its expression has not been reported in macrophages yet. Only its implication in bipolar disorder increasing suicide risk in humans is described[312].

UCP2 is found also as one of the most affected genes confirming the data showing AMPK-dependence for UCP2 up-regulation[258]. In addition, PPARδ regulates the thermogenesis in muscle cells[311] influencing UCP2 expression[107]. Considering its anti-atherosclerotic effect[259], UCP2 could serve as another therapeutic target during atherosclerosis treatment, as well as ABCA1, regulated by AMPK. A therapeutic benefit therefore may be enhanced by increased activities of both proteins, ABCA1 and UCP2.

Summarizing, microarray results show the high complexity of human macrophages indicating the regulation of FAO by PPARδ and AMPK, but also other metabolic pathways like ATP synthesis, pyruvate metabolism, and ER organization (Table 21). Besides, new gene regulation by AMPK and PPARδ was found, with targets possessing ubiquitin hydrolase/ligase and thermogenesis activities (Table 22).

6.3. Impact of VLDL and LPL in human macrophages

As described in previous studies the exposure of macrophages to VLDL stimulates foam cell formation[313, 314]. Figure 19 shows significant reduction of VLDL-induced TG accumulation by PPARδ activation, a result which is observed also by Bojic *et.al*[279]. LPL serves as a rate-limiting lipase of lipid metabolism hydrolyzing TG-rich lipoproteins releasing FFA and glycerol to promote TG clearance in plasma[315] (Figure 37). Remnant TG-poor and cholesterol-enriched lipoprotein particles and FFA induce inflammation and lipid accumulation. Therefore, LPL is implicated in atherosclerosis pathogenesis[59]. The inhibition of LPL by Angptl4 is confirmed not only by *in vitro* assays, but also during the OE and KO experiments. Angptl4 OE leads to a significant increase of plasma TG amounts in mice, whereas KO exhibits elevated LPL activity and hypotriglyceridemia[316, 317]. The mechanism of

LPL inhibition by Angptl4 is not completely clarified but is described as noncompetitive and reversible[318].

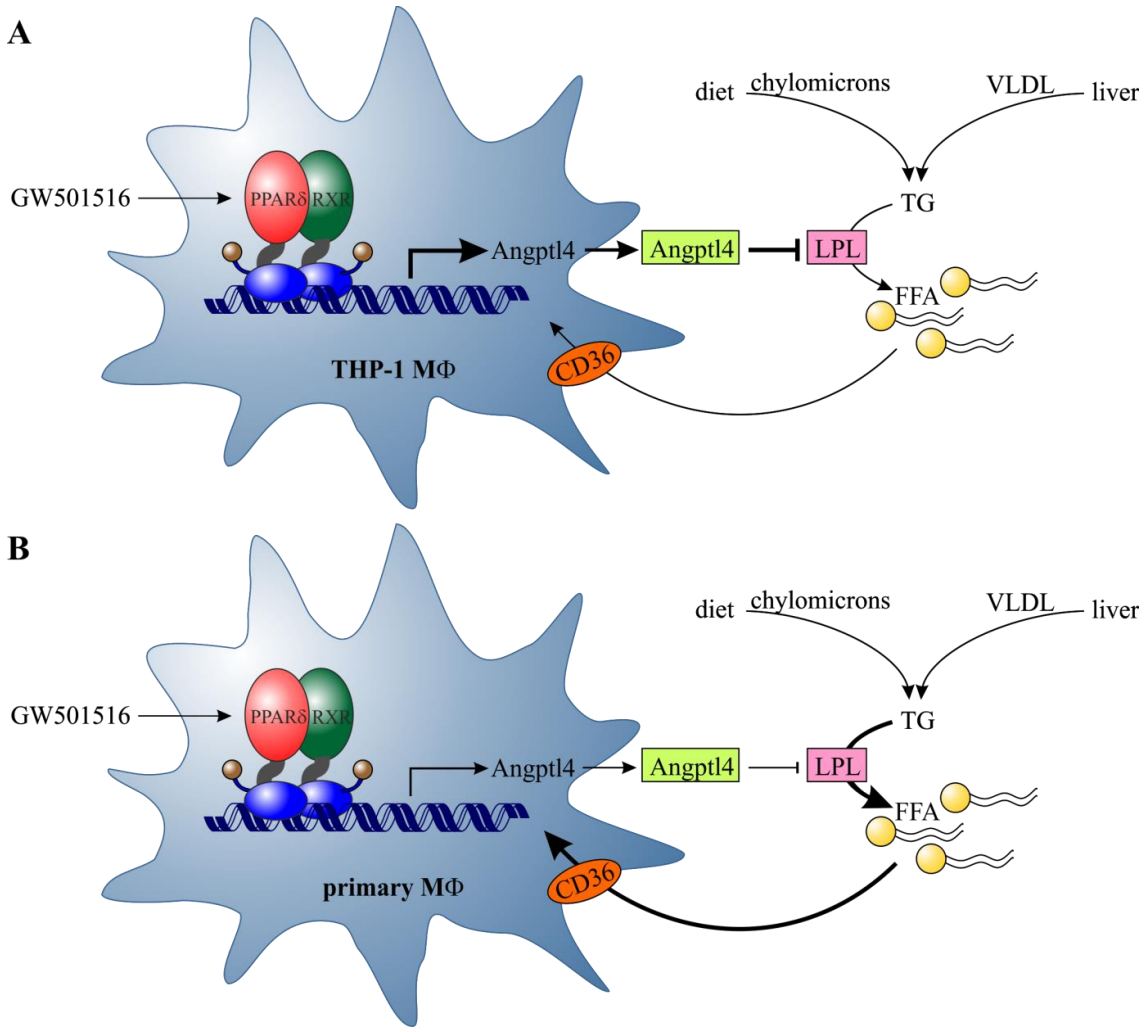

Figure 37: TG degradation depends on transcription activity of PPARδ and is cell type-dependent.
The same PPARδ activation by GW501516 leads to different Angptl4 expression levels in THP-1 and primary macrophages. **A** PPARδ activation induces high Angptl4 expression in THP-1 macrophages inhibiting LPL activity and leading to TG accumulation. **B** In primary macrophages only low content of Angptl4 will be transcribed leading finally to increased LPL activity and higher FFA concentration. In both cases TG have two sources in human blood: packaged into chylomicrons provided by diet and VLDL produced by the liver. FFA can be transported into macrophages by a membrane receptor CD36. Angptl4, angiopoietin-like 4; CD36, cluster of differentiation 36; FFA, free fatty acids; TG, triglycerides; VLDL, very low-density lipoproteins.

PPARδ is a predominant PPAR isotype regulating LPL expression in macrophages[319]. As Figure 18 A presents increased Angptl4 mRNA levels in PPARδ-activated THP-1 macrophages, LPL activity might be decreased leading to TG-rich lipoprotein accumulation. This data is consistent with previous findings. Increased Angptl4 expression and down-

regulation of LPL activity are observed during GW501516 treatment in THP-1 macrophages causing attenuated foam cell formation[279, 280]. Also *in vivo*, Angptl4 leads to dramatically reduced foam cell formation and atherosclerosis development[320]. In contrast, my observations in primary macrophages reveal an unaltered Angptl4 expression upon PPARδ activation and hence uninhibited LPL activity and hydrolysis of TG. Still, a reduction of TG amount was detected in GW501516-stimulated primary cells (Figure 19). This effect can lead back to the role of PPARδ in macrophages protecting cells from lipotoxicity, stimulating FAO[42, 79] and preventing fatty acid accumulation. Lipotoxicity describes consequences of fat overload and is related to oxidative stress, accumulation of lipotoxic intermediates, and storage of TG[321]. To avoid the lipid burden during VLDL treatment and GW501516-stimulation, PPARδ switches into the active state inducing FAO gene expression in macrophages and resulting in significantly lower TG amounts as shown in Figure 19. Steinberg and Schertzer propose AMPK-dependent FAO pathway as an inductor for anti-inflammatory macrophage state preventing the cardiovascular diseases[322]. Therefore, increased FAO in macrophages may serve as a promising treatment of obesity and type 2 diabetes[323].

According to presented data, PPARδ regulates FAO. This transcription factor is suggested to impair diabetes development and therefore to prevent insulin resistance[79]. GW501516 stimulation seems to improve diabetic symptoms decreasing blood insulin and plasma glucose levels in genetically obese *ob/ob* mice[80]. Activation of PPARδ by VLDL may orchestrate cellular response to incoming fatty acids and triglycerides storing them in PLIN2-coated lipid droplets for a short term[42]. Induction of PPARδ target genes, such as PDK4, CPT1a, and PLIN2 could also increase the uptake and clearance of the TG-rich lipoprotein particles in peripheral tissues and decrease the lipid content inside atherosclerotic plaques.

Detecting the protein expression of FAO-associated genes during AMPK activation only small increase could be observed compared to PPARδ activation (Figure 15). Additional AMPK activation of VLDL-loaded macrophages has no effect on TG content indicating only small impact on protein expression, activity of FAO genes, and regulation of TG pathway (Figure 19). The activator A-769662 may have an inhibitory effect on mitochondrial activity as shown for other AMPK activators (section 3.3.2). On the other hand, an AMPK activator berberine is described to attenuate lipid accumulation in human macrophages[225]. The explanation of the discrepancy results could be an involvement of a different pathway, but

also different treatment period. Nevertheless, AMPK seems to play an important role in FAO regulation interacting with PPARδ.

In conclusion, PPARδ serves as a sensor for fatty acids, which are provided during phagocytosis of apoptotic cells[324] or increased lipolysis by LPL[59]. The positive feedback loop including fatty acids, PPARδ, and LPL prevents arterial lipid accumulation[59, 104, 176].

6.4. AMPK increases FAO-associated gene expression via PPARδ activation

PPARδ-dependent up-regulation of PDK4, CPT1a, and ACAA2 mRNA during GW501516 stimulation is reported[325]. The same results could be observed in Figure 20 C-D, H, showing significant increase of PPARδ target genes CPT1a, PLIN2, and ACADVL by single treatment with GW501516.

Interesting but not surprising observation was the enhancement of target genes after PPARδ depletion to 28% expression by siRNA silencing (Figure 20 A-H). The increased expression of PPARδ target genes in PPARδ$^{-/-}$ macrophages was already observed previously[79]. PPARδ-deficient macrophages are unable to transform into M2-like phenotype accumulating fat, stimulating insulin resistance, and reducing FAO[83]. Adhikary *et.al*. report similar effects by siPPARδ as me in human myofibroblasts. The phenomenon of elevated mRNA expression during the silencing (type I and II of transcriptional regulation) can be explained by de-repressive state due to interaction with co-repressors or a direct recruitment of PPARδ in the unligated state as mentioned in section 3.2.1.1[89].

FAO-regulating genes were induced by GW501516 in siControl-treated cells, but this induction was abolished in PPARδ-silenced macrophages (Figure 20 B-H). Similar findings are reported for PLIN2 mRNA using MCSF-differentiated WT and PPARδ$^{-/-}$ murine bone marrow-derived macrophages[86]. Non-responsive PPARδ target gene mRNA during PPARδ silencing is also shown in cardiac muscle cells[301]. Similar results are obtained in hepatocytes showing reduced PDK4 mRNA expression in GW501516-treated and PPARδ-silencing cells compared to PPARδ-activated control[325].

On the contrary, deletion of PPARδ may impair not only the target gene transcriptional activity, but also the PPARδ-mediated effect of trans-repression of inflammatory gene

expression[326]. In cardiomyocytes a protein-protein interaction between PPARδ and NFκB subunit p65 after GW501516 treatment is demonstrated[99]. The interplay between AMPK and NFκB is also reported. Another study using PPARδ cardiomyocyte-restricted deletion in mice shows a down-regulation of FAO genes decreasing basal myocardial FAO[327]. As the involvement of NFκB in the down-regulation of FAO including PDK4 enzyme in cardiomyocytes is reported[328], it would be interesting to investigate whether enhanced NFκB activity under pro-inflammatory conditions may lead to PDK4 attenuation in human macrophages.

In PPARδ$^{-/-}$ mice, the electron transport chain and oxidative phosphorylation pathways are reduced[81] indicating a major role of this transcription factor in not only FAO, but also generally in oxidative metabolism. PPARδ is described to protect insulin-producing pancreatic β-cells from palmitate-induced ER stress via FAO promotion[329]. Cheang *et.al.* show the interaction between AMPK and PPARδ in obese diabetic mice leading to ER stress inhibition proposing the role of transcription factor downstream of AMPK[330].

AMPK significantly increases PDK4, CPT1a, and ACADVL mRNA in siControl cells (Figure 20 B-C, H), but Figure 20 B-H shows no AMPK effect in siPPARδ primary macrophages. These results indicate the probable association of AMPK with PPARδ in the nucleus to drive the transcription of FAO genes. Our research group was able to show that AMPK acts through PPARδ on PPARδ-target genes, but not vice versa. Interestingly, Narkar *et.al.* could not find any PPARδ phosphorylation by AMPK performing IP experiments in human embryonic kidney cells AD293[262]. Thus, it would be interesting to investigate, if there is any mediator between those two proteins. Further IP and Co-IP experiments targeting AMPK and/or PPARδ could clear the situation. In primary skeletal muscle cells an increase of AMPK phosphorylation by GW501516 via reduced cellular energy status is observed[263]. Although GW501516 may indirectly influence AMPK activity, the results in Figure 12 and Figure 14 show significant increase of FAO genes during combined AMPK-PPARδ activation in comparison to single GW501516 treatment. Besides, no AMPK activation was observed during GW501516-treatment (data not shown). So, these results indicate differences in FAO regulation in human macrophages and skeletal muscle cells. An additional factor and side-effect which may decrease ATP/AMP ratio and activate AMPK is high concentration (5-10 µM) of GW501516 used during some studies[331, 332]. In my experiments only 100 nM GW501516 were applied in macrophages. As AMPK seems not to

phosphorylate PPARδ directly[262], the question of other possible post-translational modifications arises, which can be answered by the method of mass spectrometry.

Some strategies to treat metabolic syndrome and its symptoms consist of an increase of phagocytosis to avoid the accumulation of dead cells[333], the usage of anti-inflammatory resolution mediators such as lipoxins or resolvins to attenuate inflammation[334], the activation of LXRs and PPARδ to enhance efferocytosis and cholesterol efflux, and to decrease ER stress[176, 177, 335]. Results shown here present positive but not very promising approach for type 2 diabetes treatment by simultaneous activation of AMPK and PPARδ. Although FAO-associated genes are affected, the FAO activity seems to have only inhibited enhancement indicating the possible involvement of other factors. Summarizing, simultaneous AMPK and PPARδ activation alone does not impair FAO in human macrophages.

6.5. AMPK enhances ABCA1 expression via LXRα activity

In the second part of my work, an effect of AMPK on promoting cholesterol efflux in macrophages to avoid foam cell formation with possible implications for the atherosclerosis development in humans will be discussed.

For the first time, I could show the dependence of ABCA1 expression on the important kinase AMPK. AMPK-dependent ABCA1 regulation is observed in both primary and THP-1 macrophages (Figure 21, Figure 22, Figure 23) showing consistency in human system. Besides, the increased functional activity of ABCA1 was confirmed by measuring cholesterol efflux during AMPK activation (Figure 23 B). Meanwhile, other groups could show the indirect effect of AMPK on ABCA1 regulation[285, 336, 337]. These and other publications indicate LXRα as the primary ABCA1 effector[166, 264]. My results can confirm these findings showing that LXRα silencing, but not siLXRβ, has an impact on ABCA1 expression level in primary cells (Figure 25 and Figure 27).

Interestingly, other transcription factors are proposed as regulators of ABCA1 expression in human macrophages. J.J. Boyle and his group suggest the involvement of ATF1 and LXRβ in the AMPK-LXRα-ABCA1 signaling pathway[285, 336]. To test this hypothesis, I used siRNA inducing silencing of ATF1 and LXRβ. Figure 27 and Figure 28 show ABCA1 independency of those transcription factors. The discrepancy regarding the ABCA1 regulation by ATF1 may be based on the differences during the macrophage treatment. Activation of AMPK by

heme[336] could function differently from A-769662 mechanism activating also other metabolic pathways.

Related to the LXRβ silencing experiments, some other studies confirm my results showing no influence on cholesterol efflux by LXRβ in macrophages. Ignatova *et.al.* observe ABCA1 regulation by LXRα, but not LXRβ, using ChIP, Western analysis, and luciferase assays[283]. This might be the reason for no effect on atherosclerosis development in LXRβ knockout mice compared to LXRα knockout mice, where increased atherosclerosis is found[190]. Another study shows similar results using KD of LXRα affecting cholesterol efflux without compensation by LXRβ in human macrophages[338].

Figure 29 shows the maximal luciferase activation of 3.3-fold (from 1 to 3.3) in ABCA1-transfected cells, whereas the LXRα overexpressing cells achieve maximal 2.5-fold induction by T0901317 (from 4 to 10). The elevation during OE seems to be reduced compared to the activation. The reason for this attenuated increase of LXRα activity could be the LXRα ability to transcribe many mRNAs of *Abca1* gene, which is limited by occupation of LXRE sites on *Abca1* promoter. My ChIP experiments in Figure 30 show the binding of LXRα to the LXRE site of *Abca1* promoter, which confirms also the data from my reporter assays (Figure 29). Similar result was achieved in the study observing the DR4-dependent ABCA1 expression and HDL biogenesis induced by niacin[339], which is used in the treatment of atherosclerosis[340]. Niacin-bound chromium treatment was also shown to up-regulate AMPK in murine system[341]. So maybe, niacin action goes through AMPK activation further leading to LXRα activation to induce ABCA1 expression in human macrophages.

6.6. AMPK regulates ABCA1 by dephosphorylation of LXRα

Different pathways can contribute to LXRα phosphorylation[342, 343]. My data in Table 23 and Figure 35 represent convincing results of performed mass spectrometry with LXRα protein showing dephosphorylation at Ser198 by activated AMPK. Using tandem mass spectrometry analysis, Torra *et.al.* identified the phosphorylation site at Ser198 which is located in the hinge region of LXRα but is absent in LXRβ protein[344]. This may be the reason for LXRα-dependent and LXRβ-independent ABCA1 regulation as shown in Figure 27. The Ser198 residue of LXRα is conserved between human, mouse, and rat suggesting the conservation of function. The phosphorylation state is not affected by RXR ligand 9-*cis*-

retinoic acid. LXRα phosphorylation at Ser198 in RAW264.7 macrophages is reported, whereas the phosphorylation-deficient mutant S198A of LXRα shows enhanced LPL mRNA expression during T0901317 stimulation implicating the phosphorylation process in a ligand-dependent LXRα transcription activity. Conformational change of LXRα by phosphorylation at Ser198 is hypothesized to recruit co-repressor NCoR, whereas the S198A LXRα mutant does not bind any NCoR in RAW264.7 cells. So, dephosphorylated LXRα mutant leads to NCoR dissociation[344]. Releasing of LXRα-bound co-repressors from *Abca1* promoter leads to increased ABCA1 transcription[283].

According to my results using mass spectrometry and finding possible dephosphorylation site during AMPK activation, a new mediator like a kinase or phosphatase could be involved. According to http://scansite.mit.edu/ LXRα protein is not a direct target of AMPK showing only a binding domain for ERK1/2. ERK1/2 are ubiquitously expressed mitogen-activated protein kinases implicated in embryogenesis, differentiation, and apoptosis[345]. Göransson *et.al*. investigated A-769662 mechanism of action and found different kinases as targets of A-769662 including ERK1/2[231]. The cross-talk between AMPK and ERK1/2 has been reported[346]. AMPK is described to inhibit ERK1/2 in cardiac fibroblasts[347]. In THP-1 macrophages, ERK1/2 are reported to inhibit ABCA1-mediated cholesterol efflux[172]. Another AMPK activator berberine is observed to block ERK1/2 pathway in vascular smooth muscle cells[226]. Furthermore, Salvado *et.al*. report ERK inhibition by PPARδ through AMPK activation in skeletal muscle[348]. Besides, the implication of AMPK into ERK pathway using adenoviral AMPKα1 constructs in cardiomyocytes is shown[349]. Additional study observed a phosphorylation of the protein kinase B-Raf, which regulates proliferation, by AMPK affecting ERK signaling[350]. There is already a strong evidence to propose that ABCA1 expression is negatively regulated by ERK1/2 according to publications. Two independent groups reveal increased ABCA1 expression levels and elevated cholesterol efflux during the inhibition of ERK1/2 in RAW264.7 macrophages[351, 352]. Mentioned results in the literature indicate ERK1/2 as possible mediators between AMPK and LXRα regulating ABCA1 expression and its activity. To investigate, if these kinases are really AMPK-dependent and participate in ABCA1 mechanism, further experiments with ERK inhibitors, AMPK KD or AMPK KO must be performed. Figure 38 shows possible interaction between activated AMPK and LXRα through ERK1/2 in human macrophages.

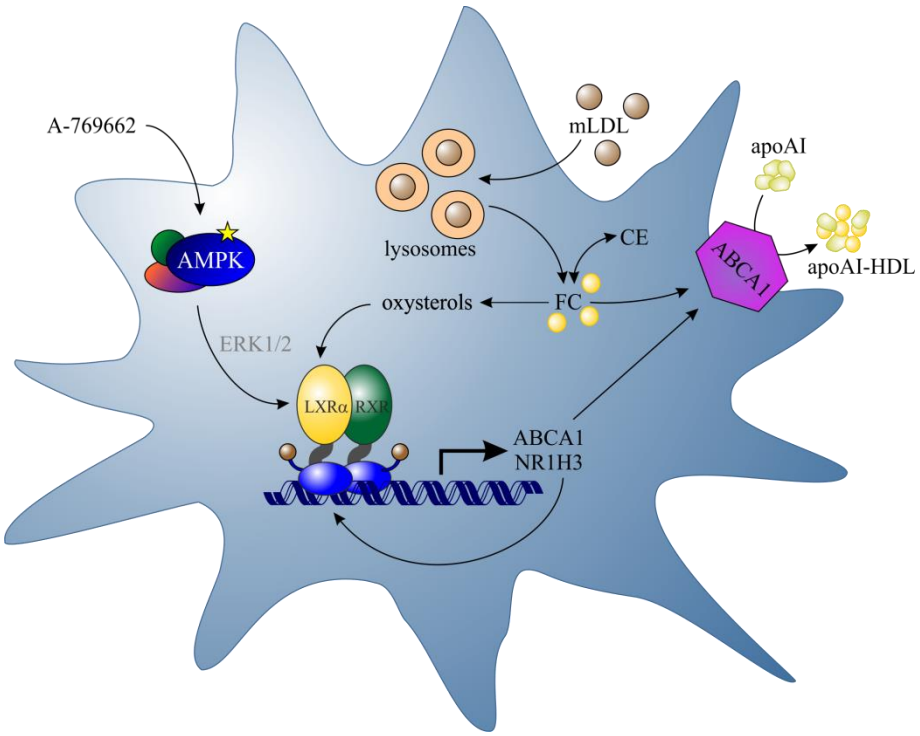

Figure 38: Proposed mechanism of cholesterol metabolism regulation by AMPK in human MΦ.
AMPK activation by A-769662 leads to dephosphorylation and stimulation of LXRα. Induction of LXRα protein occurs probably by inhibition of ERK1/2 which blocks LXRα activity. Induced transcription of LXRα gene *NR1H3* and *Abca1* increase the ABCA1 protein expression and elevate transport of FC onto apoAI particle forming apoAI-HDL. FC comes from mLDL processed by lysosomes and can be transformed into CE or oxysterols, endogenous LXRα ligands, activating LXRα activity on one hand and facilitating cholesterol efflux on the other. ABCA1, ATP-binding cassette transporter A1; apoAI-HDL, apolipoprotein AI-high-density lipoproteins; CE, cholesterol esters; ERK1/2, extracellular signal-regulated kinase 1/2; FC, free cholesterol; mLDL, modified low-density lipoproteins.

Further mediators of ABCA1 regulation may be HDAC. HDAC inhibitors are described to attenuate diabetes and atherosclerosis decreasing inflammatory response[353]. LXRs promote the recruitment of NCoR and SMRT to inhibit target gene expression. These co-repressors of LXRα block its expression by HDAC activation[354, 355]. LXR$^{-/-}$ cells show significant increase of histone H3 acetylation, because of inability to recruit co-repressors[356]. On the other hand, dehydroxytrichostatin A, a HDAC inhibitor, is observed to promote ABCA1 transcription in RAW264.7 macrophages[357] indicating a possible role of HDAC in ABCA1 regulation. A link between histone acetylation and ABCA1 regulation is also found in bone marrow-derived macrophages. In addition, the interaction between class I HDAC, such as HDAC1-3, and PPARδ is found to exhibit transcriptional repression activity in murine fibroblasts[358]. In mouse models a link between AMPK and class II HDACs (4, 5, and 7) was found. AMPK is

shown to phosphorylate these modulators keeping them out of nucleus and thus inhibiting their activity resulting in lower blood glucose and increased glycogen storage[359]. Although the mouse immune system is well understood, many pathways differ in the human system[360]. As activated AMPK induces both LXRα and PPARδ activities in primary human macrophages (Figure 29, Table 23, Figure 14, Figure 20), further investigations in human cell lines, but also *ex vivo* and *in vivo* are necessary to better understand the appropriate regulatory pathways relevant for atherosclerosis and its treatment. Methods such as contrast-enhanced ultrasound, magnetic resonance imaging, near-infrared fluorescence, and usage of isotope-tagged ligands could help to clarify the processes happening in humans[53].

6.7. The impact of AMPK, PPARs, and LXRs on lipid and cholesterol metabolism.

AMPK plays an important role in cholesterol homeostasis regulating rate-limiting enzyme of cholesterol synthesis HMG-CoA reductase which converts HMG-CoA into mevalonate, a progenitor of cholesterol synthesis[196]. Accumulation of free cholesterol in the ER leads to apoptosis of macrophages[361], the process which may cause increased inflammatory response and destabilization of atherosclerotic plaques[362]. Additional study described a decrease of ABCA1 expression and cholesterol efflux induced by high glucose concentration in murine macrophages[351] affirming the role of AMPK in this mechanism. As literature indicates an impact of PPARs on ABCA1 activity and of LXRα on some FAO-associated genes in human macrophages and my experiments show an involvement of AMPK in these pathways, I decided to discuss possible interaction of these regulators in following part (Figure 39).

The involvement of PPARs into LXRα-ABCA1 pathway is shown in Figure 26 observing the dependency of LXRα on PPARγ (Figure 26 C). This phenomenon can be explained by some publications which present the basal LXRα expression regulation by PPARγ agonists[178, 363]. Further studies report the dependency on PPARγ of LXRα-ABCA1 pathway in macrophages where PPARγ, but not PPARδ, is described to significantly induce CD36 or LXRα expression[42, 178, 179, 184, 364]. Interestingly, ABCA1 is not affected by PPARγ silencing (Figure 24 F). Our previous report showed AICAR causing reduction of PPARγ while simultaneously increasing ABCA1 mRNA expression during primary monocyte differentiation suggesting independent regulation of PPARγ and ABCA1, similar to

observations in my work[281]. In conclusion, as PPARγ-silenced cells respond to A-769662 (Figure 26 C), AMPK may act PPARγ-independently regulating LXRα and ABCA1.

Regarding atherosclerosis, the functions of PPARδ and PPARγ were mostly studied during initial stages of lesion progression, characterized by the infiltration of classically activated macrophages[365], whereas how PPARs affect later stages of atherosclerosis, including necrotic core formation and plaque stability should be addressed by future research. Evans and his group propose protecting effect by PPARδ from lipid overload in macrophages[79]. Although PPARδ KD has no effect on ABCA1 mRNA expression (Figure 24 D), several studies using PPARδ$^{-/-}$ mice indicate anti-atherogenic effects of PPARδ. PPARδ deletion leads to increased plasma glucose, TG levels, and elevated LPL[81, 366]. Additionally, an increase of plasma HDL-cholesterol levels by PPARδ was found[81, 367]. The activation of PPARδ is also described to induce angiogenesis in diabetic mice and higher HDL levels in obese rhesus monkeys inhibiting atherosclerosis[101, 368]. Besides GW501516, a novel PPARδ agonist MBX-8025 is found lowering VLDL content and improving dyslipidemia in overweight patients[369, 370]. A study in humans reveals beneficial effects after PPARδ activation regarding the composition and the content of lipoprotein particles in blood plasma[181].

In summary, PPARδ decreases TG levels, which serves as a risk factor for atherosclerosis. This transcription factor prevents atherosclerosis also by acting anti-inflammatory. Although the link between type 2 diabetes and atherosclerosis is poorly understood[371], a common factor seems to be insulin resistance promoting atherogenesis at artery walls and finally cardiovascular diseases[372]. As PPARδ is a key regulator of lipid metabolism, its activation has beneficial effects on metabolic diseases such as dyslipidemia, obesity, insulin resistance, diabetes, and atherosclerosis[85, 104, 105, 373-375].

To connect my two projects regarding the cholesterol efflux regulation, AMPK could activate not only LXRα to induce ABCA1 expression, but also PPARδ. The role of PPARδ has already been described in elevation of apoA1-specific cholesterol efflux[101]. As it is known that ABCA1 is a PPARδ target gene in skeletal muscle cells[107], no effect of ABCA1 mRNA expression was revealed during PPARδ silencing in human macrophages (Figure 24 D). Nevertheless, GW501516 treatment may enhance the ABCA1 expression in human macrophages, fibroblasts, and intestine cells increasing cholesterol efflux. In THP-1 macrophages LXRα and ABCA1 mRNA expression are increased, but also cholesterol efflux

is elevated during compound F-induced PPARδ stimulation[180]. At least, experiments with humans show 2-fold increase of ABCA1 expression after GW501516 administration accompanied by induced FAO[102]. Further investigations of PPARδ involvement into AMPK-LXRα-ABCA1 pathway would be required to find out the impact of PPARδ here.

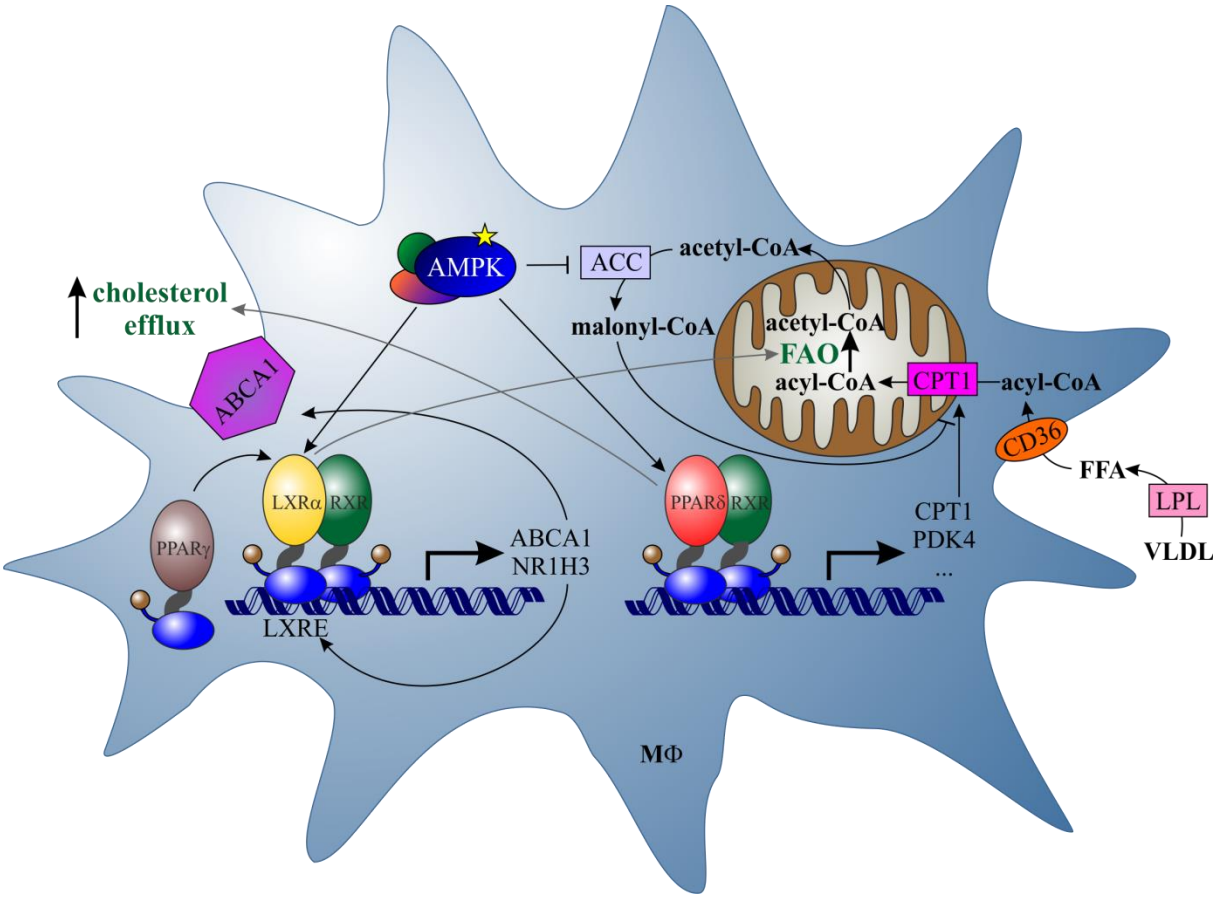

Figure 39: Regulation of LXRα and PPARδ pathways by AMPK in human MΦ.

Activated AMPK increases LXRα activity up-regulating ABCA1 expression and cholesterol efflux. PPARγ stimulates the mRNA expression of LXRα, which is autoregulated in human macrophages. VLDL particles in blood will be transformed into triglycerides by LPL. Later formed FFA can be taken up by macrophages through CD36 and be converted to acyl-CoA. CPT1 transfers acyl-CoA into the mitochondrium where FAO occurs, leading to acetyl-CoA formation. CPT1 can be positively regulated by AMPK by increasing gene expression through PPARδ protein on one hand and through inhibition of ACC on the other. Both pathways LXRα-ABCA1 and PPARδ-CPT1/PDK4 seem to have an impact on each other increasing simultaneously both cholesterol efflux and FAO (grey arrows). ABCA1, ATP-binding cassette transporter 1; ACC, acetyl-CoA carboxylase; AMPK, AMP-activated protein kinase; CD36, cluster of differentiation 36; CPT1, carnitine palmitoyltransferase 1; FAO, fatty acid oxidation; FFA, free fatty acids; LPL, lipoprotein lipase; LXRα, liver X receptor α; LXRE, LXR response element; MΦ, macrophage; NR1H3, protein-coding gene of LXRα; PDK4, pyruvate dehydrogenase kinase 4; PPAR, peroxisome proliferator-activated receptor; RXR, retinoid X receptor.

On the other hand, active LXR is described to influence FAO pathway. It up-regulates PDK4 and CPT1a expression enhancing FAO in skeletal muscle[376] and induces, like PPARδ, the expression of genes such as *Acsl3* (long-chain fatty acid-CoA ligase 3) regulating fatty acid degradation[377]. Besides, LXR regulates LPL and therefore TG amount inside the macrophages[378] having similar effect as PPARδ.

A competition between PPARδ and LXRα for their common partner RXR during ligand-induced PPARδ activation should be considered here[379]. The role of RXR is enormous according to its obligate dimerization partners PPARs and LXRs, but remains still poorly understood especially in processes such as atherosclerosis[380]. In conclusion, further investigations are required to determine the interplay of LXRα and PPARδ in the context of metabolic diseases, such as diabetes mellitus, obesity, insulin resistance, and atherosclerosis, and the impact of AMPK in those to achieve better therapeutic benefits of treatments targeting these nuclear receptors.

6.8. Outlook for the future investigations

The LXR-dependent macrophage lipogenesis is suggested as a pharmacological response to synthetic, but not endogenous ligands, indicating the absence of physiological response to increased cholesterol levels[283]. Further studies on LXRα- but also PPARδ-dependent pathway regulated by AMPK using pharmacological and genetic approaches will clarify the optimal therapeutic profiles for atherosclerosis, but also type 2 diabetes treatments. One aim would be to reduce the activation or down-regulate the recruitment of monocytes to the inflammatory plaque site. Elimination of macrophages from the atherosclerotic plaques would serve as additional treatment, which requires selective drugs. As macrophages play an important role in atherosclerosis development, they should be considered in future therapeutic approaches.

Thinking of future science interesting discovery is made few years ago. David J.P. Barker established a theory that the birth weight determines the risk of type 2 diabetes of everybody´s life. This theory was confirmed by a study in India showing an association of low BMI in infancy and rapid BMI gain in childhood and adolescence with increased risk of metabolic syndrome[381]. Another study shows significant effects of infancy on adolescence bringing placenta surface and later overweight of humans. Here, Barker observed the association of large placental surface with high body fat content and increased risk of overweight in adult

life. Recent experiments show reduced concentrations of Angptl4 and increased serum triacylglycerol, which correlate with up-regulated neonatal fat mass in pregnant women with gestational type 2 diabetes. This phenomenon could lead to a higher fatty acid placental transfer and finally to the fat accumulation in fetus. Newborns of women with gestational diabetes mellitus exhibit the highest fat mass to body weight ratio and the highest concentration of insulin in comparison to control group[382] showing possible influence on human development already during the infancy. Believing in Barker´s theory, further investigations in pregnant women, but also the trace of child´s life should be performed to better understand the up-coming diseases, their development, and treatment.

7. References

1. Odegaard, J.I. & Chawla, A. Alternative macrophage activation and metabolism. *Annual review of pathology* **6**, 275-97 (2011).
2. Eckel, R.H., Grundy, S.M. & Zimmet, P.Z. The metabolic syndrome. *Lancet* **365**, 1415-28 (2005).
3. Malik, S. et al. Impact of the metabolic syndrome on mortality from coronary heart disease, cardiovascular disease, and all causes in United States adults. *Circulation* **110**, 1245-50 (2004).
4. Hanson, R.L., Imperatore, G., Bennett, P.H. & Knowler, W.C. Components of the "metabolic syndrome" and incidence of type 2 diabetes. *Diabetes* **51**, 3120-7 (2002).
5. Stern, M.P., Williams, K., Gonzalez-Villalpando, C., Hunt, K.J. & Haffner, S.M. Does the metabolic syndrome improve identification of individuals at risk of type 2 diabetes and/or cardiovascular disease? *Diabetes Care* **27**, 2676-81 (2004).
6. Nathan, D.M. et al. Medical management of hyperglycaemia in type 2 diabetes mellitus: a consensus algorithm for the initiation and adjustment of therapy: a consensus statement from the American Diabetes Association and the European Association for the Study of Diabetes. *Diabetologia* **52**, 17-30 (2009).
7. prevention, C.f.d.c.a. (2014).
8. Conroy, R.M. et al. Estimation of ten-year risk of fatal cardiovascular disease in Europe: the SCORE project. *Eur Heart J* **24**, 987-1003 (2003).
9. Grundy, S.M. et al. Diagnosis and management of the metabolic syndrome. An American Heart Association/National Heart, Lung, and Blood Institute Scientific Statement. Executive summary. *Cardiol Rev* **13**, 322-7 (2005).
10. O'Neill, L.A. & Hardie, D.G. Metabolism of inflammation limited by AMPK and pseudo-starvation. *Nature* **493**, 346-55 (2013).
11. Ridker, P.M., Cushman, M., Stampfer, M.J., Tracy, R.P. & Hennekens, C.H. Inflammation, aspirin, and the risk of cardiovascular disease in apparently healthy men. *N Engl J Med* **336**, 973-9 (1997).
12. Lindberg, G., Eklund, G.A., Gullberg, B. & Rastam, L. Serum sialic acid concentration and cardiovascular mortality. *BMJ* **302**, 143-6 (1991).
13. Ridker, P.M., Hennekens, C.H., Buring, J.E. & Rifai, N. C-reactive protein and other markers of inflammation in the prediction of cardiovascular disease in women. *N Engl J Med* **342**, 836-43 (2000).
14. Blake, G.J. & Ridker, P.M. Inflammatory bio-markers and cardiovascular risk prediction. *J Intern Med* **252**, 283-94 (2002).
15. Pickup, J.C. Inflammation and activated innate immunity in the pathogenesis of type 2 diabetes. *Diabetes Care* **27**, 813-23 (2004).
16. Libby, P. Inflammation in atherosclerosis. *Nature* **420**, 868-74 (2002).
17. Binder, C.J. et al. Innate and acquired immunity in atherogenesis. *Nature medicine* **8**, 1218-26 (2002).
18. Azzam, K.M. & Fessler, M.B. Crosstalk between reverse cholesterol transport and innate immunity. *Trends Endocrinol Metab* **23**, 169-78 (2012).
19. Orr, J.S. et al. Toll-like receptor 4 deficiency promotes the alternative activation of adipose tissue macrophages. *Diabetes* **61**, 2718-27 (2012).
20. Pickup, J.C. & Mattock, M.B. Activation of the innate immune system as a predictor of cardiovascular mortality in Type 2 diabetes mellitus. *Diabet Med* **20**, 723-6 (2003).
21. de Lemos, E.T., Oliveira, J., Pinheiro, J.P. & Reis, F. Regular physical exercise as a strategy to improve antioxidant and anti-inflammatory status: benefits in type 2 diabetes mellitus. *Oxid Med Cell Longev* **2012**, 741545 (2012).

22. Hotamisligil, G.S. Inflammation and metabolic disorders. *Nature* **444**, 860-7 (2006).
23. Moore, K.J. & Tabas, I. Macrophages in the pathogenesis of atherosclerosis. *Cell* **145**, 341-55 (2011).
24. Huang, S. et al. Saturated fatty acids activate TLR-mediated proinflammatory signaling pathways. *J Lipid Res* **53**, 2002-13 (2012).
25. Brune, B. et al. Redox control of inflammation in macrophages. *Antioxid Redox Signal* **19**, 595-637 (2013).
26. Geissmann, F. et al. Development of monocytes, macrophages, and dendritic cells. *Science* **327**, 656-61 (2010).
27. Chawla, A. Control of macrophage activation and function by PPARs. *Circulation research* **106**, 1559-69 (2010).
28. Gordon, S. Alternative activation of macrophages. *Nature reviews. Immunology* **3**, 23-35 (2003).
29. Odegaard, J.I. & Chawla, A. Pleiotropic actions of insulin resistance and inflammation in metabolic homeostasis. *Science* **339**, 172-7 (2013).
30. Nathan, C. & Ding, A. Nonresolving inflammation. *Cell* **140**, 871-82 (2010).
31. Reichardt, H.M. et al. Repression of inflammatory responses in the absence of DNA binding by the glucocorticoid receptor. *EMBO J* **20**, 7168-73 (2001).
32. Wu, Z. et al. Mechanisms controlling mitochondrial biogenesis and respiration through the thermogenic coactivator PGC-1. *Cell* **98**, 115-24 (1999).
33. Biswas, S.K. & Mantovani, A. Orchestration of metabolism by macrophages. *Cell Metab* **15**, 432-7 (2012).
34. Wynn, T.A., Chawla, A. & Pollard, J.W. Macrophage biology in development, homeostasis and disease. *Nature* **496**, 445-55 (2013).
35. McNelis, J.C. & Olefsky, J.M. Macrophages, immunity, and metabolic disease. *Immunity* **41**, 36-48 (2014).
36. Osborn, O. & Olefsky, J.M. The cellular and signaling networks linking the immune system and metabolism in disease. *Nature medicine* **18**, 363-74 (2012).
37. Steppan, C.M. et al. The hormone resistin links obesity to diabetes. *Nature* **409**, 307-12 (2001).
38. Ozcan, U. et al. Endoplasmic reticulum stress links obesity, insulin action, and type 2 diabetes. *Science* **306**, 457-61 (2004).
39. Furukawa, S. et al. Increased oxidative stress in obesity and its impact on metabolic syndrome. *J Clin Invest* **114**, 1752-61 (2004).
40. Holland, W.L. et al. Lipid-induced insulin resistance mediated by the proinflammatory receptor TLR4 requires saturated fatty acid-induced ceramide biosynthesis in mice. *The Journal of clinical investigation* **121**, 1858-70 (2011).
41. Shelness, G.S. & Sellers, J.A. Very-low-density lipoprotein assembly and secretion. *Current opinion in lipidology* **12**, 151-7 (2001).
42. Chawla, A. et al. PPARdelta is a very low-density lipoprotein sensor in macrophages. *Proceedings of the National Academy of Sciences of the United States of America* **100**, 1268-73 (2003).
43. Hussain, M.M., Strickland, D.K. & Bakillah, A. The mammalian low-density lipoprotein receptor family. *Annu Rev Nutr* **19**, 141-72 (1999).
44. Rader, D.J. & Daugherty, A. Translating molecular discoveries into new therapies for atherosclerosis. *Nature* **451**, 904-13 (2008).
45. Lee, C.D., Folsom, A.R., Pankow, J.S. & Brancati, F.L. Cardiovascular events in diabetic and nondiabetic adults with or without history of myocardial infarction. *Circulation* **109**, 855-60 (2004).

46. Mokdad, A.H. et al. Prevalence of obesity, diabetes, and obesity-related health risk factors, 2001. *JAMA* **289**, 76-9 (2003).
47. Zhao, C. & Dahlman-Wright, K. Liver X receptor in cholesterol metabolism. *J Endocrinol* **204**, 233-40 (2010).
48. Brown, M.S. & Goldstein, J.L. The SREBP pathway: regulation of cholesterol metabolism by proteolysis of a membrane-bound transcription factor. *Cell* **89**, 331-40 (1997).
49. Williams, K.J. & Tabas, I. The response-to-retention hypothesis of early atherogenesis. *Arteriosclerosis, thrombosis, and vascular biology* **15**, 551-61 (1995).
50. De Meyer, I., Martinet, W. & De Meyer, G.R. Therapeutic strategies to deplete macrophages in atherosclerotic plaques. *Br J Clin Pharmacol* **74**, 246-63 (2012).
51. Libby, P., Ridker, P.M. & Maseri, A. Inflammation and atherosclerosis. *Circulation* **105**, 1135-43 (2002).
52. Boyle, J.J. Macrophage activation in atherosclerosis: pathogenesis and pharmacology of plaque rupture. *Curr Vasc Pharmacol* **3**, 63-8 (2005).
53. Libby, P., Ridker, P.M. & Hansson, G.K. Progress and challenges in translating the biology of atherosclerosis. *Nature* **473**, 317-25 (2011).
54. Johnson, J.L. & Newby, A.C. Macrophage heterogeneity in atherosclerotic plaques. *Current opinion in lipidology* **20**, 370-8 (2009).
55. Tabas, I., Williams, K.J. & Boren, J. Subendothelial lipoprotein retention as the initiating process in atherosclerosis: update and therapeutic implications. *Circulation* **116**, 1832-44 (2007).
56. Kruth, H.S. et al. Macropinocytosis is the endocytic pathway that mediates macrophage foam cell formation with native low density lipoprotein. *J Biol Chem* **280**, 2352-60 (2005).
57. Tabas, I. et al. Lipoprotein lipase and sphingomyelinase synergistically enhance the association of atherogenic lipoproteins with smooth muscle cells and extracellular matrix. A possible mechanism for low density lipoprotein and lipoprotein(a) retention and macrophage foam cell formation. *J Biol Chem* **268**, 20419-32 (1993).
58. Brown, M.S., Ho, Y.K. & Goldstein, J.L. The cholesteryl ester cycle in macrophage foam cells. Continual hydrolysis and re-esterification of cytoplasmic cholesteryl esters. *J Biol Chem* **255**, 9344-52 (1980).
59. Li, Y. et al. Lipoprotein lipase: From gene to atherosclerosis. *Atherosclerosis* **237**, 597-608 (2014).
60. Coll, T. et al. Peroxisome proliferator-activated receptor (PPAR) beta/delta: a new potential therapeutic target for the treatment of metabolic syndrome. *Curr Mol Pharmacol* **2**, 46-55 (2009).
61. Boyle, J.J., Weissberg, P.L. & Bennett, M.R. Human macrophage-induced vascular smooth muscle cell apoptosis requires NO enhancement of Fas/Fas-L interactions. *Arteriosclerosis, thrombosis, and vascular biology* **22**, 1624-30 (2002).
62. Newby, A.C. et al. Vulnerable atherosclerotic plaque metalloproteinases and foam cell phenotypes. *Thromb Haemost* **101**, 1006-11 (2009).
63. Tabas, I. & Ron, D. Integrating the mechanisms of apoptosis induced by endoplasmic reticulum stress. *Nat Cell Biol* **13**, 184-90 (2011).
64. Rader, D.J. Molecular regulation of HDL metabolism and function: implications for novel therapies. *J Clin Invest* **116**, 3090-100 (2006).
65. Rye, K.A., Bursill, C.A., Lambert, G., Tabet, F. & Barter, P.J. The metabolism and anti-atherogenic properties of HDL. *J Lipid Res* **50 Suppl**, S195-200 (2009).
66. Tabas, I., Garcia-Cardena, G. & Owens, G.K. Recent insights into the cellular biology of atherosclerosis. *J Cell Biol* **209**, 13-22 (2015).

67. Kiss, M., Czimmerer, Z. & Nagy, L. The role of lipid-activated nuclear receptors in shaping macrophage and dendritic cell function: From physiology to pathology. *J Allergy Clin Immunol* **132**, 264-86 (2013).
68. Aranda, A. & Pascual, A. Nuclear hormone receptors and gene expression. *Physiol Rev* **81**, 1269-304 (2001).
69. Chinetti, G., Fruchart, J.C. & Staels, B. Peroxisome proliferator-activated receptors (PPARs): nuclear receptors at the crossroads between lipid metabolism and inflammation. *Inflamm Res* **49**, 497-505 (2000).
70. Glass, C.K. & Saijo, K. Nuclear receptor transrepression pathways that regulate inflammation in macrophages and T cells. *Nature reviews. Immunology* **10**, 365-76 (2010).
71. Desvergne, B., Michalik, L. & Wahli, W. Transcriptional regulation of metabolism. *Physiol Rev* **86**, 465-514 (2006).
72. Marx, N., Duez, H., Fruchart, J.C. & Staels, B. Peroxisome proliferator-activated receptors and atherogenesis: regulators of gene expression in vascular cells. *Circ Res* **94**, 1168-78 (2004).
73. Nielsen, R., Grontved, L., Stunnenberg, H.G. & Mandrup, S. Peroxisome proliferator-activated receptor subtype- and cell-type-specific activation of genomic target genes upon adenoviral transgene delivery. *Mol Cell Biol* **26**, 5698-714 (2006).
74. Kersten, S. et al. Peroxisome proliferator-activated receptor alpha mediates the adaptive response to fasting. *J Clin Invest* **103**, 1489-98 (1999).
75. Moraes, L.A., Piqueras, L. & Bishop-Bailey, D. Peroxisome proliferator-activated receptors and inflammation. *Pharmacol Ther* **110**, 371-85 (2006).
76. Nagy, L., Szanto, A., Szatmari, I. & Szeles, L. Nuclear hormone receptors enable macrophages and dendritic cells to sense their lipid environment and shape their immune response. *Physiol Rev* **92**, 739-89 (2012).
77. Barak, Y. et al. PPAR gamma is required for placental, cardiac, and adipose tissue development. *Molecular cell* **4**, 585-95 (1999).
78. Kubota, N. et al. PPAR gamma mediates high-fat diet-induced adipocyte hypertrophy and insulin resistance. *Molecular cell* **4**, 597-609 (1999).
79. Lee, C.H. et al. Peroxisome proliferator-activated receptor delta promotes very low-density lipoprotein-derived fatty acid catabolism in the macrophage. *Proceedings of the National Academy of Sciences of the United States of America* **103**, 2434-9 (2006).
80. Tanaka, T. et al. Activation of peroxisome proliferator-activated receptor delta induces fatty acid beta-oxidation in skeletal muscle and attenuates metabolic syndrome. *Proc Natl Acad Sci U S A* **100**, 15924-9 (2003).
81. Sanderson, L.M., Boekschoten, M.V., Desvergne, B., Muller, M. & Kersten, S. Transcriptional profiling reveals divergent roles of PPARalpha and PPARbeta/delta in regulation of gene expression in mouse liver. *Physiol Genomics* **41**, 42-52 (2010).
82. Desvergne, B. PPARdelta/beta: the lobbyist switching macrophage allegiance in favor of metabolism. *Cell Metab* **7**, 467-9 (2008).
83. Odegaard, J.I. et al. Alternative M2 activation of Kupffer cells by PPARdelta ameliorates obesity-induced insulin resistance. *Cell metabolism* **7**, 496-507 (2008).
84. Lee, C.H. et al. PPARdelta regulates glucose metabolism and insulin sensitivity. *Proc Natl Acad Sci U S A* **103**, 3444-9 (2006).
85. Wang, Y.X. et al. Peroxisome-proliferator-activated receptor delta activates fat metabolism to prevent obesity. *Cell* **113**, 159-70 (2003).
86. Lee, C.H. et al. Transcriptional repression of atherogenic inflammation: modulation by PPARdelta. *Science* **302**, 453-7 (2003).

87. Barish, G.D., Narkar, V.A. & Evans, R.M. PPAR delta: a dagger in the heart of the metabolic syndrome. *J Clin Invest* **116**, 590-7 (2006).
88. Kang, K. et al. Adipocyte-derived Th2 cytokines and myeloid PPARdelta regulate macrophage polarization and insulin sensitivity. *Cell metabolism* **7**, 485-95 (2008).
89. Adhikary, T. et al. Genomewide analyses define different modes of transcriptional regulation by peroxisome proliferator-activated receptor-beta/delta (PPARbeta/delta). *Plos One* **6**, e16344 (2011).
90. Coll, T. et al. The Role of Peroxisome Proliferator-Activated Receptor beta/delta on the Inflammatory Basis of Metabolic Disease. *PPAR Res* **2010** (2010).
91. Daynes, R.A. & Jones, D.C. Emerging roles of PPARs in inflammation and immunity. *Nature reviews. Immunology* **2**, 748-59 (2002).
92. Ghisletti, S. et al. Cooperative NCoR/SMRT interactions establish a corepressor-based strategy for integration of inflammatory and anti-inflammatory signaling pathways. *Genes & development* **23**, 681-93 (2009).
93. Bishop-Bailey, D. & Bystrom, J. Emerging roles of peroxisome proliferator-activated receptor-beta/delta in inflammation. *Pharmacol Ther* **124**, 141-50 (2009).
94. Takata, Y. et al. PPARdelta-mediated antiinflammatory mechanisms inhibit angiotensin II-accelerated atherosclerosis. *Proceedings of the National Academy of Sciences of the United States of America* **105**, 4277-82 (2008).
95. Fan, Y. et al. Suppression of pro-inflammatory adhesion molecules by PPAR-delta in human vascular endothelial cells. *Arteriosclerosis, thrombosis, and vascular biology* **28**, 315-21 (2008).
96. Kilgore, K.S. & Billin, A.N. PPARbeta/delta ligands as modulators of the inflammatory response. *Curr Opin Investig Drugs* **9**, 463-9 (2008).
97. Sznaidman, M.L. et al. Novel selective small molecule agonists for peroxisome proliferator-activated receptor delta (PPARdelta)--synthesis and biological activity. *Bioorg Med Chem Lett* **13**, 1517-21 (2003).
98. Randle, P.J. Fuel selection in animals. *Biochem Soc Trans* **14**, 799-806 (1986).
99. Alvarez-Guardia, D. et al. PPARbeta/delta activation blocks lipid-induced inflammatory pathways in mouse heart and human cardiac cells. *Biochimica et biophysica acta* **1811**, 59-67 (2011).
100. Rodriguez-Calvo, R. et al. Activation of peroxisome proliferator-activated receptor beta/delta inhibits lipopolysaccharide-induced cytokine production in adipocytes by lowering nuclear factor-kappaB activity via extracellular signal-related kinase 1/2. *Diabetes* **57**, 2149-57 (2008).
101. Oliver, W.R., Jr. et al. A selective peroxisome proliferator-activated receptor delta agonist promotes reverse cholesterol transport. *Proc Natl Acad Sci U S A* **98**, 5306-11 (2001).
102. Sprecher, D.L. et al. Triglyceride:high-density lipoprotein cholesterol effects in healthy subjects administered a peroxisome proliferator activated receptor delta agonist. *Arteriosclerosis, thrombosis, and vascular biology* **27**, 359-65 (2007).
103. Ooi, E.M., Watts, G.F., Sprecher, D.L., Chan, D.C. & Barrett, P.H. Mechanism of action of a peroxisome proliferator-activated receptor (PPAR)-delta agonist on lipoprotein metabolism in dyslipidemic subjects with central obesity. *J Clin Endocrinol Metab* **96**, E1568-76 (2011).
104. Bojic, L.A. & Huff, M.W. Peroxisome proliferator-activated receptor delta: a multifaceted metabolic player. *Current opinion in lipidology* **24**, 171-7 (2013).
105. Riserus, U. et al. Activation of peroxisome proliferator-activated receptor (PPAR)delta promotes reversal of multiple metabolic abnormalities, reduces oxidative stress, and increases fatty acid oxidation in moderately obese men. *Diabetes* **57**, 332-9 (2008).

106. Brasaemle, D.L. et al. Adipose differentiation-related protein is an ubiquitously expressed lipid storage droplet-associated protein. *J Lipid Res* **38**, 2249-63 (1997).
107. Dressel, U. et al. The peroxisome proliferator-activated receptor beta/delta agonist, GW501516, regulates the expression of genes involved in lipid catabolism and energy uncoupling in skeletal muscle cells. *Molecular endocrinology* **17**, 2477-93 (2003).
108. Zhu, P., Goh, Y.Y., Chin, H.F., Kersten, S. & Tan, N.S. Angiopoietin-like 4: a decade of research. *Biosci Rep* **32**, 211-9 (2012).
109. Mandard, S. et al. The fasting-induced adipose factor/angiopoietin-like protein 4 is physically associated with lipoproteins and governs plasma lipid levels and adiposity. *J Biol Chem* **281**, 934-44 (2006).
110. Adhikary, T. et al. Inverse PPARbeta/delta agonists suppress oncogenic signaling to the ANGPTL4 gene and inhibit cancer cell invasion. *Oncogene* **32**, 5241-52 (2013).
111. Eckel, R.H. Lipoprotein lipase. A multifunctional enzyme relevant to common metabolic diseases. *N Engl J Med* **320**, 1060-8 (1989).
112. Sukonina, V., Lookene, A., Olivecrona, T. & Olivecrona, G. Angiopoietin-like protein 4 converts lipoprotein lipase to inactive monomers and modulates lipase activity in adipose tissue. *Proc Natl Acad Sci U S A* **103**, 17450-5 (2006).
113. Nahle, Z. et al. CD36-dependent regulation of muscle FoxO1 and PDK4 in the PPAR delta/beta-mediated adaptation to metabolic stress. *J Biol Chem* **283**, 14317-26 (2008).
114. Sugden, M.C., Kraus, A., Harris, R.A. & Holness, M.J. Fibre-type specific modification of the activity and regulation of skeletal muscle pyruvate dehydrogenase kinase (PDK) by prolonged starvation and refeeding is associated with targeted regulation of PDK isoenzyme 4 expression. *Biochem J* **346 Pt 3**, 651-7 (2000).
115. Foster, D.W. Malonyl-CoA: the regulator of fatty acid synthesis and oxidation. *J Clin Invest* **122**, 1958-9 (2012).
116. Nakamura, M.T., Yudell, B.E. & Loor, J.J. Regulation of energy metabolism by long-chain fatty acids. *Prog Lipid Res* **53**, 124-44 (2014).
117. Schuler, M. et al. PGC1alpha expression is controlled in skeletal muscles by PPARbeta, whose ablation results in fiber-type switching, obesity, and type 2 diabetes. *Cell Metab* **4**, 407-14 (2006).
118. Peters, J.M., Shah, Y.M. & Gonzalez, F.J. The role of peroxisome proliferator-activated receptors in carcinogenesis and chemoprevention. *Nat Rev Cancer* **12**, 181-95 (2012).
119. N, A.G. & Castrillo, A. Liver X receptors as regulators of macrophage inflammatory and metabolic pathways. *Biochimica et biophysica acta* **1812**, 982-94 (2011).
120. Lehmann, J.M. et al. Activation of the nuclear receptor LXR by oxysterols defines a new hormone response pathway. *The Journal of biological chemistry* **272**, 3137-40 (1997).
121. Michalik, L. et al. International Union of Pharmacology. LXI. Peroxisome proliferator-activated receptors. *Pharmacol Rev* **58**, 726-41 (2006).
122. Erbay, E. et al. Reducing endoplasmic reticulum stress through a macrophage lipid chaperone alleviates atherosclerosis. *Nature medicine* **15**, 1383-91 (2009).
123. Levin, N. et al. Macrophage liver X receptor is required for antiatherogenic activity of LXR agonists. *Arteriosclerosis, thrombosis, and vascular biology* **25**, 135-42 (2005).
124. Valledor, A.F. et al. Activation of liver X receptors and retinoid X receptors prevents bacterial-induced macrophage apoptosis. *Proc Natl Acad Sci U S A* **101**, 17813-8 (2004).
125. Nomiyama, T. & Bruemmer, D. Liver X receptors as therapeutic targets in metabolism and atherosclerosis. *Current atherosclerosis reports* **10**, 88-95 (2008).

126. Jakobsson, T., Treuter, E., Gustafsson, J.A. & Steffensen, K.R. Liver X receptor biology and pharmacology: new pathways, challenges and opportunities. *Trends Pharmacol Sci* **33**, 394-404 (2012).
127. Joseph, S.B., Castrillo, A., Laffitte, B.A., Mangelsdorf, D.J. & Tontonoz, P. Reciprocal regulation of inflammation and lipid metabolism by liver X receptors. *Nature medicine* **9**, 213-9 (2003).
128. Fontaine, C. et al. Liver X receptor activation potentiates the lipopolysaccharide response in human macrophages. *Circulation research* **101**, 40-9 (2007).
129. Macphee, C.H., Nelson, J. & Zalewski, A. Role of lipoprotein-associated phospholipase A2 in atherosclerosis and its potential as a therapeutic target. *Curr Opin Pharmacol* **6**, 154-61 (2006).
130. Morbitzer, D., Namgaladze, D. & Brune, B. Phospholipase A(2)-modified low-density lipoprotein activates liver X receptor in human macrophages. *Cell biochemistry and biophysics* **63**, 143-9 (2012).
131. Laffitte, B.A. et al. LXRs control lipid-inducible expression of the apolipoprotein E gene in macrophages and adipocytes. *Proc Natl Acad Sci U S A* **98**, 507-12 (2001).
132. Peet, D.J. et al. Cholesterol and bile acid metabolism are impaired in mice lacking the nuclear oxysterol receptor LXR alpha. *Cell* **93**, 693-704 (1998).
133. Alberti, S. et al. Hepatic cholesterol metabolism and resistance to dietary cholesterol in LXRbeta-deficient mice. *J Clin Invest* **107**, 565-73 (2001).
134. Laffitte, B.A. et al. Autoregulation of the human liver X receptor alpha promoter. *Mol Cell Biol* **21**, 7558-68 (2001).
135. Li, Y. et al. Induction of human liver X receptor alpha gene expression via an autoregulatory loop mechanism. *Molecular endocrinology* **16**, 506-14 (2002).
136. Chen, M., Bradley, M.N., Beaven, S.W. & Tontonoz, P. Phosphorylation of the liver X receptors. *FEBS Lett* **580**, 4835-41 (2006).
137. Li, X. et al. SIRT1 deacetylates and positively regulates the nuclear receptor LXR. *Molecular cell* **28**, 91-106 (2007).
138. Ghisletti, S. et al. Parallel SUMOylation-dependent pathways mediate gene- and signal-specific transrepression by LXRs and PPARgamma. *Molecular cell* **25**, 57-70 (2007).
139. Anthonisen, E.H. et al. Nuclear receptor liver X receptor is O-GlcNAc-modified in response to glucose. *J Biol Chem* **285**, 1607-15 (2010).
140. Repa, J.J. et al. Regulation of absorption and ABC1-mediated efflux of cholesterol by RXR heterodimers. *Science* **289**, 1524-9 (2000).
141. Venkateswaran, A. et al. Human white/murine ABC8 mRNA levels are highly induced in lipid-loaded macrophages. A transcriptional role for specific oxysterols. *J Biol Chem* **275**, 14700-7 (2000).
142. Naik, S.U. et al. Pharmacological activation of liver X receptors promotes reverse cholesterol transport in vivo. *Circulation* **113**, 90-7 (2006).
143. Beyea, M.M. et al. Selective up-regulation of LXR-regulated genes ABCA1, ABCG1, and APOE in macrophages through increased endogenous synthesis of 24(S),25-epoxycholesterol. *J Biol Chem* **282**, 5207-16 (2007).
144. Dean, M. & Allikmets, R. Evolution of ATP-binding cassette transporter genes. *Curr Opin Genet Dev* **5**, 779-85 (1995).
145. Wang, N., Silver, D.L., Thiele, C. & Tall, A.R. ATP-binding cassette transporter A1 (ABCA1) functions as a cholesterol efflux regulatory protein. *J Biol Chem* **276**, 23742-7 (2001).
146. Tall, A.R. & Wang, N. Tangier disease as a test of the reverse cholesterol transport hypothesis. *J Clin Invest* **106**, 1205-7 (2000).

147. Zelcer, N. & Tontonoz, P. Liver X receptors as integrators of metabolic and inflammatory signaling. *J Clin Invest* **116**, 607-14 (2006).
148. Remaley, A.T. et al. Human ATP-binding cassette transporter 1 (ABC1): genomic organization and identification of the genetic defect in the original Tangier disease kindred. *Proc Natl Acad Sci U S A* **96**, 12685-90 (1999).
149. Langmann, T. et al. Molecular cloning of the human ATP-binding cassette transporter 1 (hABC1): evidence for sterol-dependent regulation in macrophages. *Biochem Biophys Res Commun* **257**, 29-33 (1999).
150. Aiello, R.J., Brees, D. & Francone, O.L. ABCA1-deficient mice: insights into the role of monocyte lipid efflux in HDL formation and inflammation. *Arteriosclerosis, thrombosis, and vascular biology* **23**, 972-80 (2003).
151. Francone, O.L. & Aiello, R.J. ABCA1: regulation, function and relationship to atherosclerosis. *Curr Opin Investig Drugs* **3**, 415-9 (2002).
152. Lv, Y.C. et al. Posttranscriptional regulation of ATP-binding cassette transporter A1 in lipid metabolism. *DNA Cell Biol* **32**, 348-58 (2013).
153. Schultz, J.R. et al. Role of LXRs in control of lipogenesis. *Genes & development* **14**, 2831-8 (2000).
154. Collins, J.L. et al. Identification of a nonsteroidal liver X receptor agonist through parallel array synthesis of tertiary amines. *J Med Chem* **45**, 1963-6 (2002).
155. Chambenoit, O. et al. Specific docking of apolipoprotein A-I at the cell surface requires a functional ABCA1 transporter. *J Biol Chem* **276**, 9955-60 (2001).
156. Nissen, S.E. et al. Effect of recombinant ApoA-I Milano on coronary atherosclerosis in patients with acute coronary syndromes: a randomized controlled trial. *JAMA* **290**, 2292-300 (2003).
157. Tardif, J.C. et al. Effects of reconstituted high-density lipoprotein infusions on coronary atherosclerosis: a randomized controlled trial. *JAMA* **297**, 1675-82 (2007).
158. Zhu, X. et al. Macrophage ABCA1 reduces MyD88-dependent Toll-like receptor trafficking to lipid rafts by reduction of lipid raft cholesterol. *J Lipid Res* **51**, 3196-206 (2010).
159. Yvan-Charvet, L. et al. Increased inflammatory gene expression in ABC transporter-deficient macrophages: free cholesterol accumulation, increased signaling via toll-like receptors, and neutrophil infiltration of atherosclerotic lesions. *Circulation* **118**, 1837-47 (2008).
160. Zhu, X. et al. Increased cellular free cholesterol in macrophage-specific Abca1 knock-out mice enhances pro-inflammatory response of macrophages. *J Biol Chem* **283**, 22930-41 (2008).
161. Yvan-Charvet, L. et al. ATP-binding cassette transporters and HDL suppress hematopoietic stem cell proliferation. *Science* **328**, 1689-93 (2010).
162. Yvan-Charvet, L. et al. Combined deficiency of ABCA1 and ABCG1 promotes foam cell accumulation and accelerates atherosclerosis in mice. *J Clin Invest* **117**, 3900-8 (2007).
163. Singaraja, R.R. et al. Increased ABCA1 activity protects against atherosclerosis. *J Clin Invest* **110**, 35-42 (2002).
164. Aiello, R.J. et al. Increased atherosclerosis in hyperlipidemic mice with inactivation of ABCA1 in macrophages. *Arteriosclerosis, thrombosis, and vascular biology* **22**, 630-7 (2002).
165. Ma, L., Dong, F., Zaid, M., Kumar, A. & Zha, X. ABCA1 protein enhances Toll-like receptor 4 (TLR4)-stimulated interleukin-10 (IL-10) secretion through protein kinase A (PKA) activation. *J Biol Chem* **287**, 40502-12 (2012).

166. Larrede, S. et al. Stimulation of cholesterol efflux by LXR agonists in cholesterol-loaded human macrophages is ABCA1-dependent but ABCG1-independent. *Arteriosclerosis, thrombosis, and vascular biology* **29**, 1930-6 (2009).
167. Ma, A.Z., Song, Z.Y. & Zhang, Q. Cholesterol efflux is LXRalpha isoform-dependent in human macrophages. *BMC Cardiovasc Disord* **14**, 80 (2014).
168. Hao, X.R. et al. IFN-gamma down-regulates ABCA1 expression by inhibiting LXRalpha in a JAK/STAT signaling pathway-dependent manner. *Atherosclerosis* **203**, 417-28 (2009).
169. Chen, M., Li, W., Wang, N., Zhu, Y. & Wang, X. ROS and NF-kappaB but not LXR mediate IL-1beta signaling for the downregulation of ATP-binding cassette transporter A1. *Am J Physiol Cell Physiol* **292**, C1493-501 (2007).
170. Wang, Y.F. et al. Protective effect of Astragalus polysaccharides on ATP binding cassette transporter A1 in THP-1 derived foam cells exposed to tumor necrosis factor-alpha. *Phytother Res* **24**, 393-8 (2010).
171. Pascual-Garcia, M. et al. Reciprocal negative cross-talk between liver X receptors (LXRs) and STAT1: effects on IFN-gamma-induced inflammatory responses and LXR-dependent gene expression. *Journal of immunology* **190**, 6520-32 (2013).
172. Wang, X. et al. C-reactive protein inhibits cholesterol efflux from human macrophage-derived foam cells. *Arteriosclerosis, thrombosis, and vascular biology* **28**, 519-26 (2008).
173. Chan, E.S. et al. Effect of cyclooxygenase inhibition on cholesterol efflux proteins and atheromatous foam cell transformation in THP-1 human macrophages: a possible mechanism for increased cardiovascular risk. *Arthritis Res Ther* **9**, R4 (2007).
174. Han, X., Kitamoto, S., Lian, Q. & Boisvert, W.A. Interleukin-10 facilitates both cholesterol uptake and efflux in macrophages. *J Biol Chem* **284**, 32950-8 (2009).
175. Panousis, C.G., Evans, G. & Zuckerman, S.H. TGF-beta increases cholesterol efflux and ABC-1 expression in macrophage-derived foam cells: opposing the effects of IFN-gamma. *J Lipid Res* **42**, 856-63 (2001).
176. Mukundan, L. et al. PPAR-delta senses and orchestrates clearance of apoptotic cells to promote tolerance. *Nature medicine* **15**, 1266-72 (2009).
177. N, A.G. et al. Apoptotic cells promote their own clearance and immune tolerance through activation of the nuclear receptor LXR. *Immunity* **31**, 245-58 (2009).
178. Chawla, A. et al. A PPAR gamma-LXR-ABCA1 pathway in macrophages is involved in cholesterol efflux and atherogenesis. *Molecular cell* **7**, 161-71 (2001).
179. Chinetti, G. et al. PPAR-alpha and PPAR-gamma activators induce cholesterol removal from human macrophage foam cells through stimulation of the ABCA1 pathway. *Nature medicine* **7**, 53-8 (2001).
180. Vosper, H. et al. The peroxisome proliferator-activated receptor delta promotes lipid accumulation in human macrophages. *J Biol Chem* **276**, 44258-65 (2001).
181. Olson, E.J., Pearce, G.L., Jones, N.P. & Sprecher, D.L. Lipid effects of peroxisome proliferator-activated receptor-delta agonist GW501516 in subjects with low high-density lipoprotein cholesterol: characteristics of metabolic syndrome. *Arteriosclerosis, thrombosis, and vascular biology* **32**, 2289-94 (2012).
182. Li, A.C. et al. Differential inhibition of macrophage foam-cell formation and atherosclerosis in mice by PPARalpha, beta/delta, and gamma. *The Journal of clinical investigation* **114**, 1564-76 (2004).
183. Graham, T.L., Mookherjee, C., Suckling, K.E., Palmer, C.N. & Patel, L. The PPARdelta agonist GW0742X reduces atherosclerosis in LDLR(-/-) mice. *Atherosclerosis* **181**, 29-37 (2005).

184. Nakaya, K. et al. Telmisartan enhances cholesterol efflux from THP-1 macrophages by activating PPARgamma. *J Atheroscler Thromb* **14**, 133-41 (2007).
185. Zhang, L. et al. DNA topoisomerase II inhibitors induce macrophage ABCA1 expression and cholesterol efflux-an LXR-dependent mechanism. *Biochimica et biophysica acta* **1831**, 1134-45 (2013).
186. Calkin, A.C. & Tontonoz, P. Liver x receptor signaling pathways and atherosclerosis. *Arteriosclerosis, thrombosis, and vascular biology* **30**, 1513-8 (2010).
187. Peng, D., Hiipakka, R.A., Reardon, C.A., Getz, G.S. & Liao, S. Differential anti-atherosclerotic effects in the innominate artery and aortic sinus by the liver X receptor agonist T0901317. *Atherosclerosis* **203**, 59-66 (2009).
188. Grefhorst, A. et al. Stimulation of lipogenesis by pharmacological activation of the liver X receptor leads to production of large, triglyceride-rich very low density lipoprotein particles. *J Biol Chem* **277**, 34182-90 (2002).
189. Tangirala, R.K. et al. Identification of macrophage liver X receptors as inhibitors of atherosclerosis. *Proceedings of the National Academy of Sciences of the United States of America* **99**, 11896-901 (2002).
190. Bischoff, E.D. et al. Non-redundant roles for LXRalpha and LXRbeta in atherosclerosis susceptibility in low density lipoprotein receptor knockout mice. *J Lipid Res* **51**, 900-6 (2010).
191. Schuster, G.U. et al. Accumulation of foam cells in liver X receptor-deficient mice. *Circulation* **106**, 1147-53 (2002).
192. Imamura, K., Ogura, T., Kishimoto, A., Kaminishi, M. & Esumi, H. Cell cycle regulation via p53 phosphorylation by a 5'-AMP activated protein kinase activator, 5-aminoimidazole- 4-carboxamide-1-beta-D-ribofuranoside, in a human hepatocellular carcinoma cell line. *Biochem Biophys Res Commun* **287**, 562-7 (2001).
193. Jones, R.G. et al. AMP-activated protein kinase induces a p53-dependent metabolic checkpoint. *Molecular cell* **18**, 283-93 (2005).
194. Corton, J.M., Gillespie, J.G., Hawley, S.A. & Hardie, D.G. 5-aminoimidazole-4-carboxamide ribonucleoside. A specific method for activating AMP-activated protein kinase in intact cells? *Eur J Biochem* **229**, 558-65 (1995).
195. Towler, M.C. & Hardie, D.G. AMP-activated protein kinase in metabolic control and insulin signaling. *Circ Res* **100**, 328-41 (2007).
196. Misra, P. AMP activated protein kinase: a next generation target for total metabolic control. *Expert Opin Ther Targets* **12**, 91-100 (2008).
197. Chen, L. et al. AMP-activated protein kinase undergoes nucleotide-dependent conformational changes. *Nat Struct Mol Biol* **19**, 716-8 (2012).
198. Sanders, M.J. et al. Defining the mechanism of activation of AMP-activated protein kinase by the small molecule A-769662, a member of the thienopyridone family. *J Biol Chem* **282**, 32539-48 (2007).
199. Lizcano, J.M. et al. LKB1 is a master kinase that activates 13 kinases of the AMPK subfamily, including MARK/PAR-1. *EMBO J* **23**, 833-43 (2004).
200. Sakamoto, K., Goransson, O., Hardie, D.G. & Alessi, D.R. Activity of LKB1 and AMPK-related kinases in skeletal muscle: effects of contraction, phenformin, and AICAR. *Am J Physiol Endocrinol Metab* **287**, E310-7 (2004).
201. Carling, D., Sanders, M.J. & Woods, A. The regulation of AMP-activated protein kinase by upstream kinases. *Int J Obes (Lond)* **32 Suppl 4**, S55-9 (2008).
202. Hawley, S.A. et al. Calmodulin-dependent protein kinase kinase-beta is an alternative upstream kinase for AMP-activated protein kinase. *Cell Metab* **2**, 9-19 (2005).
203. Stein, S.C., Woods, A., Jones, N.A., Davison, M.D. & Carling, D. The regulation of AMP-activated protein kinase by phosphorylation. *Biochem J* **345 Pt 3**, 437-43 (2000).

204. Crute, B.E., Seefeld, K., Gamble, J., Kemp, B.E. & Witters, L.A. Functional domains of the alpha1 catalytic subunit of the AMP-activated protein kinase. *J Biol Chem* **273**, 35347-54 (1998).
205. Gadalla, A.E. et al. AICA riboside both activates AMP-activated protein kinase and competes with adenosine for the nucleoside transporter in the CA1 region of the rat hippocampus. *J Neurochem* **88**, 1272-82 (2004).
206. Bai, A. et al. AMPK agonist downregulates innate and adaptive immune responses in TNBS-induced murine acute and relapsing colitis. *Biochemical pharmacology* **80**, 1708-17 (2010).
207. Gaidhu, M.P. et al. Chronic AMP-kinase activation with AICAR reduces adiposity by remodeling adipocyte metabolism and increasing leptin sensitivity. *J Lipid Res* **52**, 1702-11 (2011).
208. Longnus, S.L., Wambolt, R.B., Parsons, H.L., Brownsey, R.W. & Allard, M.F. 5-Aminoimidazole-4-carboxamide 1-beta -D-ribofuranoside (AICAR) stimulates myocardial glycogenolysis by allosteric mechanisms. *Am J Physiol Regul Integr Comp Physiol* **284**, R936-44 (2003).
209. Vincent, M.F., Erion, M.D., Gruber, H.E. & Van den Berghe, G. Hypoglycaemic effect of AICAriboside in mice. *Diabetologia* **39**, 1148-55 (1996).
210. Guigas, B. et al. 5-Aminoimidazole-4-carboxamide-1-beta-D-ribofuranoside and metformin inhibit hepatic glucose phosphorylation by an AMP-activated protein kinase-independent effect on glucokinase translocation. *Diabetes* **55**, 865-74 (2006).
211. Labuzek, K., Liber, S., Gabryel, B. & Okopien, B. AICAR (5-aminoimidazole-4-carboxamide-1-beta-4-ribofuranoside) increases the production of toxic molecules and affects the profile of cytokines release in LPS-stimulated rat primary microglial cultures. *Neurotoxicology* **31**, 134-46 (2010).
212. Zhou, G. et al. Role of AMP-activated protein kinase in mechanism of metformin action. *J Clin Invest* **108**, 1167-74 (2001).
213. Soranna, D. et al. Cancer risk associated with use of metformin and sulfonylurea in type 2 diabetes: a meta-analysis. *Oncologist* **17**, 813-22 (2012).
214. Zang, M. et al. AMP-activated protein kinase is required for the lipid-lowering effect of metformin in insulin-resistant human HepG2 cells. *J Biol Chem* **279**, 47898-905 (2004).
215. Miller, R.A. et al. Biguanides suppress hepatic glucagon signalling by decreasing production of cyclic AMP. *Nature* **494**, 256-60 (2013).
216. Dykens, J.A. et al. Biguanide-induced mitochondrial dysfunction yields increased lactate production and cytotoxicity of aerobically-poised HepG2 cells and human hepatocytes in vitro. *Toxicol Appl Pharmacol* **233**, 203-10 (2008).
217. Owen, M.R., Doran, E. & Halestrap, A.P. Evidence that metformin exerts its anti-diabetic effects through inhibition of complex 1 of the mitochondrial respiratory chain. *Biochem J* **348 Pt 3**, 607-14 (2000).
218. El-Mir, M.Y. et al. Dimethylbiguanide inhibits cell respiration via an indirect effect targeted on the respiratory chain complex I. *J Biol Chem* **275**, 223-8 (2000).
219. Hardie, D.G. Neither LKB1 nor AMPK are the direct targets of metformin. *Gastroenterology* **131**, 973; author reply 974-5 (2006).
220. Hawley, S.A., Gadalla, A.E., Olsen, G.S. & Hardie, D.G. The antidiabetic drug metformin activates the AMP-activated protein kinase cascade via an adenine nucleotide-independent mechanism. *Diabetes* **51**, 2420-5 (2002).
221. Lee, Y.S. et al. Berberine, a natural plant product, activates AMP-activated protein kinase with beneficial metabolic effects in diabetic and insulin-resistant states. *Diabetes* **55**, 2256-64 (2006).

222. Yin, J., Zhang, H. & Ye, J. Traditional chinese medicine in treatment of metabolic syndrome. *Endocr Metab Immune Disord Drug Targets* **8**, 99-111 (2008).
223. Jeong, H.W. et al. Berberine suppresses proinflammatory responses through AMPK activation in macrophages. *Am J Physiol Endocrinol Metab* **296**, E955-64 (2009).
224. Guo, Y. et al. Biochemical pathways in the antiatherosclerotic effect of berberine. *Chin Med J (Engl)* **121**, 1197-203 (2008).
225. Lee, T.S. et al. Anti-atherogenic effect of berberine on LXRalpha-ABCA1-dependent cholesterol efflux in macrophages. *Journal of cellular biochemistry* **111**, 104-10 (2010).
226. Cho, B.J. et al. Berberine inhibits the production of lysophosphatidylcholine-induced reactive oxygen species and the ERK1/2 pathway in vascular smooth muscle cells. *Mol Cells* **20**, 429-34 (2005).
227. Hawley, S.A. et al. The ancient drug salicylate directly activates AMP-activated protein kinase. *Science* **336**, 918-22 (2012).
228. Steinberg, G.R., Dandapani, M. & Hardie, D.G. AMPK: mediating the metabolic effects of salicylate-based drugs? *Trends Endocrinol Metab* **24**, 481-7 (2013).
229. Cool, B. et al. Identification and characterization of a small molecule AMPK activator that treats key components of type 2 diabetes and the metabolic syndrome. *Cell Metab* **3**, 403-16 (2006).
230. Scott, J.W. et al. Thienopyridone drugs are selective activators of AMP-activated protein kinase beta1-containing complexes. *Chem Biol* **15**, 1220-30 (2008).
231. Goransson, O. et al. Mechanism of action of A-769662, a valuable tool for activation of AMP-activated protein kinase. *J Biol Chem* **282**, 32549-60 (2007).
232. Hardie, D.G. Minireview: the AMP-activated protein kinase cascade: the key sensor of cellular energy status. *Endocrinology* **144**, 5179-83 (2003).
233. Carling, D. The AMP-activated protein kinase cascade--a unifying system for energy control. *Trends Biochem Sci* **29**, 18-24 (2004).
234. Scott, J.W., Norman, D.G., Hawley, S.A., Kontogiannis, L. & Hardie, D.G. Protein kinase substrate recognition studied using the recombinant catalytic domain of AMP-activated protein kinase and a model substrate. *J Mol Biol* **317**, 309-23 (2002).
235. Hardie, D.G. AMPK and Raptor: matching cell growth to energy supply. *Molecular cell* **30**, 263-5 (2008).
236. Zheng, D. et al. Regulation of muscle GLUT-4 transcription by AMP-activated protein kinase. *J Appl Physiol (1985)* **91**, 1073-83 (2001).
237. Carling, D. & Hardie, D.G. The substrate and sequence specificity of the AMP-activated protein kinase. Phosphorylation of glycogen synthase and phosphorylase kinase. *Biochimica et biophysica acta* **1012**, 81-6 (1989).
238. Young, M.E., Radda, G.K. & Leighton, B. Activation of glycogen phosphorylase and glycogenolysis in rat skeletal muscle by AICAR--an activator of AMP-activated protein kinase. *FEBS Lett* **382**, 43-7 (1996).
239. Ponticos, M. et al. Dual regulation of the AMP-activated protein kinase provides a novel mechanism for the control of creatine kinase in skeletal muscle. *EMBO J* **17**, 1688-99 (1998).
240. Kimura, N. et al. A possible linkage between AMP-activated protein kinase (AMPK) and mammalian target of rapamycin (mTOR) signalling pathway. *Genes Cells* **8**, 65-79 (2003).
241. Gwinn, D.M. et al. AMPK phosphorylation of raptor mediates a metabolic checkpoint. *Molecular cell* **30**, 214-26 (2008).
242. Inoki, K., Zhu, T. & Guan, K.L. TSC2 mediates cellular energy response to control cell growth and survival. *Cell* **115**, 577-90 (2003).

243. Vincent, E.E. et al. Differential effects of AMPK agonists on cell growth and metabolism. *Oncogene* (2014).
244. Carling, D., Zammit, V.A. & Hardie, D.G. A common bicyclic protein kinase cascade inactivates the regulatory enzymes of fatty acid and cholesterol biosynthesis. *FEBS Lett* **223**, 217-22 (1987).
245. McGarry, J.D., Mills, S.E., Long, C.S. & Foster, D.W. Observations on the affinity for carnitine, and malonyl-CoA sensitivity, of carnitine palmitoyltransferase I in animal and human tissues. Demonstration of the presence of malonyl-CoA in non-hepatic tissues of the rat. *Biochem J* **214**, 21-8 (1983).
246. Saha, A.K. et al. Activation of malonyl-CoA decarboxylase in rat skeletal muscle by contraction and the AMP-activated protein kinase activator 5-aminoimidazole-4-carboxamide-1-beta -D-ribofuranoside. *J Biol Chem* **275**, 24279-83 (2000).
247. Velasco, G., Geelen, M.J. & Guzman, M. Control of hepatic fatty acid oxidation by 5'-AMP-activated protein kinase involves a malonyl-CoA-dependent and a malonyl-CoA-independent mechanism. *Arch Biochem Biophys* **337**, 169-75 (1997).
248. Merrill, G.F., Kurth, E.J., Hardie, D.G. & Winder, W.W. AICA riboside increases AMP-activated protein kinase, fatty acid oxidation, and glucose uptake in rat muscle. *Am J Physiol* **273**, E1107-12 (1997).
249. Reznick, R.M. & Shulman, G.I. The role of AMP-activated protein kinase in mitochondrial biogenesis. *J Physiol* **574**, 33-9 (2006).
250. Yang, Z., Kahn, B.B., Shi, H. & Xue, B.Z. Macrophage alpha1 AMP-activated protein kinase (alpha1AMPK) antagonizes fatty acid-induced inflammation through SIRT1. *The Journal of biological chemistry* **285**, 19051-9 (2010).
251. Sag, D., Carling, D., Stout, R.D. & Suttles, J. Adenosine 5'-monophosphate-activated protein kinase promotes macrophage polarization to an anti-inflammatory functional phenotype. *Journal of immunology* **181**, 8633-41 (2008).
252. Marsin, A.S., Bouzin, C., Bertrand, L. & Hue, L. The stimulation of glycolysis by hypoxia in activated monocytes is mediated by AMP-activated protein kinase and inducible 6-phosphofructo-2-kinase. *J Biol Chem* **277**, 30778-83 (2002).
253. Krawczyk, C.M. et al. Toll-like receptor-induced changes in glycolytic metabolism regulate dendritic cell activation. *Blood* **115**, 4742-9 (2010).
254. Galic, S. et al. Hematopoietic AMPK beta1 reduces mouse adipose tissue macrophage inflammation and insulin resistance in obesity. *The Journal of clinical investigation* **121**, 4903-15 (2011).
255. Vatish, M., Yamada, E., Pessin, J.E. & Bastie, C.C. Fyn kinase function in lipid utilization: a new upstream regulator of AMPK activity? *Arch Physiol Biochem* **115**, 191-8 (2009).
256. Koo, S.H. et al. The CREB coactivator TORC2 is a key regulator of fasting glucose metabolism. *Nature* **437**, 1109-11 (2005).
257. Zong, H. et al. AMP kinase is required for mitochondrial biogenesis in skeletal muscle in response to chronic energy deprivation. *Proc Natl Acad Sci U S A* **99**, 15983-7 (2002).
258. Wang, Q. et al. Activation of AMP-activated protein kinase is required for berberine-induced reduction of atherosclerosis in mice: the role of uncoupling protein 2. *Plos One* **6**, e25436 (2011).
259. Blanc, J. et al. Protective role of uncoupling protein 2 in atherosclerosis. *Circulation* **107**, 388-90 (2003).
260. Winder, W.W. & Hardie, D.G. AMP-activated protein kinase, a metabolic master switch: possible roles in type 2 diabetes. *Am J Physiol* **277**, E1-10 (1999).

261. Hardie, D.G. Role of AMP-activated protein kinase in the metabolic syndrome and in heart disease. *FEBS Lett* **582**, 81-9 (2008).
262. Narkar, V.A. et al. AMPK and PPARdelta agonists are exercise mimetics. *Cell* **134**, 405-15 (2008).
263. Kramer, D.K. et al. Role of AMP kinase and PPARdelta in the regulation of lipid and glucose metabolism in human skeletal muscle. *J Biol Chem* **282**, 19313-20 (2007).
264. Phelan, C.A. et al. Selective partial agonism of liver X receptor alpha is related to differential corepressor recruitment. *Molecular endocrinology* **22**, 2241-9 (2008).
265. Gantner, F., Kupferschmidt, R., Schudt, C., Wendel, A. & Hatzelmann, A. In vitro differentiation of human monocytes to macrophages: change of PDE profile and its relationship to suppression of tumour necrosis factor-alpha release by PDE inhibitors. *Br J Pharmacol* **121**, 221-31 (1997).
266. Gentleman, R.C. et al. Bioconductor: open software development for computational biology and bioinformatics. *Genome Biol* **5**, R80 (2004).
267. Dunning, M.J., Smith, M.L., Ritchie, M.E. & Tavare, S. beadarray: R classes and methods for Illumina bead-based data. *Bioinformatics* **23**, 2183-4 (2007).
268. Smyth, G.K., Michaud, J. & Scott, H.S. Use of within-array replicate spots for assessing differential expression in microarray experiments. *Bioinformatics* **21**, 2067-75 (2005).
269. Subramanian, A. et al. Gene set enrichment analysis: a knowledge-based approach for interpreting genome-wide expression profiles. *Proc Natl Acad Sci U S A* **102**, 15545-50 (2005).
270. Cerami, E.G. et al. Pathway Commons, a web resource for biological pathway data. *Nucleic Acids Res* **39**, D685-90 (2011).
271. Flicek, P. et al. Ensembl 2013. *Nucleic Acids Res* **41**, D48-55 (2013).
272. Lowry, O.H., Rosebrough, N.J., Farr, A.L. & Randall, R.J. Protein measurement with the Folin phenol reagent. *J Biol Chem* **193**, 265-75 (1951).
273. Woods, A. et al. Characterization of the role of AMP-activated protein kinase in the regulation of glucose-activated gene expression using constitutively active and dominant negative forms of the kinase. *Mol Cell Biol* **20**, 6704-11 (2000).
274. Zhao, C. et al. Adenovirus-mediated gene transfer in mesenchymal stem cells can be significantly enhanced by the cationic polymer polybrene. *Plos One* **9**, e92908 (2014).
275. Mayne, G.C. et al. Centrifugation facilitates transduction of green fluorescent protein in human monocytes and macrophages by adenovirus at low multiplicity of infection. *J Immunol Methods* **278**, 45-56 (2003).
276. Erkkila, K. et al. Regulation of human male germ cell death by modulators of ATP production. *Am J Physiol Endocrinol Metab* **290**, E1145-54 (2006).
277. Serrill, J.D. et al. Apoptolidins A and C Activate AMPK in Metabolically Sensitive Cell Types and are Mechanistically Distinct from Oligomycin A. *Biochemical pharmacology* (2014).
278. Kersten, S. Physiological regulation of lipoprotein lipase. *Biochimica et biophysica acta* **1841**, 919-33 (2014).
279. Bojic, L.A. et al. Activation of peroxisome proliferator-activated receptor delta inhibits human macrophage foam cell formation and the inflammatory response induced by very low-density lipoprotein. *Arteriosclerosis, thrombosis, and vascular biology* **32**, 2919-28 (2012).
280. Makoveichuk, E. et al. Inactivation of lipoprotein lipase occurs on the surface of THP-1 macrophages where oligomers of angiopoietin-like protein 4 are formed. *Biochem Biophys Res Commun* **425**, 138-43 (2012).

281. Namgaladze, D., Kemmerer, M., von Knethen, A. & Brune, B. AICAR inhibits PPARgamma during monocyte differentiation to attenuate inflammatory responses to atherogenic lipids. *Cardiovascular research* **98**, 479-87 (2013).
282. Xia, X. et al. Liver X receptor beta and peroxisome proliferator-activated receptor delta regulate cholesterol transport in murine cholangiocytes. *Hepatology* **56**, 2288-96 (2012).
283. Ignatova, I.D., Angdisen, J., Moran, E. & Schulman, I.G. Differential regulation of gene expression by LXRs in response to macrophage cholesterol loading. *Molecular endocrinology* **27**, 1036-47 (2013).
284. Chinetti-Gbaguidi, G. et al. Human atherosclerotic plaque alternative macrophages display low cholesterol handling but high phagocytosis because of distinct activities of the PPARgamma and LXRalpha pathways. *Circulation research* **108**, 985-95 (2011).
285. Boyle, J.J. et al. Activating transcription factor 1 directs Mhem atheroprotective macrophages through coordinated iron handling and foam cell protection. *Circ Res* **110**, 20-33 (2012).
286. Luu, W., Sharpe, L.J. & Brown, A.J. Protein tyrosine phosphatase inhibition down-regulates ligand-induced ABCA1 expression. *Atherosclerosis* **228**, 362-9 (2013).
287. Costet, P., Luo, Y., Wang, N. & Tall, A.R. Sterol-dependent transactivation of the ABC1 promoter by the liver X receptor/retinoid X receptor. *J Biol Chem* **275**, 28240-5 (2000).
288. Langmann, T. et al. Identification of sterol-independent regulatory elements in the human ATP-binding cassette transporter A1 promoter: role of Sp1/3, E-box binding factors, and an oncostatin M-responsive element. *J Biol Chem* **277**, 14443-50 (2002).
289. Noto, P.B. et al. Regulation of sphingomyelin phosphodiesterase acid-like 3A gene (SMPDL3A) by liver X receptors. *Mol Pharmacol* **82**, 719-27 (2012).
290. Roepstorff, P. & Fohlman, J. Proposal for a common nomenclature for sequence ions in mass spectra of peptides. *Biomed Mass Spectrom* **11**, 601 (1984).
291. Leyva, F.J., Anzinger, J.J., McCoy, J.P., Jr. & Kruth, H.S. Evaluation of transduction efficiency in macrophage colony-stimulating factor differentiated human macrophages using HIV-1 based lentiviral vectors. *BMC Biotechnol* **11**, 13 (2011).
292. Moreno, D., Knecht, E., Viollet, B. & Sanz, P. A769662, a novel activator of AMP-activated protein kinase, inhibits non-proteolytic components of the 26S proteasome by an AMPK-independent mechanism. *FEBS Lett* **582**, 2650-4 (2008).
293. Xiao, B. et al. Structural basis of AMPK regulation by small molecule activators. *Nat Commun* **4**, 3017 (2013).
294. Fritz, T. et al. Low-intensity exercise increases skeletal muscle protein expression of PPARdelta and UCP3 in type 2 diabetic patients. *Diabetes Metab Res Rev* **22**, 492-8 (2006).
295. Watt, M.J., Southgate, R.J., Holmes, A.G. & Febbraio, M.A. Suppression of plasma free fatty acids upregulates peroxisome proliferator-activated receptor (PPAR) alpha and delta and PPAR coactivator 1alpha in human skeletal muscle, but not lipid regulatory genes. *J Mol Endocrinol* **33**, 533-44 (2004).
296. Ehrenborg, E. & Krook, A. Regulation of skeletal muscle physiology and metabolism by peroxisome proliferator-activated receptor delta. *Pharmacol Rev* **61**, 373-93 (2009).
297. Wallner, S. et al. Monocyte to macrophage differentiation goes along with modulation of the plasmalogen pattern through transcriptional regulation. *Plos One* **9**, e94102 (2014).
298. Gan, Z. et al. The nuclear receptor PPARbeta/delta programs muscle glucose metabolism in cooperation with AMPK and MEF2. *Genes & development* **25**, 2619-30 (2011).

299. Michael, L.F. et al. Restoration of insulin-sensitive glucose transporter (GLUT4) gene expression in muscle cells by the transcriptional coactivator PGC-1. *Proc Natl Acad Sci U S A* **98**, 3820-5 (2001).
300. Holloway, G.P., Bonen, A. & Spriet, L.L. Regulation of skeletal muscle mitochondrial fatty acid metabolism in lean and obese individuals. *Am J Clin Nutr* **89**, 455S-62S (2009).
301. Kleiner, S. et al. PPAR{delta} agonism activates fatty acid oxidation via PGC-1{alpha} but does not increase mitochondrial gene expression and function. *J Biol Chem* **284**, 18624-33 (2009).
302. Namgaladze, D. & Brune, B. Fatty acid oxidation is dispensable for human macrophage IL-4-induced polarization. *Biochimica et biophysica acta* **1841**, 1329-35 (2014).
303. McCarthy, C. et al. Macrophage PPAR gamma Co-activator-1 alpha participates in repressing foam cell formation and atherosclerosis in response to conjugated linoleic acid. *EMBO Mol Med* **5**, 1443-57 (2013).
304. Pilegaard, H. & Neufer, P.D. Transcriptional regulation of pyruvate dehydrogenase kinase 4 in skeletal muscle during and after exercise. *Proc Nutr Soc* **63**, 221-6 (2004).
305. Xu, J., Han, J., Epstein, P.N. & Liu, Y.Q. Regulation of PDK mRNA by high fatty acid and glucose in pancreatic islets. *Biochem Biophys Res Commun* **344**, 827-33 (2006).
306. Houten, S.M. et al. Pyruvate dehydrogenase kinase 4 expression is synergistically induced by AMP-activated protein kinase and fatty acids. *Cell Mol Life Sci* **66**, 1283-94 (2009).
307. Wan, Z. et al. Epinephrine-mediated regulation of PDK4 mRNA in rat adipose tissue. *Am J Physiol Cell Physiol* **299**, C1162-70 (2010).
308. Namgaladze, D. et al. Inhibition of macrophage fatty acid beta-oxidation exacerbates palmitate-induced inflammatory and endoplasmic reticulum stress responses. *Diabetologia* (2014).
309. Jara, J.H., Frank, D.D. & Ozdinler, P.H. Could dysregulation of UPS be a common underlying mechanism for cancer and neurodegeneration? Lessons from UCHL1. *Cell biochemistry and biophysics* **67**, 45-53 (2013).
310. Zhang, M., Cai, F., Zhang, S. & Song, W. Overexpression of ubiquitin carboxyl-terminal hydrolase L1 (UCHL1) delays Alzheimer's progression in vivo. *Sci Rep* **4**, 7298 (2014).
311. Jucker, B.M. et al. Selective PPARdelta agonist treatment increases skeletal muscle lipid metabolism without altering mitochondrial energy coupling: an in vivo magnetic resonance spectroscopy study. *Am J Physiol Endocrinol Metab* **293**, E1256-64 (2007).
312. Jimenez, E. et al. Genetic variability at IMPA2, INPP1 and GSK3beta increases the risk of suicidal behavior in bipolar patients. *Eur Neuropsychopharmacol* **23**, 1452-62 (2013).
313. Whitman, S.C. et al. Uptake of type IV hypertriglyceridemic VLDL by cultured macrophages is enhanced by interferon-gamma. *J Lipid Res* **40**, 1017-28 (1999).
314. Whitman, S.C. et al. Modification of type III VLDL, their remnants, and VLDL from ApoE-knockout mice by p-hydroxyphenylacetaldehyde, a product of myeloperoxidase activity, causes marked cholesteryl ester accumulation in macrophages. *Arteriosclerosis, thrombosis, and vascular biology* **19**, 1238-49 (1999).
315. Ziouzenkova, O. et al. Lipolysis of triglyceride-rich lipoproteins generates PPAR ligands: evidence for an antiinflammatory role for lipoprotein lipase. *Proc Natl Acad Sci U S A* **100**, 2730-5 (2003).
316. Koster, A. et al. Transgenic angiopoietin-like (angptl)4 overexpression and targeted disruption of angptl4 and angptl3: regulation of triglyceride metabolism. *Endocrinology* **146**, 4943-50 (2005).

317. Yoshida, K., Shimizugawa, T., Ono, M. & Furukawa, H. Angiopoietin-like protein 4 is a potent hyperlipidemia-inducing factor in mice and inhibitor of lipoprotein lipase. *J Lipid Res* **43**, 1770-2 (2002).
318. Lafferty, M.J., Bradford, K.C., Erie, D.A. & Neher, S.B. Angiopoietin-like protein 4 inhibition of lipoprotein lipase: evidence for reversible complex formation. *J Biol Chem* **288**, 28524-34 (2013).
319. Lichtenstein, L. et al. Angptl4 protects against severe proinflammatory effects of saturated fat by inhibiting fatty acid uptake into mesenteric lymph node macrophages. *Cell Metab* **12**, 580-92 (2010).
320. Georgiadi, A. et al. Overexpression of angiopoietin-like protein 4 protects against atherosclerosis development. *Arteriosclerosis, thrombosis, and vascular biology* **33**, 1529-37 (2013).
321. Schaffer, J.E. Lipotoxicity: when tissues overeat. *Current opinion in lipidology* **14**, 281-7 (2003).
322. Steinberg, G.R. & Schertzer, J.D. AMPK promotes macrophage fatty acid oxidative metabolism to mitigate inflammation: implications for diabetes and cardiovascular disease. *Immunol Cell Biol* **92**, 340-5 (2014).
323. Malandrino, M.I. et al. Enhanced fatty acid oxidation in adipocytes and macrophages reduces lipid-induced triglyceride accumulation and inflammation. *Am J Physiol Endocrinol Metab* **308**, E756-69 (2015).
324. Erwig, L.P. & Henson, P.M. Clearance of apoptotic cells by phagocytes. *Cell Death Differ* **15**, 243-50 (2008).
325. Shrivastav, S. et al. HIV-1 Vpr enhances PPARbeta/delta-mediated transcription, increases PDK4 expression, and reduces PDC activity. *Molecular endocrinology* **27**, 1564-76 (2013).
326. Welch, J.S., Ricote, M., Akiyama, T.E., Gonzalez, F.J. & Glass, C.K. PPARgamma and PPARdelta negatively regulate specific subsets of lipopolysaccharide and IFN-gamma target genes in macrophages. *Proc Natl Acad Sci U S A* **100**, 6712-7 (2003).
327. Cheng, L. et al. Cardiomyocyte-restricted peroxisome proliferator-activated receptor-delta deletion perturbs myocardial fatty acid oxidation and leads to cardiomyopathy. *Nature medicine* **10**, 1245-50 (2004).
328. Smeets, P.J. et al. Inflammatory pathways are activated during cardiomyocyte hypertrophy and attenuated by peroxisome proliferator-activated receptors PPARalpha and PPARdelta. *J Biol Chem* **283**, 29109-18 (2008).
329. Cao, M. et al. PPARdelta Activation Rescues Pancreatic beta-Cell Line INS-1E from Palmitate-Induced Endoplasmic Reticulum Stress through Enhanced Fatty Acid Oxidation. *PPAR Res* **2012**, 680684 (2012).
330. Cheang, W.S. et al. Metformin protects endothelial function in diet-induced obese mice by inhibition of endoplasmic reticulum stress through 5' adenosine monophosphate-activated protein kinase-peroxisome proliferator-activated receptor delta pathway. *Arteriosclerosis, thrombosis, and vascular biology* **34**, 830-6 (2014).
331. Serrano-Marco, L. et al. The peroxisome proliferator-activated receptor (PPAR) beta/delta agonist GW501516 inhibits IL-6-induced signal transducer and activator of transcription 3 (STAT3) activation and insulin resistance in human liver cells. *Diabetologia* **55**, 743-51 (2012).
332. Coll, T. et al. Activation of peroxisome proliferator-activated receptor-{delta} by GW501516 prevents fatty acid-induced nuclear factor-{kappa}B activation and insulin resistance in skeletal muscle cells. *Endocrinology* **151**, 1560-9 (2010).
333. Tabas, I. Macrophage death and defective inflammation resolution in atherosclerosis. *Nature reviews. Immunology* **10**, 36-46 (2010).

334. Serhan, C.N., Chiang, N. & Van Dyke, T.E. Resolving inflammation: dual anti-inflammatory and pro-resolution lipid mediators. *Nature reviews. Immunology* **8**, 349-61 (2008).
335. Yvan-Charvet, L. et al. ABCA1 and ABCG1 protect against oxidative stress-induced macrophage apoptosis during efferocytosis. *Circ Res* **106**, 1861-9 (2010).
336. Wan, X. et al. 5'-AMP-activated protein kinase-activating transcription factor 1 cascade modulates human monocyte-derived macrophages to atheroprotective functions in response to heme or metformin. *Arteriosclerosis, thrombosis, and vascular biology* **33**, 2470-80 (2013).
337. Davies, N.A. et al. The contributions of oxidative stress, oxidised lipoproteins and AMPK towards exercise-associated PPARgamma signalling within human monocytic cells. *Free Radic Res* **49**, 45-56 (2015).
338. Ishibashi, M. et al. Knock-down of the oxysterol receptor LXRalpha impairs cholesterol efflux in human primary macrophages: lack of compensation by LXRbeta activation. *Biochemical pharmacology* **86**, 122-9 (2013).
339. Zhang, L.H., Kamanna, V.S., Ganji, S.H., Xiong, X.M. & Kashyap, M.L. Niacin increases HDL biogenesis by enhancing DR4-dependent transcription of ABCA1 and lipidation of apolipoprotein A-I in HepG2 cells. *J Lipid Res* **53**, 941-50 (2012).
340. Meyers, C.D., Kamanna, V.S. & Kashyap, M.L. Niacin therapy in atherosclerosis. *Current opinion in lipidology* **15**, 659-65 (2004).
341. Penumathsa, S.V. et al. Niacin bound chromium treatment induces myocardial Glut-4 translocation and caveolar interaction via Akt, AMPK and eNOS phosphorylation in streptozotocin induced diabetic rats after ischemia-reperfusion injury. *Biochimica et biophysica acta* **1792**, 39-48 (2009).
342. Huang, C.J., Feltkamp, D., Nilsson, S. & Gustafsson, J.A. Synergistic activation of RLD-1 by agents triggering PKA and PKC dependent signalling. *Biochem Biophys Res Commun* **243**, 657-63 (1998).
343. Tamura, K. et al. LXRalpha functions as a cAMP-responsive transcriptional regulator of gene expression. *Proc Natl Acad Sci U S A* **97**, 8513-8 (2000).
344. Torra, I.P. et al. Phosphorylation of liver X receptor alpha selectively regulates target gene expression in macrophages. *Mol Cell Biol* **28**, 2626-36 (2008).
345. Pearson, G. et al. Mitogen-activated protein (MAP) kinase pathways: regulation and physiological functions. *Endocr Rev* **22**, 153-83 (2001).
346. Hwang, S.L. et al. Inhibitory cross-talk between the AMPK and ERK pathways mediates endoplasmic reticulum stress-induced insulin resistance in skeletal muscle. *Br J Pharmacol* **169**, 69-81 (2013).
347. Du, J. et al. Inhibitory crosstalk between ERK and AMPK in the growth and proliferation of cardiac fibroblasts. *Biochem Biophys Res Commun* **368**, 402-7 (2008).
348. Salvado, L. et al. PPARbeta/delta prevents endoplasmic reticulum stress-associated inflammation and insulin resistance in skeletal muscle cells through an AMPK-dependent mechanism. *Diabetologia* **57**, 2126-35 (2014).
349. Li, H.L. et al. Long-term activation of adenosine monophosphate-activated protein kinase attenuates pressure-overload-induced cardiac hypertrophy. *Journal of cellular biochemistry* **100**, 1086-99 (2007).
350. Shen, C.H. et al. Phosphorylation of BRAF by AMPK impairs BRAF-KSR1 association and cell proliferation. *Molecular cell* **52**, 161-72 (2013).
351. Chang, Y.C. et al. Hyperglycemia accelerates ATP-binding cassette transporter A1 degradation via an ERK-dependent pathway in macrophages. *Journal of cellular biochemistry* **114**, 1364-73 (2013).

352. Zhou, X., Yin, Z., Guo, X., Hajjar, D.P. & Han, J. Inhibition of ERK1/2 and activation of liver X receptor synergistically induce macrophage ABCA1 expression and cholesterol efflux. *J Biol Chem* **285**, 6316-26 (2010).
353. Dinarello, C.A., Fossati, G. & Mascagni, P. Histone deacetylase inhibitors for treating a spectrum of diseases not related to cancer. *Mol Med* **17**, 333-52 (2011).
354. Huang, E.Y. et al. Nuclear receptor corepressors partner with class II histone deacetylases in a Sin3-independent repression pathway. *Genes & development* **14**, 45-54 (2000).
355. Guenther, M.G. et al. A core SMRT corepressor complex containing HDAC3 and TBL1, a WD40-repeat protein linked to deafness. *Genes & development* **14**, 1048-57 (2000).
356. Wagner, B.L. et al. Promoter-specific roles for liver X receptor/corepressor complexes in the regulation of ABCA1 and SREBP1 gene expression. *Mol Cell Biol* **23**, 5780-9 (2003).
357. Xu, Y., Bao, Y., Hong, B. & Si, S. Identification of dehydroxytrichostatin A as a novel up-regulator of the ATP-binding cassette transporter A1 (ABCA1). *Molecules* **16**, 7183-98 (2011).
358. Shi, Y., Hon, M. & Evans, R.M. The peroxisome proliferator-activated receptor delta, an integrator of transcriptional repression and nuclear receptor signaling. *Proc Natl Acad Sci U S A* **99**, 2613-8 (2002).
359. Mihaylova, M.M. et al. Class IIa histone deacetylases are hormone-activated regulators of FOXO and mammalian glucose homeostasis. *Cell* **145**, 607-21 (2011).
360. Nussenblatt, R.B. et al. National Institutes of Health Center for Human Immunology Conference, September 2009. *Ann N Y Acad Sci* **1200 Suppl 1**, E1-23 (2010).
361. Devries-Seimon, T. et al. Cholesterol-induced macrophage apoptosis requires ER stress pathways and engagement of the type A scavenger receptor. *J Cell Biol* **171**, 61-73 (2005).
362. Arai, S. et al. A role for the apoptosis inhibitory factor AIM/Spalpha/Api6 in atherosclerosis development. *Cell Metab* **1**, 201-13 (2005).
363. Fu, X., Xu, A.G., Yao, M.Y., Guo, L. & Zhao, L.S. Emodin enhances cholesterol efflux by activating peroxisome proliferator-activated receptor-gamma in oxidized low density lipoprotein-loaded THP1 macrophages. *Clin Exp Pharmacol Physiol* **41**, 679-84 (2014).
364. Tontonoz, P., Nagy, L., Alvarez, J.G., Thomazy, V.A. & Evans, R.M. PPARgamma promotes monocyte/macrophage differentiation and uptake of oxidized LDL. *Cell* **93**, 241-52 (1998).
365. Thorp, E. & Tabas, I. Mechanisms and consequences of efferocytosis in advanced atherosclerosis. *J Leukoc Biol* **86**, 1089-95 (2009).
366. Akiyama, T.E. et al. Peroxisome proliferator-activated receptor beta/delta regulates very low density lipoprotein production and catabolism in mice on a Western diet. *J Biol Chem* **279**, 20874-81 (2004).
367. Leibowitz, M.D. et al. Activation of PPARdelta alters lipid metabolism in db/db mice. *FEBS Lett* **473**, 333-6 (2000).
368. Tian, X.Y. et al. PPARdelta activation protects endothelial function in diabetic mice. *Diabetes* **61**, 3285-93 (2012).
369. Bays, H.E. et al. MBX-8025, a novel peroxisome proliferator receptor-delta agonist: lipid and other metabolic effects in dyslipidemic overweight patients treated with and without atorvastatin. *J Clin Endocrinol Metab* **96**, 2889-97 (2011).
370. Choi, Y.J. et al. Effects of the PPAR-delta agonist MBX-8025 on atherogenic dyslipidemia. *Atherosclerosis* **220**, 470-6 (2012).

371. Mazzone, T., Chait, A. & Plutzky, J. Cardiovascular disease risk in type 2 diabetes mellitus: insights from mechanistic studies. *Lancet* **371**, 1800-9 (2008).
372. Tabas, I., Tall, A. & Accili, D. The impact of macrophage insulin resistance on advanced atherosclerotic plaque progression. *Circ Res* **106**, 58-67 (2010).
373. Billin, A.N. PPAR-beta/delta agonists for Type 2 diabetes and dyslipidemia: an adopted orphan still looking for a home. *Expert Opin Investig Drugs* **17**, 1465-71 (2008).
374. Takahashi, S., Tanaka, T. & Sakai, J. New therapeutic target for metabolic syndrome: PPARdelta. *Endocr J* **54**, 347-57 (2007).
375. Reilly, S.M. & Lee, C.H. PPAR delta as a therapeutic target in metabolic disease. *FEBS Lett* **582**, 26-31 (2008).
376. Kase, E.T. et al. Skeletal muscle lipid accumulation in type 2 diabetes may involve the liver X receptor pathway. *Diabetes* **54**, 1108-15 (2005).
377. Dong, B., Kan, C.F., Singh, A.B. & Liu, J. High-fructose diet downregulates long-chain acyl-CoA synthetase 3 expression in liver of hamsters via impairing LXR/RXR signaling pathway. *J Lipid Res* **54**, 1241-54 (2013).
378. Zhang, Y., Repa, J.J., Gauthier, K. & Mangelsdorf, D.J. Regulation of lipoprotein lipase by the oxysterol receptors, LXRalpha and LXRbeta. *J Biol Chem* **276**, 43018-24 (2001).
379. Matsusue, K., Miyoshi, A., Yamano, S. & Gonzalez, F.J. Ligand-activated PPARbeta efficiently represses the induction of LXR-dependent promoter activity through competition with RXR. *Mol Cell Endocrinol* **256**, 23-33 (2006).
380. Plutzky, J. The PPAR-RXR transcriptional complex in the vasculature: energy in the balance. *Circ Res* **108**, 1002-16 (2011).
381. Fall, C.H. et al. Adult metabolic syndrome and impaired glucose tolerance are associated with different patterns of BMI gain during infancy: Data from the New Delhi Birth Cohort. *Diabetes Care* **31**, 2349-56 (2008).
382. Ortega-Senovilla, H., Schaefer-Graf, U., Meitzner, K., Abou-Dakn, M. & Herrera, E. Decreased concentrations of the lipoprotein lipase inhibitor angiopoietin-like protein 4 and increased serum triacylglycerol are associated with increased neonatal fat mass in pregnant women with gestational diabetes mellitus. *J Clin Endocrinol Metab* **98**, 3430-7 (2013).

8. Publications and conferences

8.1. Publications

1. Muik A, Kneiske I, **Werbizki M**, Wilflingseder D, Giroglou T, Ebert O, Kraft A, Dietrich U, Zimmer G, Momma S, von Laer D. Pseudotyping vesicular stomatitis virus with lymphocytic choriomeningitis virus glycoproteins enhances infectivity for glioma cells and minimizes neurotropism. J Virol. 2011, 85(11):5679-84
2. Muik A, Dold C, Geiß Y, Volk A, **Werbizki M**, Dietrich U, von Laer D. Semireplication-competent vesicular stomatitis virus as a novel platform for oncolytic virotherapy. J Mol Med (Berl). 2012, 90(8):959-70
3. Namgaladze D, **Kemmerer M**, von Knethen A, Brüne B. AICAR inhibits PPARγ during monocyte differentiation to attenuate inflammatory responses to atherogenic lipids. Cardiovasc Res. 2013, 98(3):479-87
4. Boß M, **Kemmerer M**, Brüne B, Namgaladze D. FABP4 inhibition suppresses PPARγ activity and VLDL-induced foam cell formation in IL-4-polarized human macrophages. Atherosclerosis. 2015, 240(2):424-30
5. **Kemmerer M**, Finkernagel F, Cavalcante MF, Abdalla DS, Müller R, Brüne B, Namgaladze D. AMP-activated protein kinase interacts with the peroxisome proliferator-activated receptor δ to induce genes affecting fatty acid oxidation in human macrophages. PLoS ONE. 2015, 10(6):e0130893
6. **Kemmerer M**, Richter F, Wittig I, Brüne B, Namgaladze D. AMPK regulates cholesterol efflux by dephosphorylation of LXRα in human macrophages. (wip)

8.2. Conferences

1. Lipid Meeting Leipzig 2013 – participation in lectures and discussion meetings
2. Keystone Symposia on Molecular Cell Biology of Macrophages in Human Diseases in Santa Fe, USA 2014 – poster presentation: “AMPK and PPARδ cooperatively regulate fatty acid metabolism in human macrophages.”

9. Ackowledgements

I would like to thank all those people who were supporting me during the last years. In this time I learned a lot and gained experience not only for my work, but also for my personality. Therefore, my grateful gratitude is extended to:

Prof. Bernhard Brüne for the possibility to perform my thesis in Pathobiochemie laboratory, for providing grants and reviews. Discussion sessions were very helpful realizing my experiments and projects;

PD Dmitry Namgaladze for the assignment of my projects, frequent discussions, laboratory support, and supporting my papers and thesis;

Prof. Bernd Ludwig for great support and supervision of my thesis.

Special thanks go to my collaboration partners in Marburg, Florian Finkernagel and Prof. Rolf Müller for bioinformatics analysis of microarray, and Till Adhikary for showing me the method ChIP. At Frankfurt University I would like to thank Ilka Wittig and Florian Richter for the preparation and performance of mass spectrometry analyses. They made my projects and publications possible.

I am happy to acknowlegde my colleagues I met during my PhD. They supported me not only during discussion sessions, in laboratory and paper work, but also mentally:
Marcel Boß, Christine von Hayn, Ryan Snodgrass, Andreas Weigert,
Marcela Frota Cavalcante, Laura-Ann Seif, Daniel Morbitzer, Wei Sha, Javier Mora,
Stephanie Ley, Larissa Milke, Margarete Wiebe, Divya Sekar, Victoria Buderus,
Michael Kunze, Thilo Brauss, Sebastian Lampe, Nina Großmann, Magdalena Bajer,
Michaela Jung, Praveen Mathoor, Shahzad Nawaz Seyd, Lisa Sha, Michaela Tausendschön,
Nadine Hoffmann, Christina Mertens, Dominik Fuhrmann, Gudrun Beyer,
Simone Graf, and Manuela Diehl.

My friends helped me a lot in this sometimes very hard time. Therefore, sincere gratitude goes to all my friends and their families for great support and exchange of ideas.

Most of all, I want to thank my husband Tobias and our whole family for their everlasting support any time. They were always at my side when I needed them. I dedicate my thesis to my father who engraved me in large extent.

10. Ehrenwörtliche Erklärung

Hiermit erkläre ich ehrenwörtlich, dass ich Marina Kemmerer, geboren am 19.09.1985 in Sumy (Ukraine), die dem Fachbereich Biochemie, Chemie und Pharmazie der Goethe-Universität Frankfurt am Main zur Promotionsprüfung vorliegende Arbeit mit dem Titel

"Elucidation of lipid metabolism pathways mediated by AMPK and nuclear receptors PPARδ and LXRα in human macrophages"

im Institut für Biochemie I – Pathobiochemie unter Betreuung und Anleitung von Prof. Dr. Bernhard Brüne und PD Dr. Dmitry Namgaladze ohne sonstige Hilfe selbst durchgeführt und bei der Abfassung der Dissertation nur die angegebenen Hilfsmittel und Quellen benutzt habe.

Ich habe bisher an keiner in- oder ausländischen Universität ein Gesuch um Zulassung zur Promotion eingereicht. Die vorliegende Arbeit wurde bisher nicht als Dissertation eingereicht.

Teile der vorliegenden Arbeit wurden in dem folgenden Publikationsorgan veröffentlicht:

Kemmerer et.al. PLoS One 2015, 10(6):e0130893

Frankfurt am Main, den

_____

Marina Kemmerer